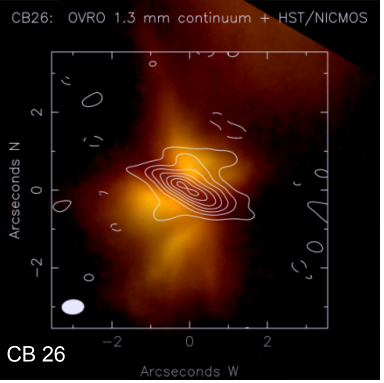

[Sauter et al. 2009]

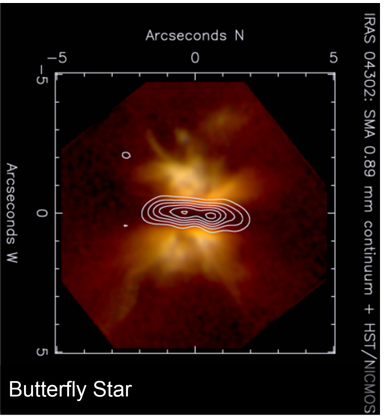

[Wolf et al. 2008]

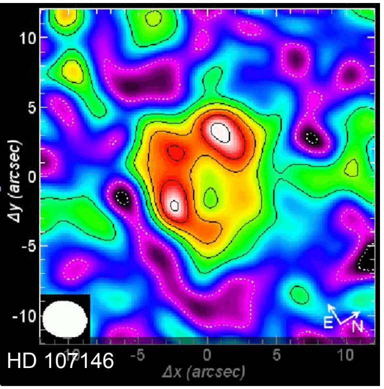

[Ertel et al. 2011]

The birthplace of planets

Observations and modeling of circumstellar disks

Sebastian Wolf

Christian Albrechts University Kiel
Germany

wolf@astrophysik.uni-kiel.de

Overview

Introduction

Young, gas-rich circumstellar disks („Protoplanetary“ disks)

Debris disks

Observations – Modeling – Disk physics

Molecular clouds – Stars – Disks

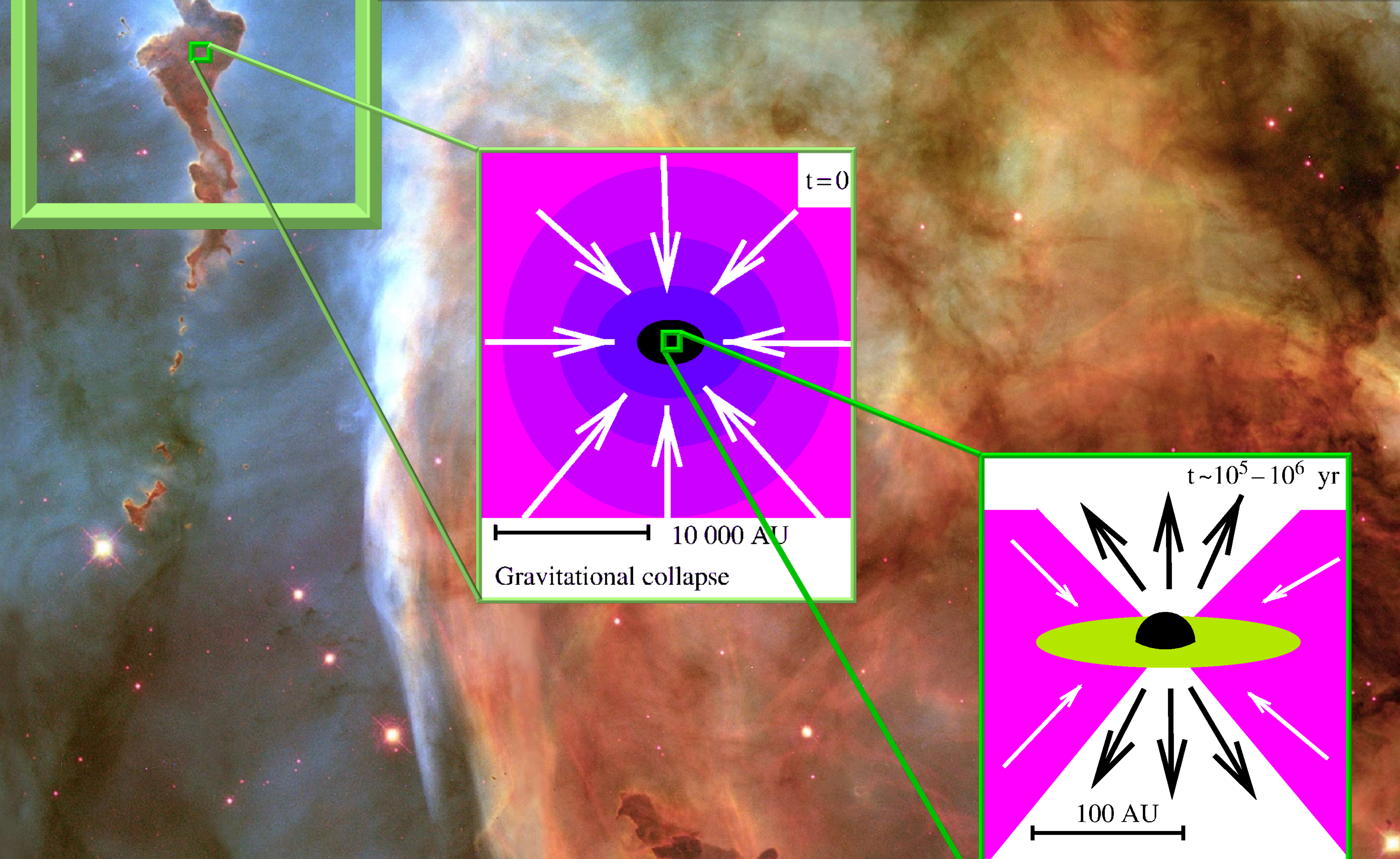

[„Keyhole Nebula“, Húbble Heritage;
figures from Waelkens 2001]

Collapse => Circumstellar disks

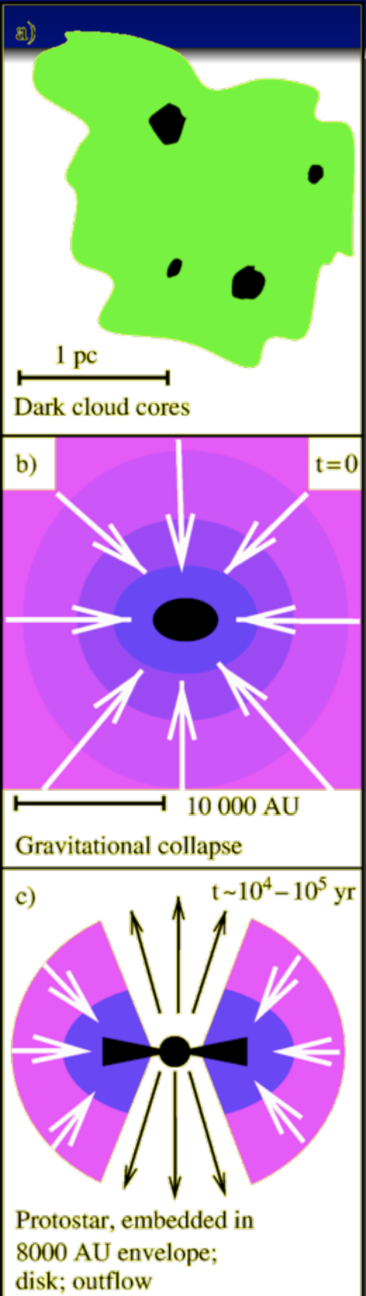

- Protostellar Disk / Protoplanetary Disk / Circumstellar Disk around a young stellar object
  - Gas- and dust disk
  - Composition: 99% Gas, 1% Dust (mass)
  - Typical diameter: several 100 AU

- Formation:
  - "By-product" of star formation
  - Gravitational collapse of a rotating molecular cloud core
  - Conservation of angular momentum

    => Material forms disk around the central object (pre-main sequence star)

- Protostellar Disk
  - "Reservoir" of mass and angular momentum
  - Environment + material for planet formation
  - Evolution of structure and composition

[from Waelkens 2001]

Molecular clouds – Stars – Planets

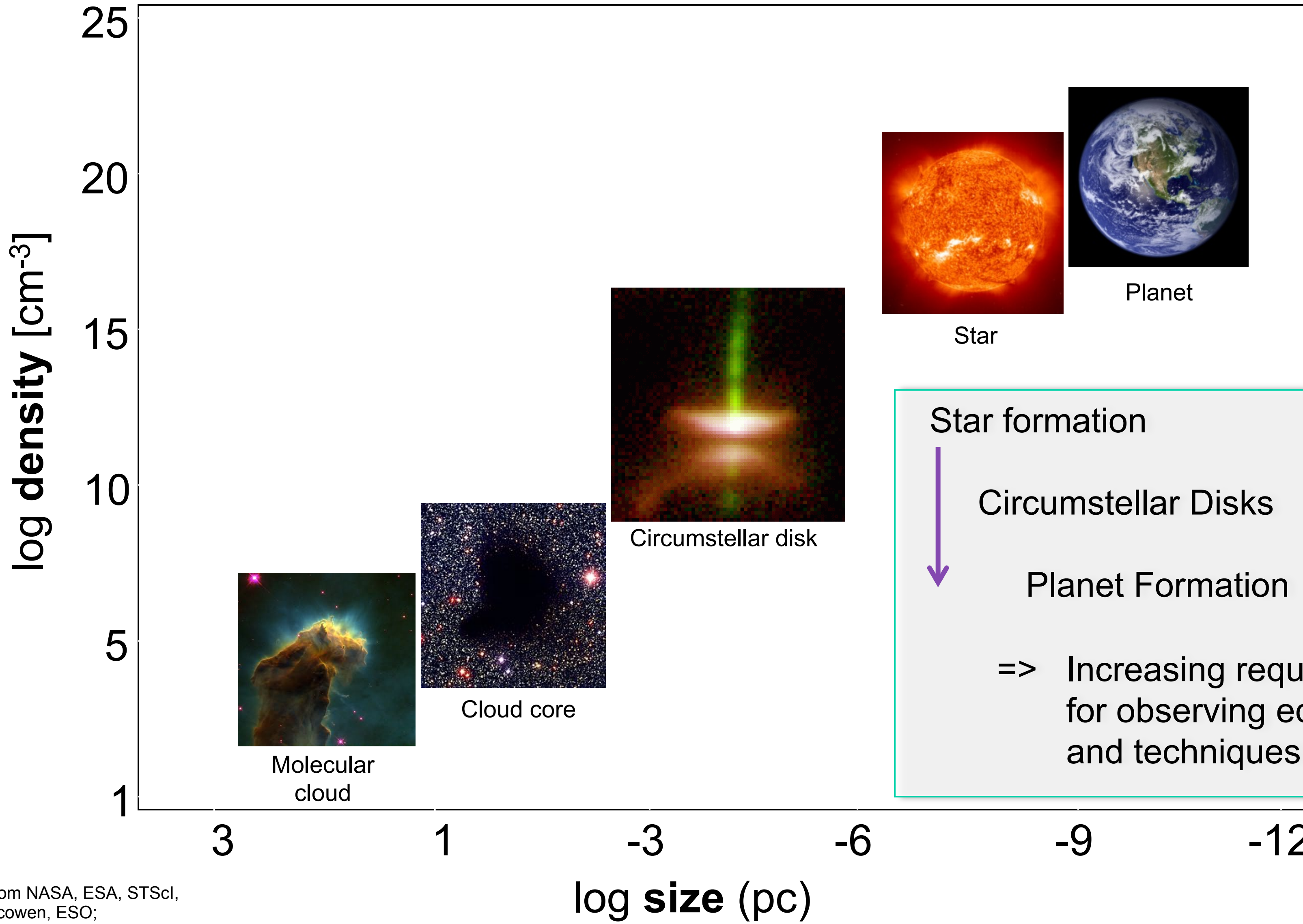

Star formation

Circumstellar Disks

Planet Formation

=> Increasing requirements for observing equipment and techniques

[figures from NASA, ESA, STScI, Hester, Scowen, ESO; Based on figure by Th. Henning]

Telescope: Angular resolution

- Angular resolution of a telescope limited by the size of its aperture:

$$d \approx 1{,}22\,\frac{\lambda}{D}$$

d - angular resolution [rad]
λ - wavelength
D - aperture diameter

but: Influence of the atmosphere

Example:
Disk diameter: 300 AU, Distance: 150pc
=> d ~ 2“
Observations in the visible wavelength range:
Typical seeing ~1“ => Disk structure hardly visible

- Possible solutions:
  Observations above the atmosphere, Adaptive Optics, Interferometry

Step 1

Investigating circumstellar disks
without spatially resolved images

Photometry of YSOs

&

Early Models

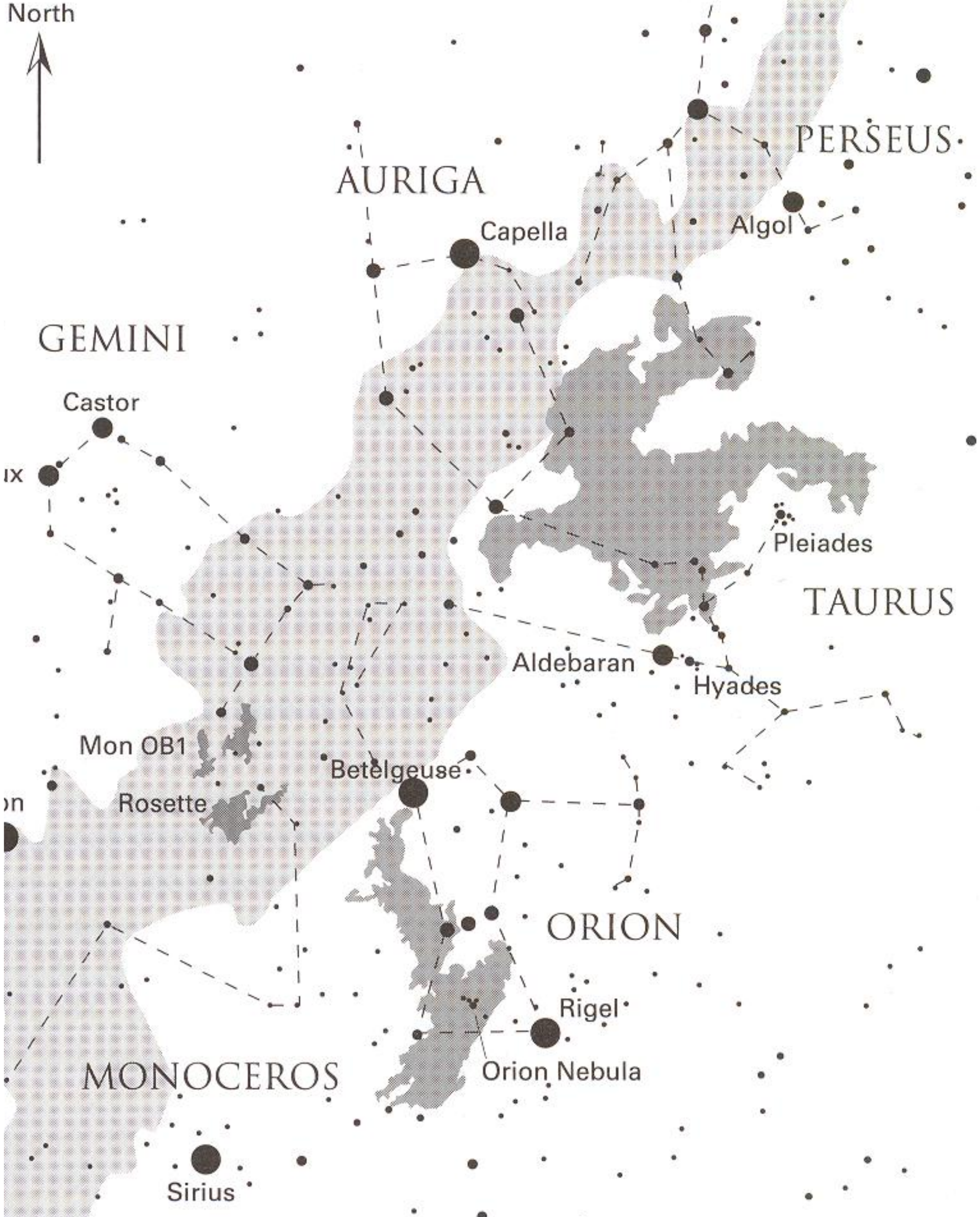

[from Stahler & Palla,
„The formation of stars“]

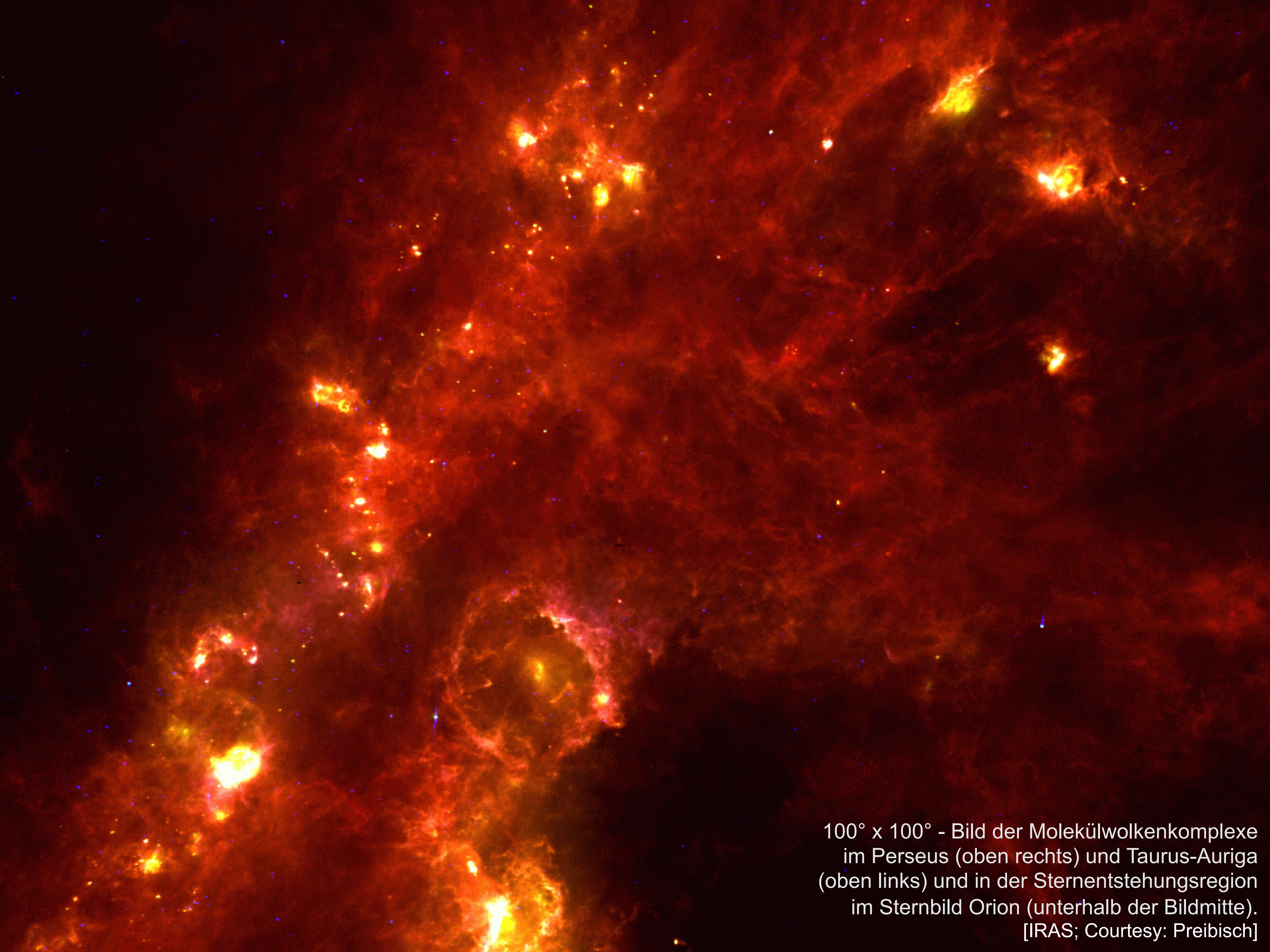

100° x 100° - Bild der Molekülwolkenkomplexe im Perseus (oben rechts) und Taurus-Auriga (oben links) und in der Sternentstehungsregion im Sternbild Orion (unterhalb der Bildmitte). [IRAS; Courtesy: Preibisch]

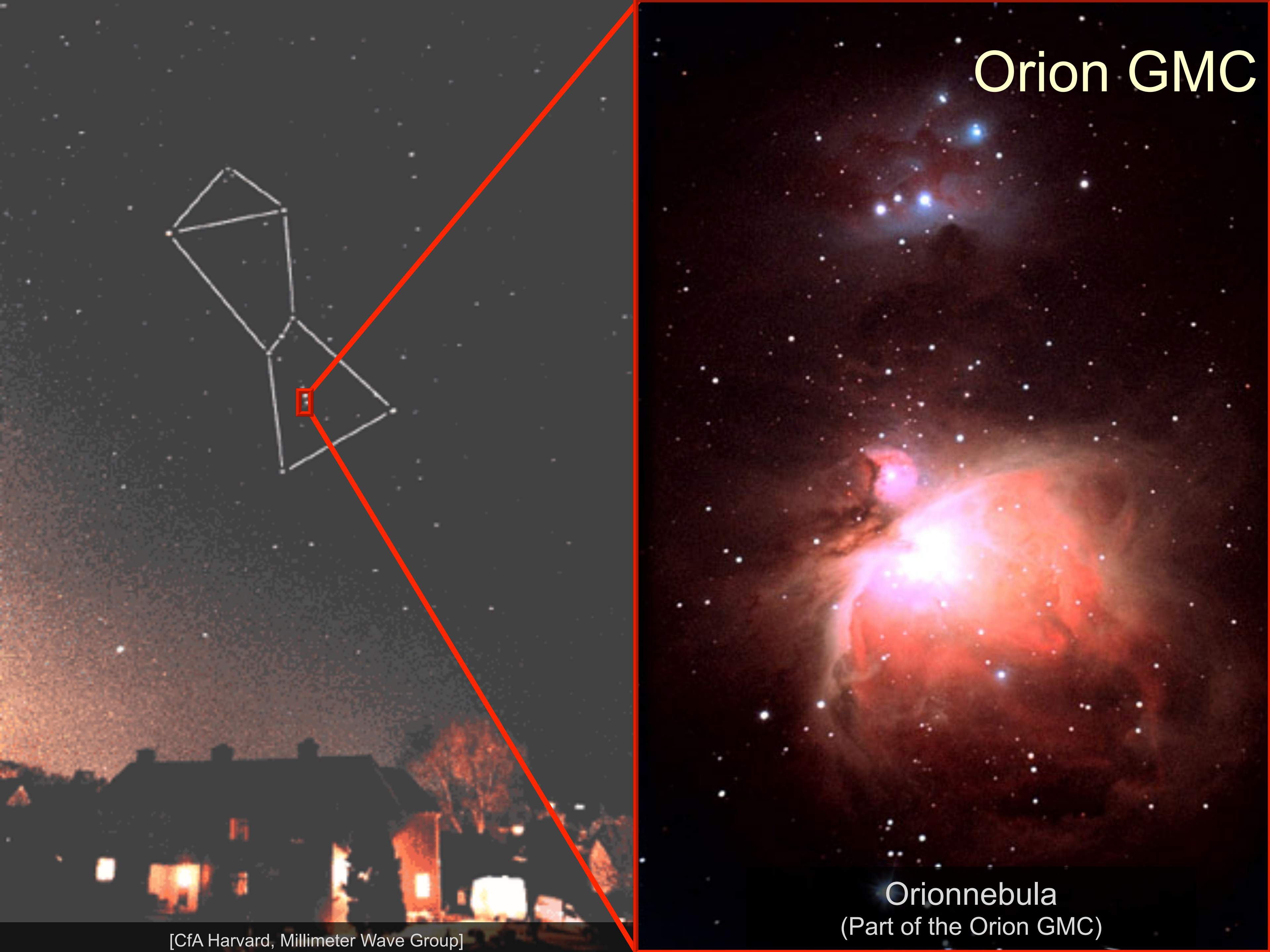
Orion GMC
Orionnebula
(Part of the Orion GMC)
[CfA Harvard, Millimeter Wave Group]

Photometry of YSO – Sampling the SED

[Exemplary Telescopes]

Herschel [2009]

JCMT

SUBARU

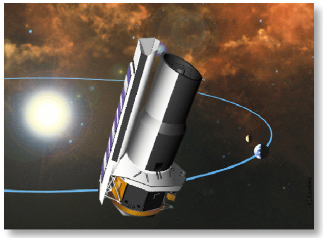

Spitzer ST [2003]

SOFIA [2011]

APEX

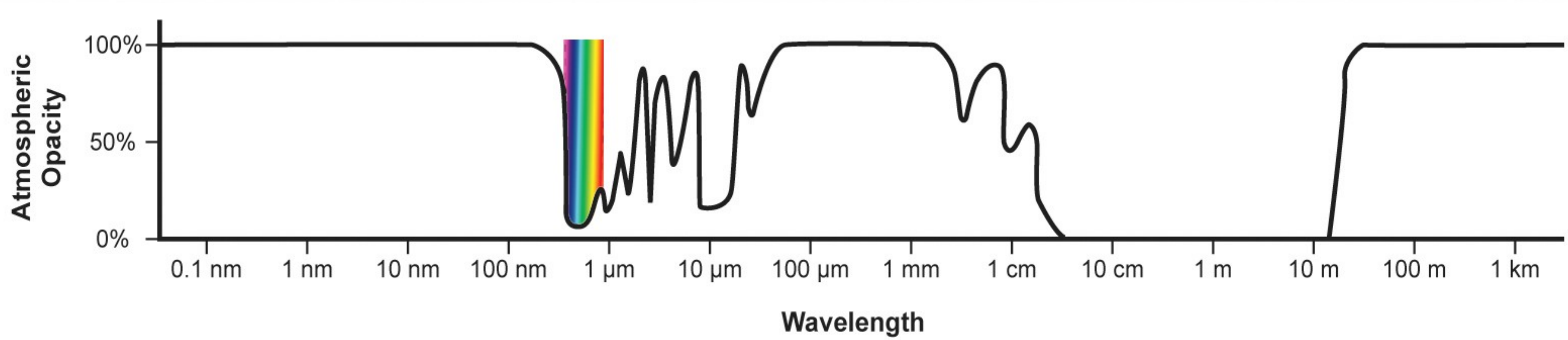

Infrared excess

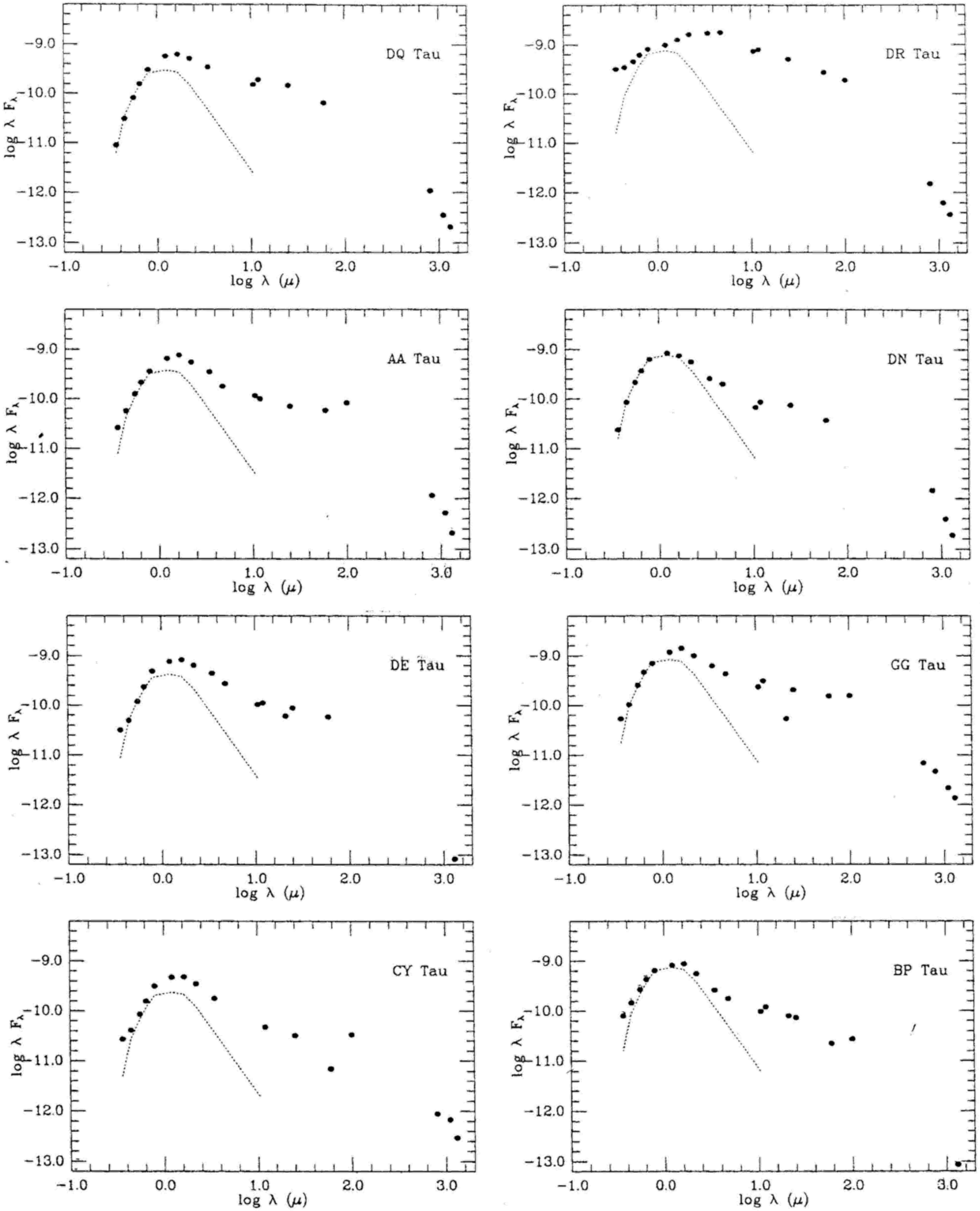

Spectral energy distribution
of T Tauri stars in
the Taurus molecular cloud

The vertical axes denote observed fluxes in erg/cm^2/s. The dotted curve denotes the SED for the WTTS LkCa7, which is a K7-M0 pre-main-sequence star that shows no evidence for accretion.

[from Kenyon & Hartmann, 1995]

Disk evolution

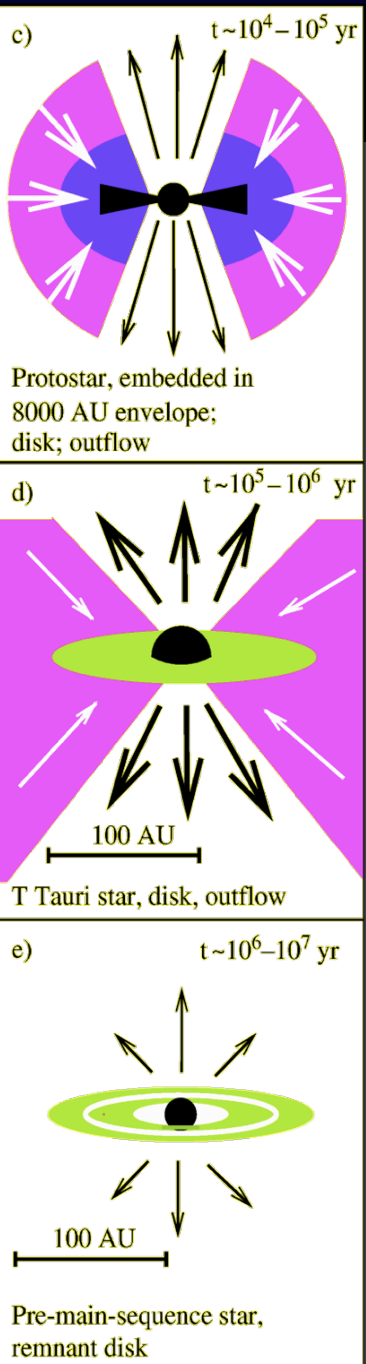

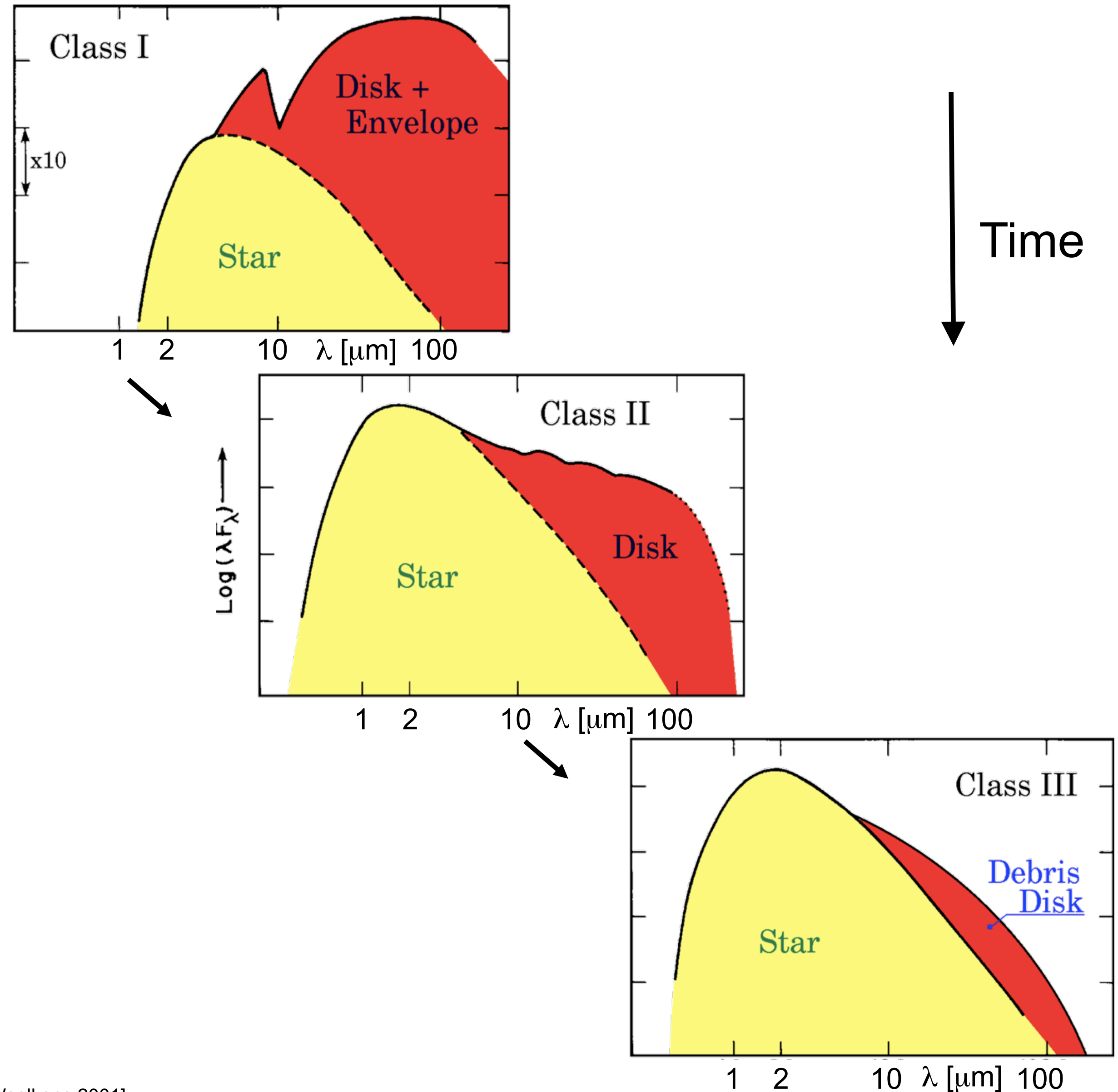

[from Waelkens 2001]

[from Lada 1987]

Disk classification

Classification scheme:

Based on spectral index *s* of the reemitted radiation in the wavelength range: 2-50μm / 100μm (Lada & Wilking 1984, Lada 1987):

$$\nu F_\nu = \lambda F_\lambda \sim \lambda^s$$

- *Class 0 (Andre et al. 1993)*
  - *Emission mainly in the submm wavelength range*

- **Class I**
  - s > 0 (flux increases with wavelength)
  - Deeply embedded objects
  - SED dominated by reemission of infalling envelope

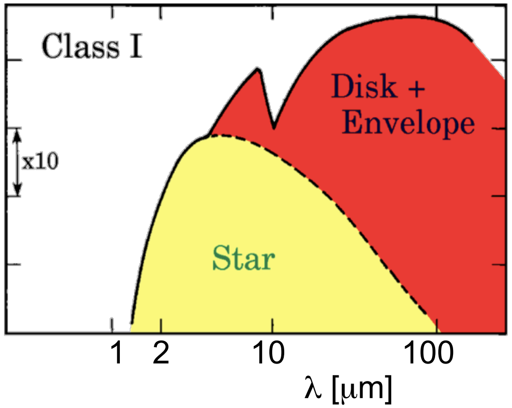

Disk classification

- **Class II**
  - -4/3 < s < 0
  - SED of the circumstellar disk (heating by star / accretion)
  - Disk optically thick
  - Observables inclination-dependent

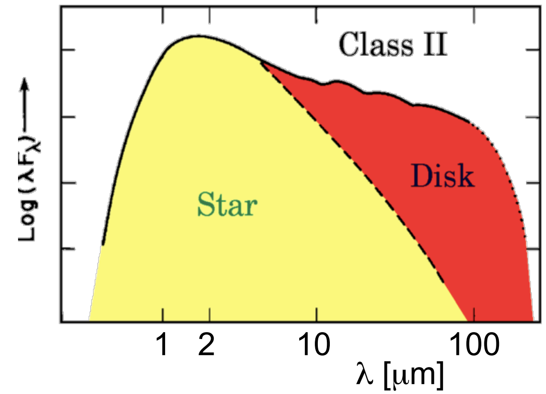

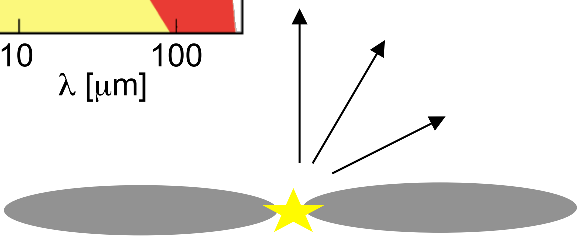

SED = f (inclination) !

- **Class III**
  - s ~ -3
  - Stellar photosphere (Rayleigh-Jeans Limit)
  - Infrared excess negligible
    - Disk evaporation / Accretion

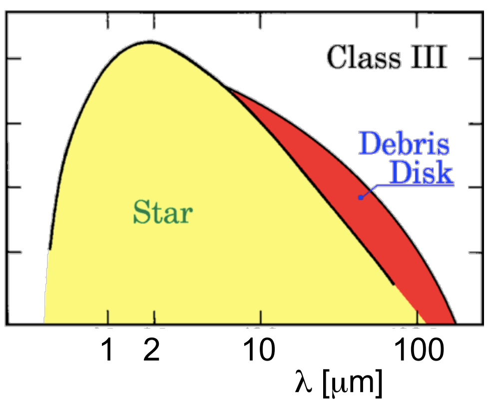

Heating of the disk: Energy sources

- **Stellar heating**
  - **Absorption** + Scattering of the stellar radiation (UV – near-infrared range)
    => Resulting dust temperature
    ~ 10 K (outer disk) … >10^3 K (inner disk boundary)
  - Reemission at near-infrared to millimeter wavelengths (Wien's law)

- **Accretion** *)
  Important:
  - During early disk evolution
  - Inside ~ 10 R_*

*) *see Appendix for an introduction to the physics of accretion*

- Terms:
  - **Passive Disk**: Stellar radiation dominates *(Adams et al. 1987)*
  - **Active Disk**: Accretion dominates *(Lynden-Bell & Pringle 1974)*

[First step] Basic SED analysis

<u>Assumption:</u>

Geometrically thin disk

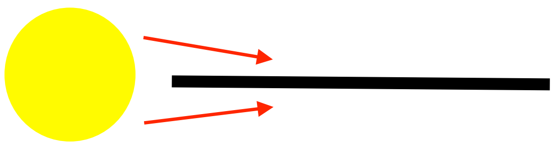

L_*, R_*

<u>Problem:</u>

Infrared excess*)
derived for this model is lower than observed

*) near-infrared – mm flux ”above” the stellar photosphere

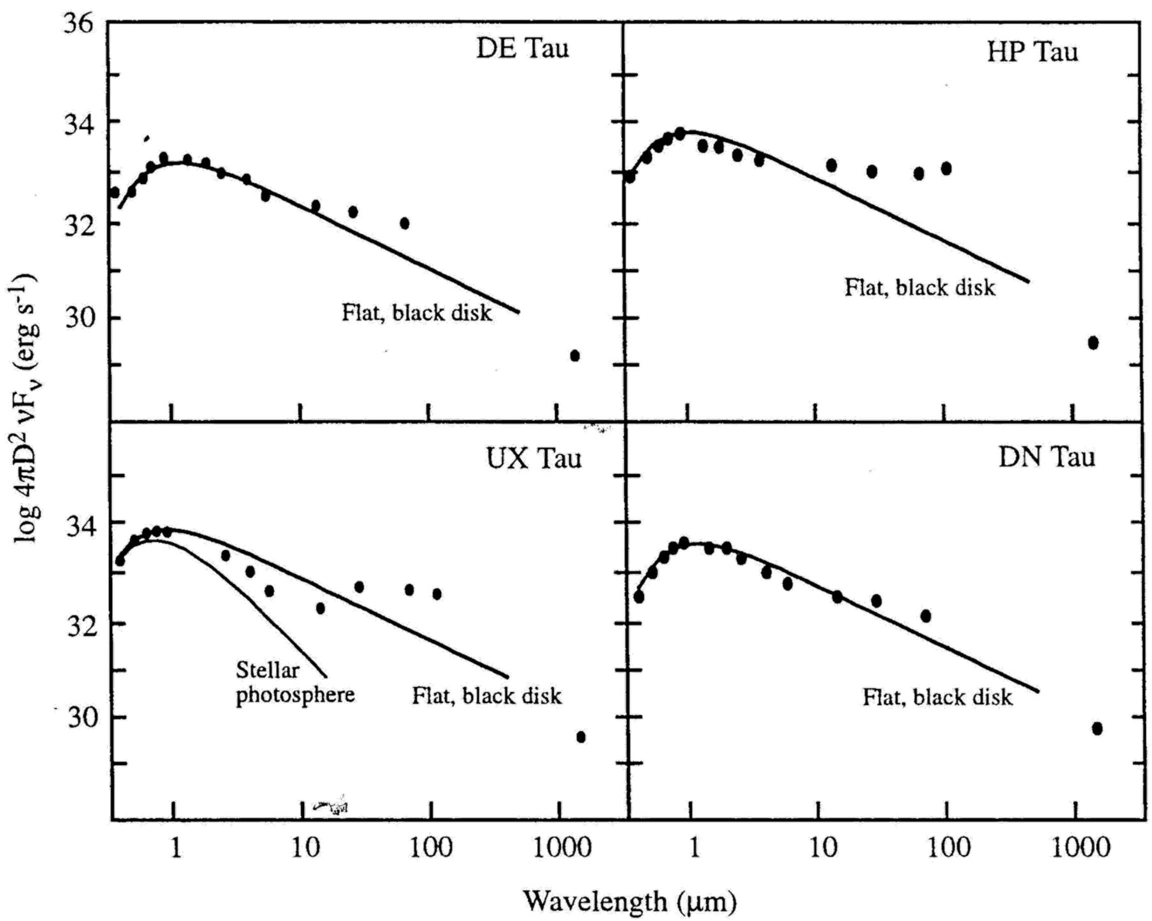

Figure 5. Observed spectral energy distributions are plotted on calculations of SEDs using the flat, black disk model. In general, the actual SEDs have more excess infrared radiation than predicted by the flat disk model. [from Beckwith, 2000]

[First step] Basic SED analysis

Vertical disk structure => “Disk flaring” (Kenyon & Hartmann 1987)

e.g.

- $T(r) \sim r^{-3/4}$
  (flat disk – Accretion or stellar heating)

- Gravitational potential dominated by central star

$$E_{vert} \sim -(z/r)\ G M_* / r \sim k\,T(r)$$

- Scale height: $\boldsymbol{h_{scale}(r)} \sim k / (G M_*)\ \boldsymbol{r^{5/4}}$

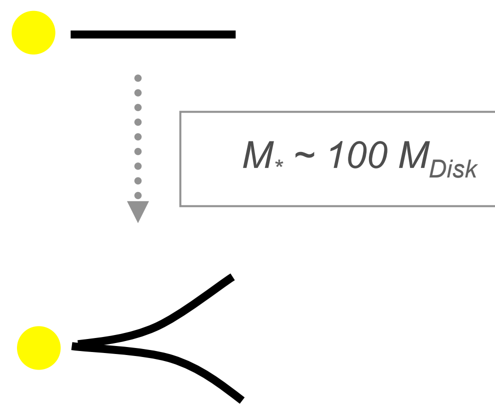

$\Rightarrow$ **Increase of the vertical disk size with radius**
“Disk flaring”

[First step] Basic SED analysis

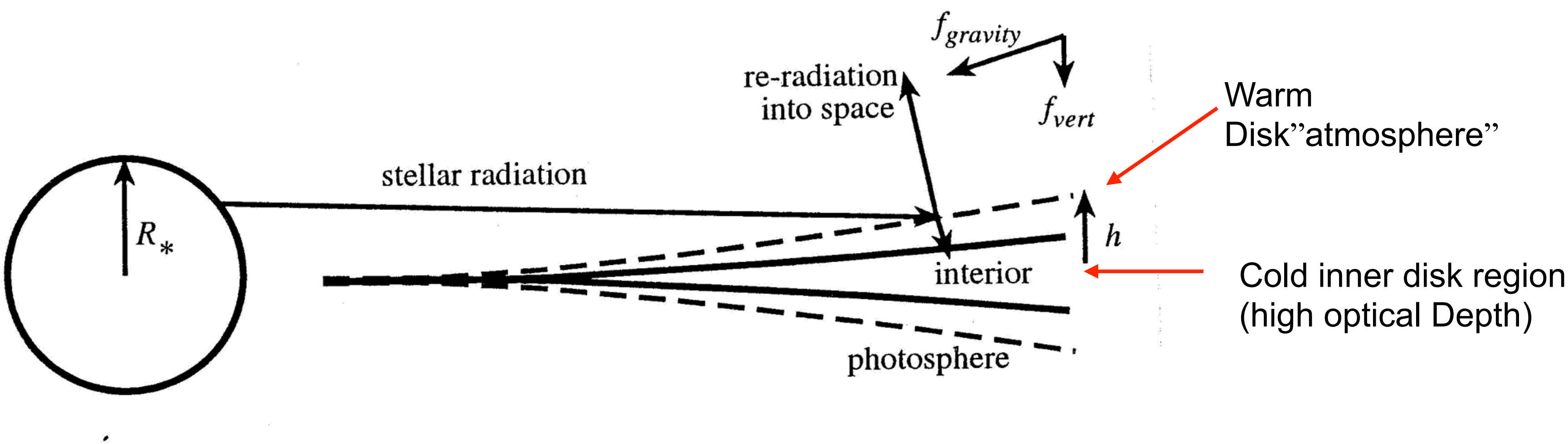

Figure 6. The flaring of a disk occurs naturally for a disk in hydrostatic equilibrium. The disk mass is assumed to be negligible; gravity from the star acts to keep the material in a plane. The scale height of the disk increases with radius, because the thermal energy decreases more slowly than the vertical gravitational energy as radius increases. The vertical gravitational force, f_{vert}, is shown as a component of the stellar gravitational force, $f_{gravity}$. The ray from the star shows the point at which short wavelength stellar radiation from the star is absorbed in the disk photosphere. The two other rays from this point show how the energy is reradiated into space and into the interior of the disk, thus heating the interior from the above.

[from Beckwith, 2000]

Flaring => Star can illuminate / heat disk more efficiently

[First step] Basic SED analysis

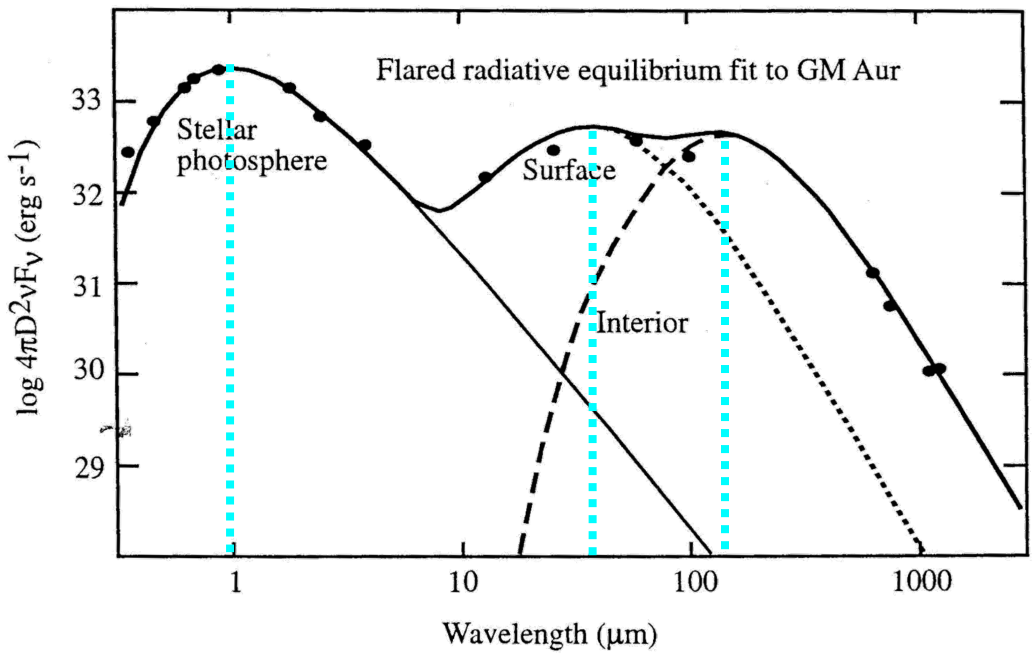

Figure 7. Figure 8 from Chiang and Goldreich (1997) showing how a flared disk with a photosphere reproduces one SED that differs substantially from a flat, black disk. They need a hole in the inner disk to account for the lack of disk emission short ward of about 5 μm.

[from Beckwith, 2000]

Simple 3 component SED

Inclination dependence:

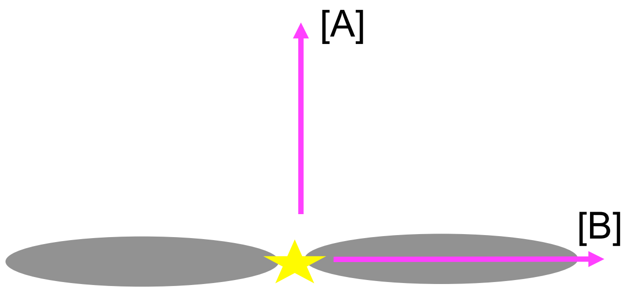

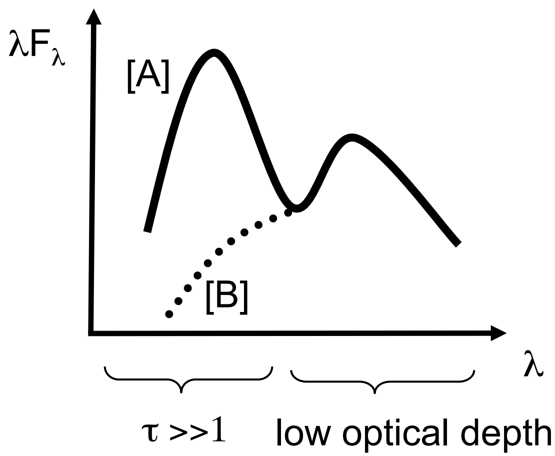

SED analysis: Next steps

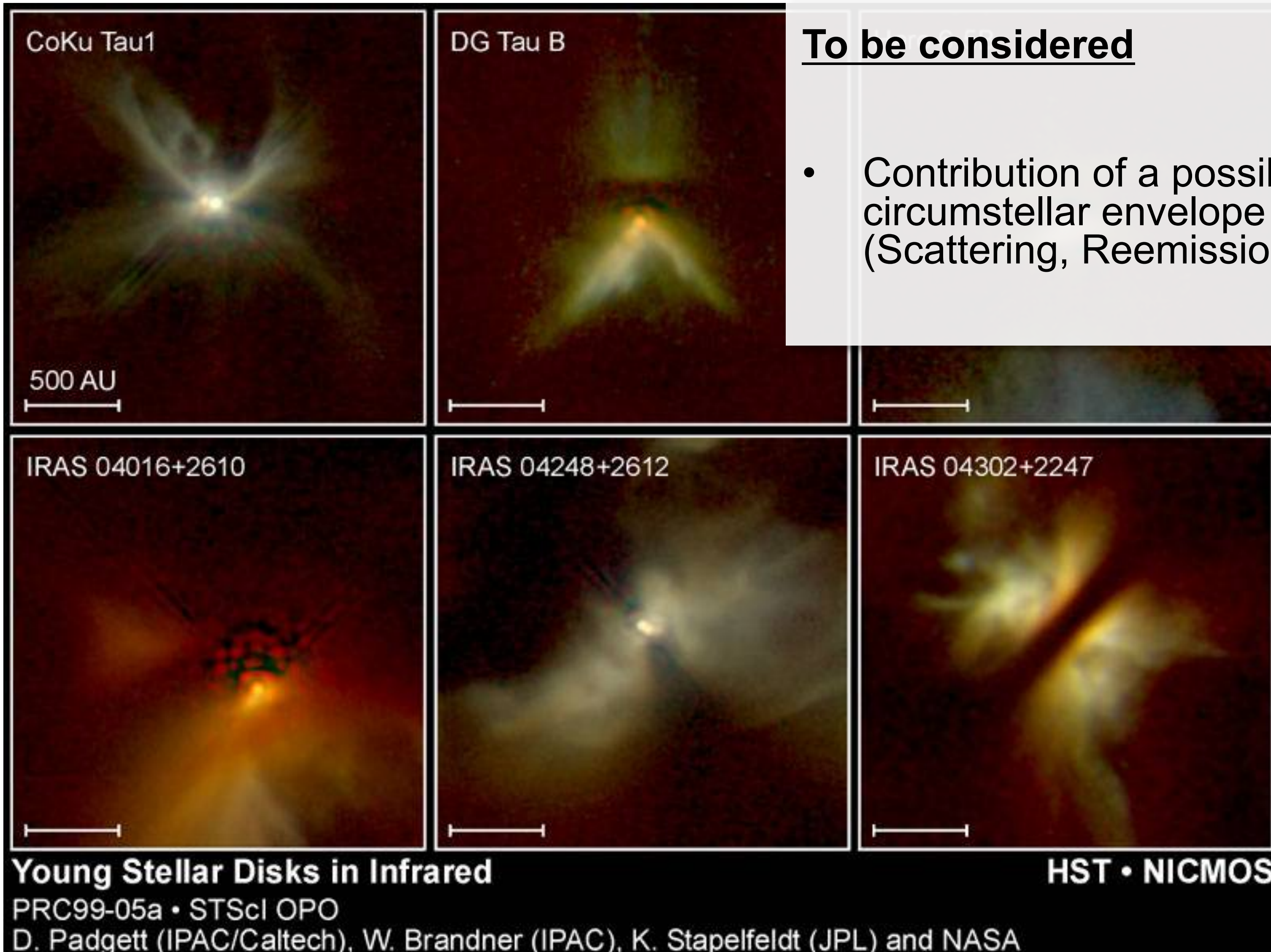

<u>To be considered</u>

- Contribution of a possibly remaining circumstellar envelope (Scattering, Reemission, Absorption)

SED analysis: Next steps

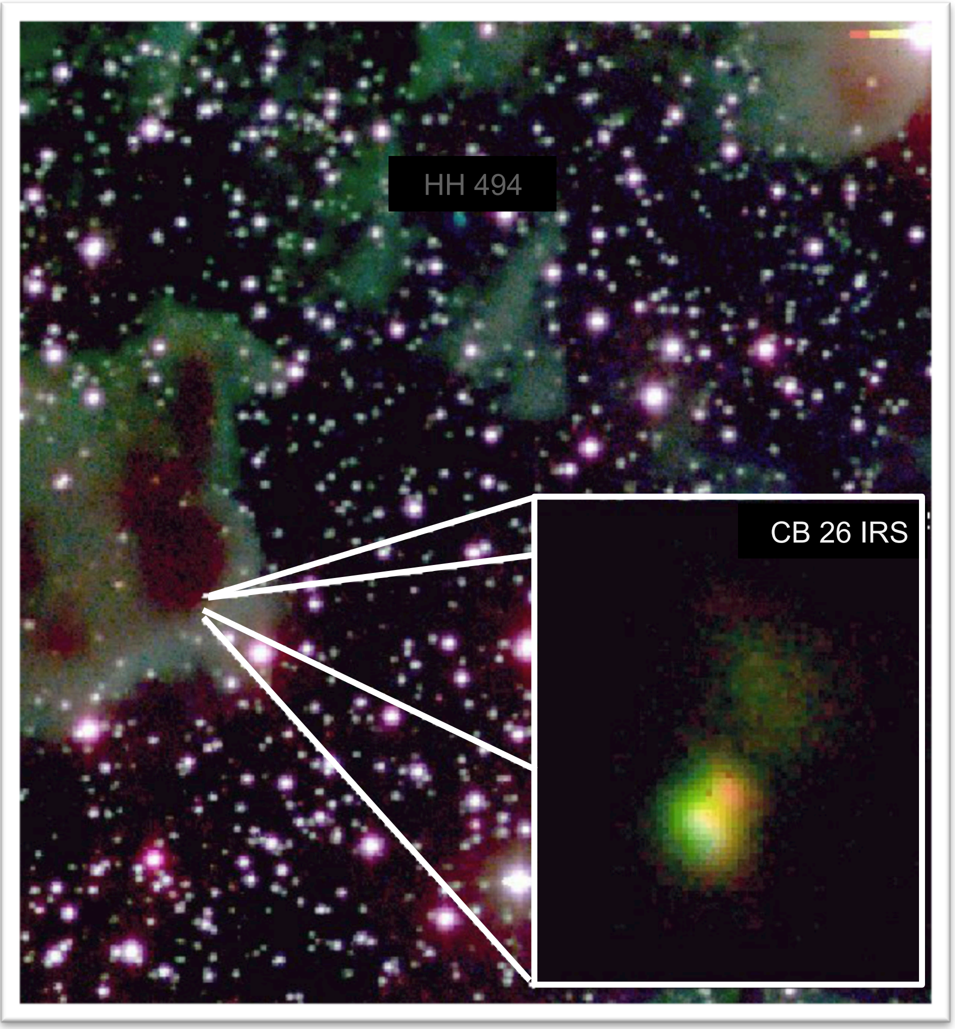

[courtesy of R. Launhardt]

To be considered

- Contribution of a possibly remaining circumstellar envelope (Scattering, Reemission, Absorption)
- Significant foreground extinction (wavelength-dependent!);

  Interstellar Polarization

SED analysis: Next steps

Analysis of individual features

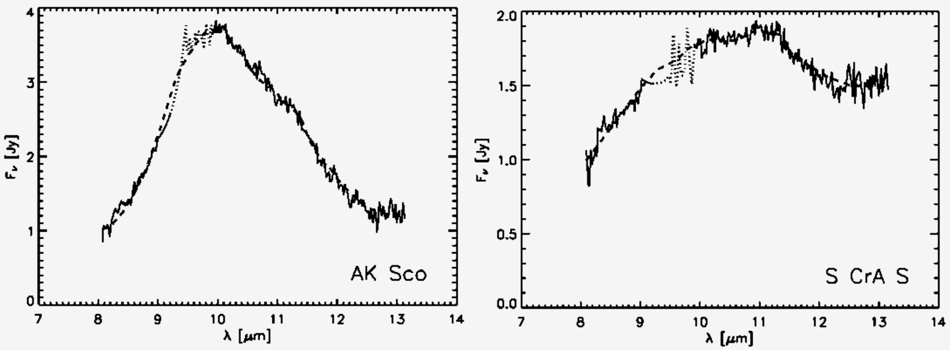

8-13micron spectra of 27 <u>T Tauri stars</u>

based on surveys by Przygodda et al. (2003) and Kessler-Silacci et al. (2004) using TIMMI2/3.6m, LWS/Keck

[Schegerer, Wolf, et al., 2006]

Prominent Example: ~10μm Silicate Feature

Size + Shape, Chemical Composition

Crystallization degree of Silicate grains

⇒ **Grain Evolution**

⇒ **Physical Conditions**

<u>To be considered</u>

- Contribution of a possibly remaining circumstellar envelope (Scattering, Reemission, Absorption)
- Significant foreground extinction (wavelength-dependent!);

  Interstellar Polarization
- Dust characteristics (constraints from emission/absorption features)

SED analysis: Next steps

Analysis of individual features

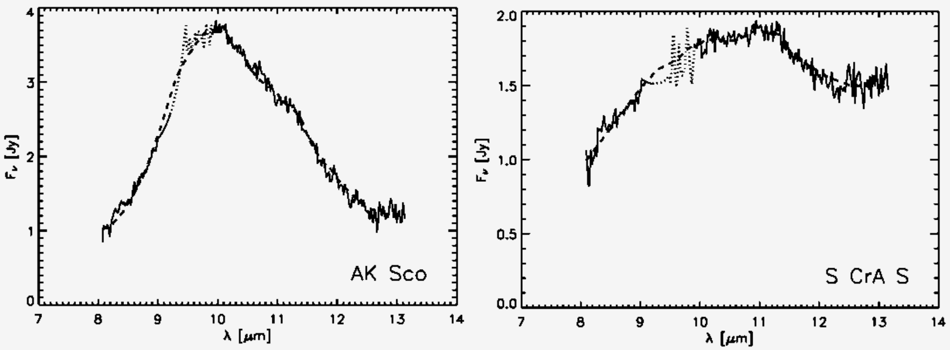

8-13micron spectra of 27 T Tauri stars

based on surveys by Przygodda et al. (2003) and Kessler-Silacci et al. (2004) using TIMMI2/3.6m, LWS/Keck

[Schegerer, Wolf, et al.. 2006]

Prominent Example: ~10μm Silicate Feature

Size + Shape, Chemical Composition

Crystallization degree of Silicate grains

$\Rightarrow$ **Grain Evolution**

$\Rightarrow$ **Physical Conditions**

To be considered

- Contribution of a possibly remaining circumstellar envelope (Scattering, Reemission, Absorption)
- Significant foreground extinction (wavelength-dependent!);

  Interstellar Polarization
- Dust characteristics (constraints from emission/absorption features)
- Characteristics of the illuminating / heating sources:
  - Spectrum of stellar photosphere
  - Accretion
  - Single star vs. binary

SED analysis: No unique results

SEDs can be well reproduced, but not unambiguously

=> Information about the spatial brightness distribution required

Goals:

- Constraints for spatial structure of disks
  (e.g., inner / outer radius, radial scale height distribution)
- Constraint for spatial distribution of
  - Dust parameters (composition, size)
  - Gas phase composition (+ excitation conditions)

Note:

Appearance of a circumstellar disk is determined by *both,*

its **Structure** (density distribution) and **Dust properties**

Thamm et al. 1994, A&A 287, 493,
"Ambiguities of parameterized dust disk models for young stellar objects"

Goal: Finding the best fit for the SED of FU Ori, DN Tau;
(8 free parameters, Metropolis algorithm)

Result: "… In all cases [the authors] find a global ambiguity in acceptable fits."

A sanity check:

How can we be sure (without images), that YSOs have disks?

SED analysis: Disk mass

Continuum SED:

Warm Dust (only ~1% of total mass, but dominates opacity)

The flux density, F_ν, from an optically thin disk at distance, D, is:

$$F_\nu = \frac{1}{D^2}\int_{R_{min}}^{R_{max}} \underbrace{B_\nu\left[T(r)\right]\tau_\nu(r)2\pi r dr}_{}\,,$$

Disks are optically thin in the mm range

$$B_\nu \approx 2kT\nu^2/c^2$$

[Rayleigh-Jeans Limit]

$$\tau_\nu(r) = \kappa_\nu \Sigma(r)$$

κ_ν – mass opacity

$\Sigma(r)$ – Surface density

$$\Longrightarrow \quad F_\nu \approx \kappa_\nu \frac{2k\nu^2}{c^2 D^2}\int_{R_{min}}^{R_{max}} T(r)\Sigma(r)2\pi r dr$$

$$\approx \kappa_\nu \frac{2k\langle T\rangle \nu^2}{c^2 D^2} M_{dust}$$

<T(r)> - average temperature

$$M_{disk} = 0.03\, M_\odot \,\frac{F_\nu}{1\,\mathrm{Jy}}\left(\frac{D}{100\,\mathrm{pc}}\right)^2\left(\frac{\lambda}{1.3\,\mathrm{mm}}\right)^3\frac{50\,\mathrm{K}}{\langle T\rangle}\,\frac{0.02\,\mathrm{cm^2\,g^{-1}}}{\kappa_{1.3\,\mathrm{mm}}}.$$

<T(r)> = 50K

κ_ν ~ 0.02 (1.3mm/λ) cm^2/g

M_{Gas}/M_{Dust} = 100

Disk mass

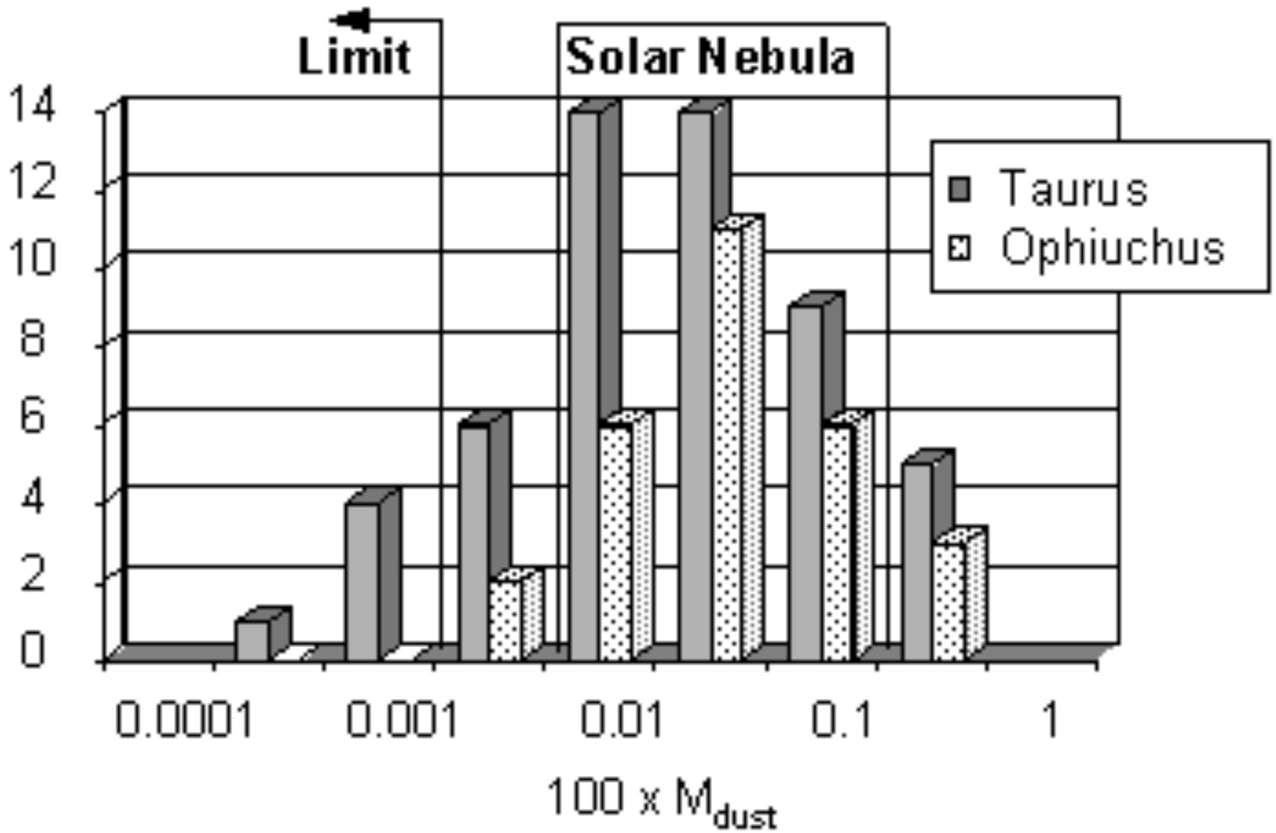

Typical disk mass:
~ 0.01 M_{sun}

Comparable to
"Minimum Mass Solar Nebula"
(Total mass of the material of solar composition from which the planetary system was built)

The histograms show the distribution of disk masses among stars in the Taurus and Ophiuchus star forming regions determined by Beckwith et al. (1990) and Andre et al. (1994).

[from Beckwith, 2000]

Opacity: Disks, no (spherical) shells

Problem:

Is the emitting dust really distributed in form of a *disk*?

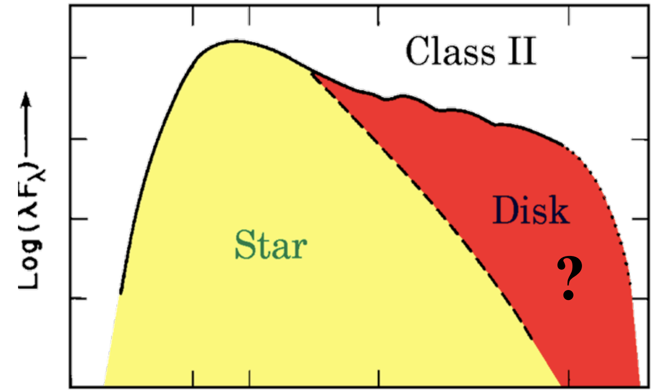

Argument #1

Millimeter observations / mm SED:

=> Disk mass (optically thin)

=> Optical depth under the assumption of spherical symmetry

=> high optical depth at near-IR wavelengths

=> T Tauri stars should be invisible in the near-IR)

=> Contradicts observations

another possible solution: Clumpy shell?

Argument #2

Observed SEDs can be well explained on the basis of disk models

… but: not unequivocally!

Indirect Evidence: Observations

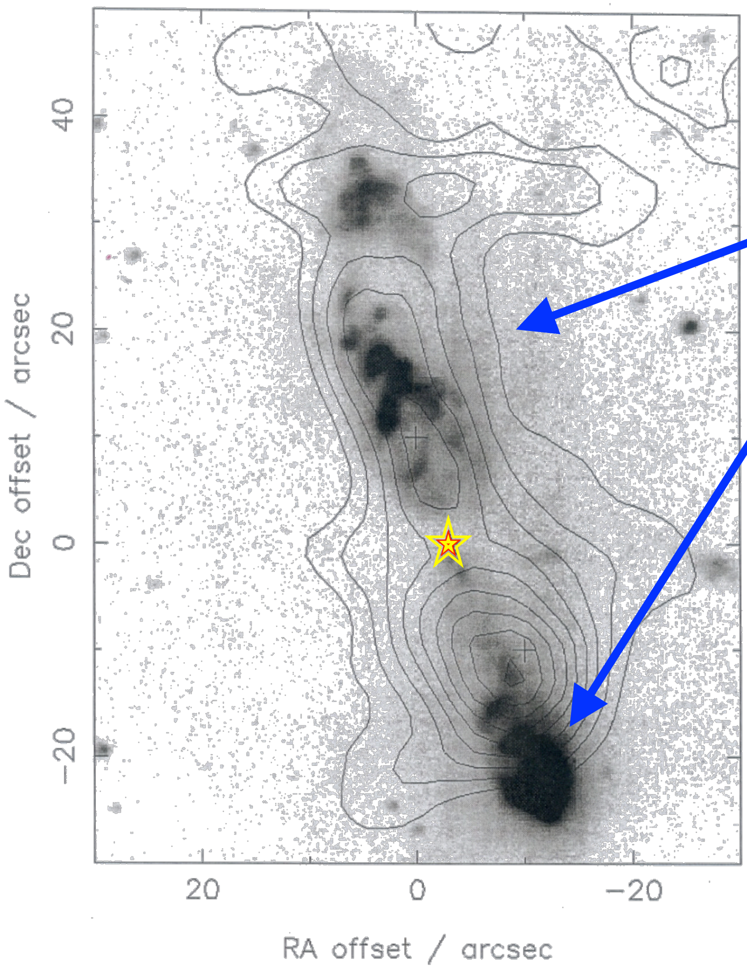

Fig. 1. Cep E ^{12}CO 4-3 map integrated from -33 to 14 km s^{-1} (contours) superimposed on continuum-subtracted H_2 2.12 μm image from Ladd & Hodapp (1997) (greyscale). Positions of CO bullet observations (to within 5″) are marked with crosses, and the driving source is marked with a star. Contours are every 30 K km s^{-1} from 60 K km s^{-1}.

[Hetchell et al. 1999]

1. **Bipolar molecular outflows**
   (weakly focussed)

2. **Jets**
   (highly focussed)

   Collimation

   => focussing processes on size scales <100 AU

3. **Polarization maps**
   (Light scattering)

Indirect Evidence: Observations

Outflows in the Orion star-forming region

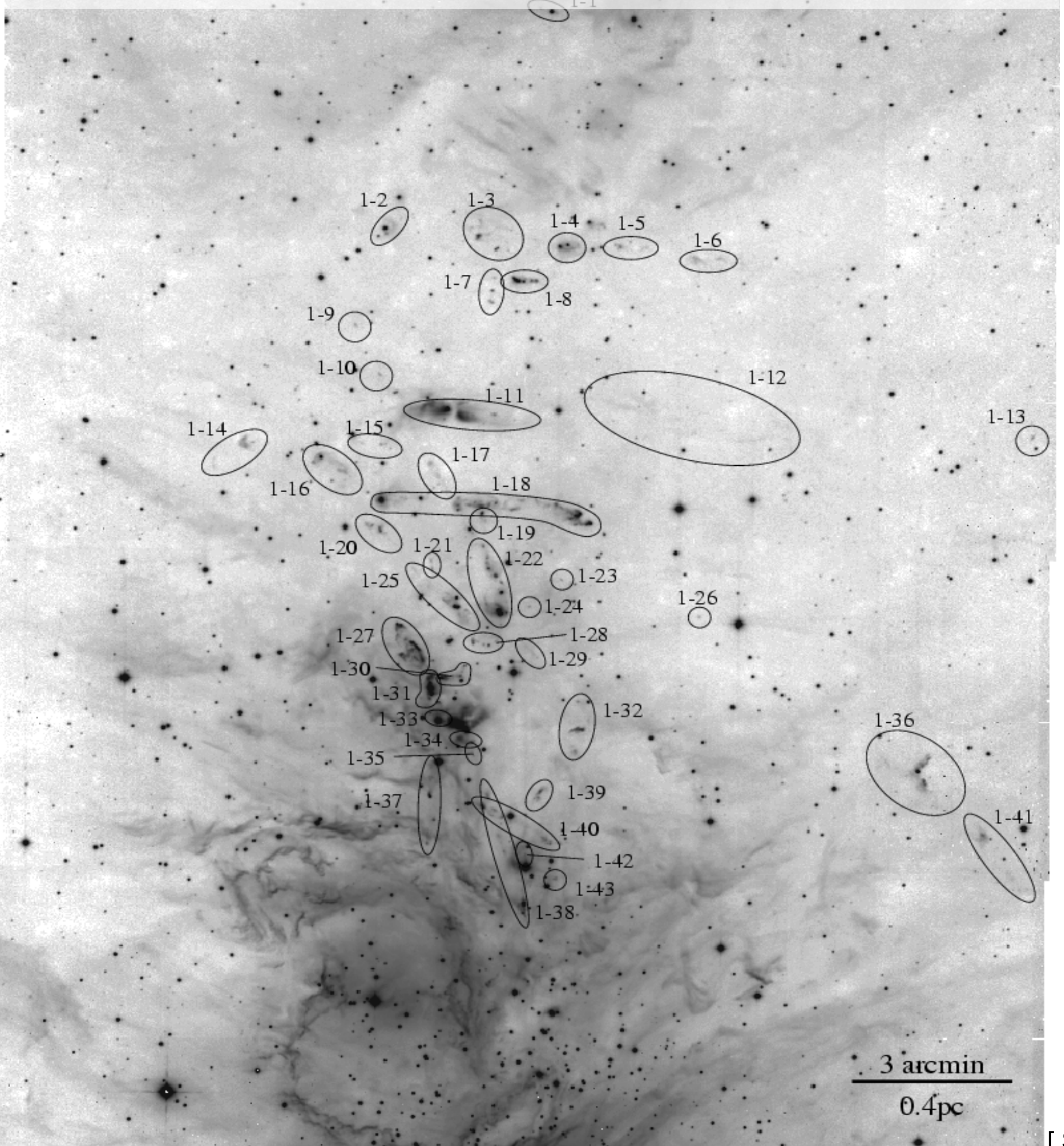

Bipolar molecular outflows
(weakly focussed)

Jets
(highly focussed)

Collimation
=> focussing processes on size scales <100 AU

Polarization maps
(Light scattering)

[Stanke et al. 2002]

Indirect Evidence: Observations

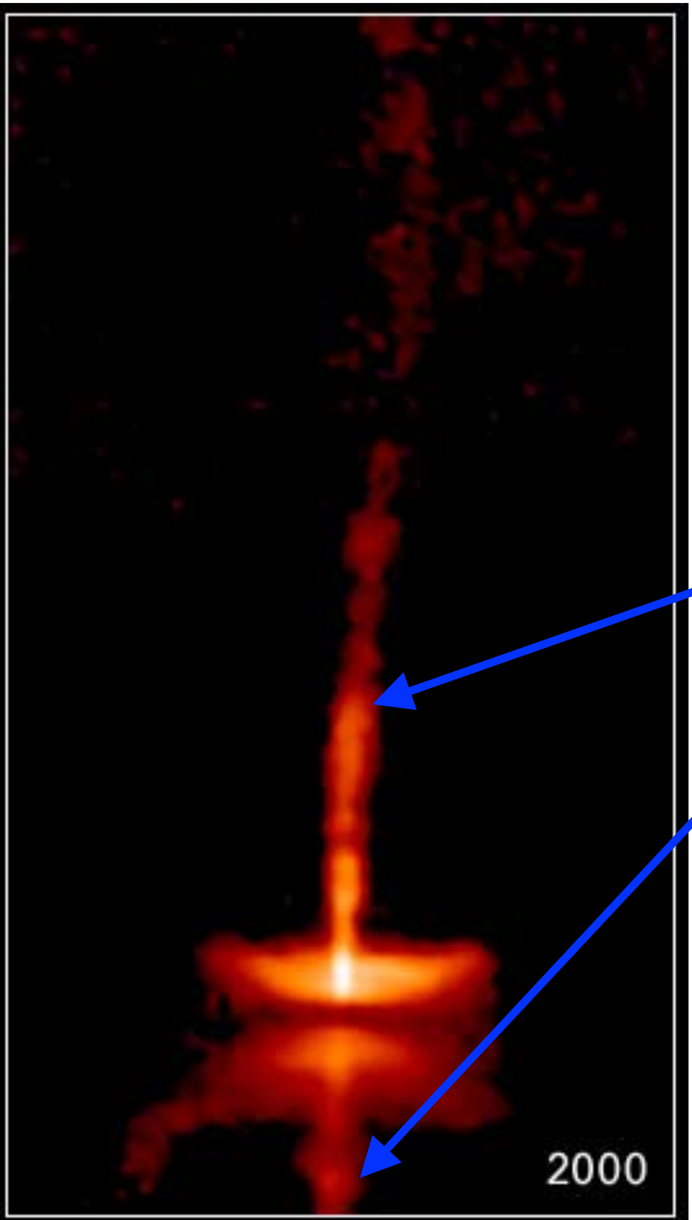

[HH30 jet, NASA/Watson 2000]

1. **Bipolar molecular outflows**
   (weakly focussed)

2. **Jets**
   (highly focussed)

   Collimation

   => focussing processes on size scales <100 AU

3. **Polarization maps**
   (Light scattering)

Indirect Evidence: Observations

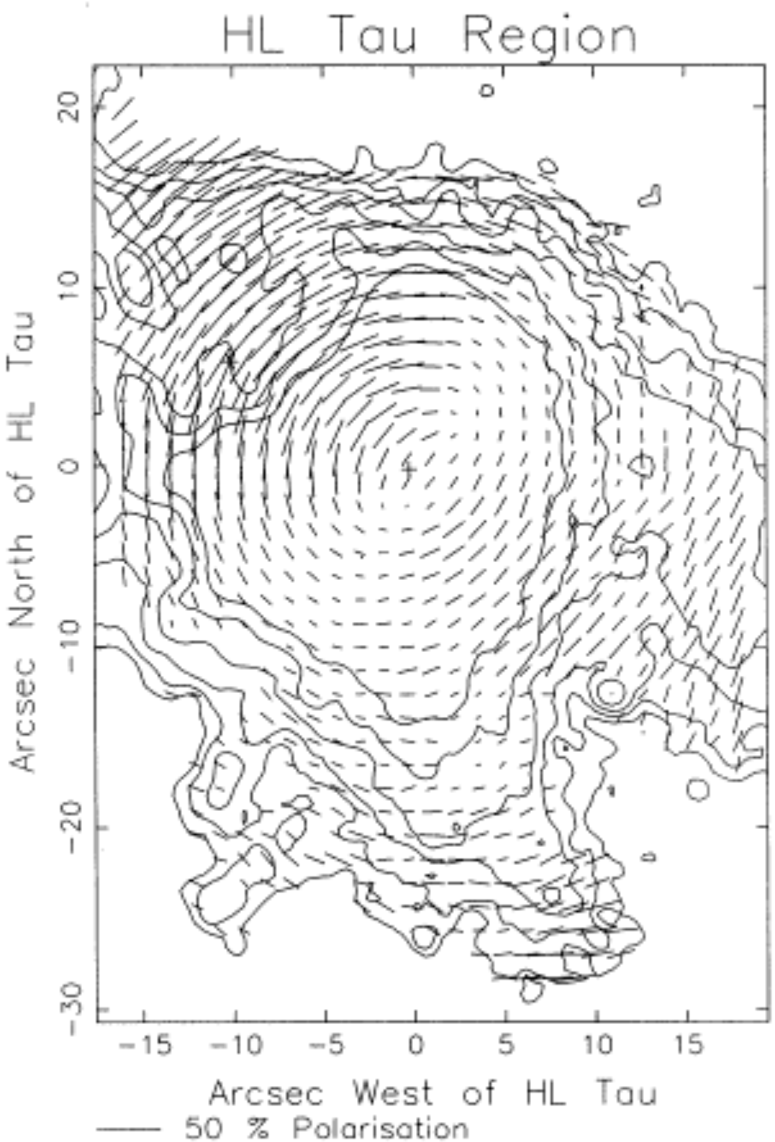

[Gledhill & Scarrott 1989]

1. **Bipolar molecular outflows**
   (weakly focussed)

2. **Jets**
   (highly focussed)

   Collimation

   => focussing processes on size scales <100 AU

3. **Polarization maps**
   (Light scattering)

Polarization maps

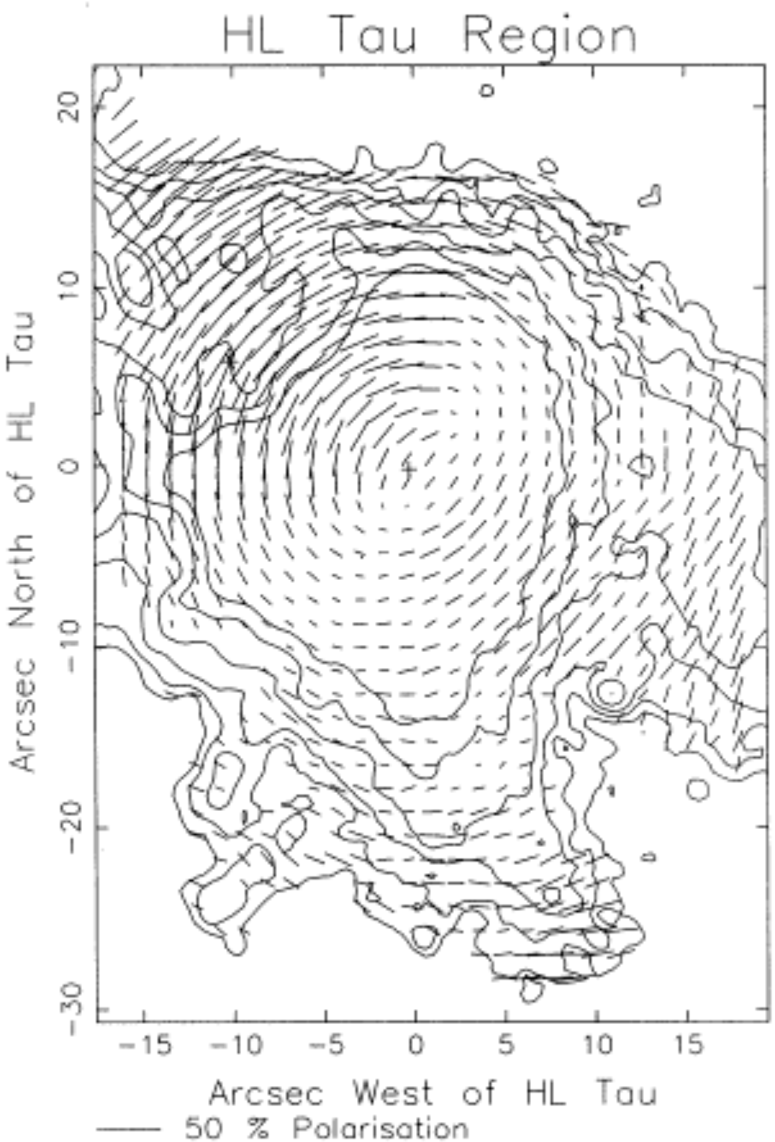

[Gledhill & Scarrott 1989]

<u>Polarization mechanisms</u>

1. **Scattering**

   Observed polarization patterns and degrees can be well explained without any limiting assumptions concerning grain shape or alignment (simple models: spherical grains)

2. **Dichroic Extinction**

   by aligned spheroidal or anisotropic particles

   - Efficient alignment mechanism required in order to explain the observed polarization degrees
   - Important for *interstellar* polarization (grain alignment by intergalactic magnetic field)

Polarization maps

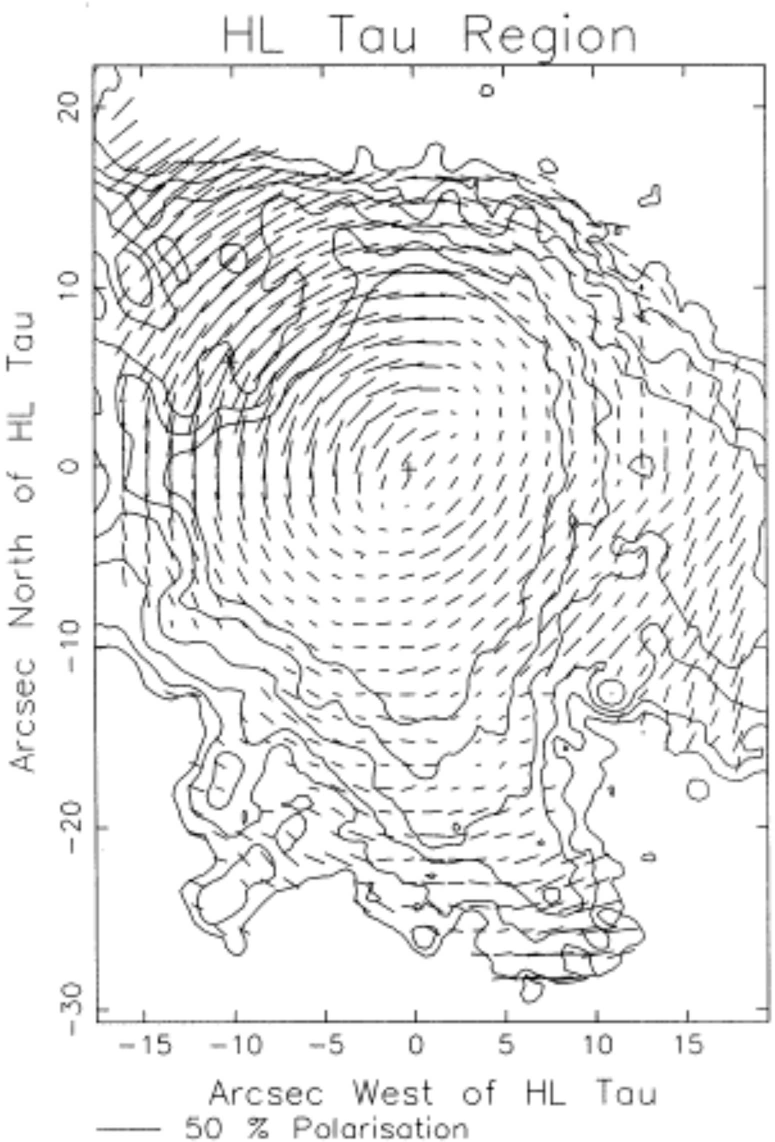

[Gledhill & Scarrott 1989]

Observed Polarization degree

- Particle size: a=5-250nm,

  n(a)~$a^{-3.5}$ (Mathis et al. 1977)

  => Large scattering cross section / Polarization in the optical / near-infrared wavelength range

- **ISM**

  P_{max} at 0.45 … 0.80 micron

  Young stellar objects

  Similar, but also at longer / shorter wavelengths

- Net polarization (optical/near-IR wavelength range) :
  - ISM < 5%
  - YSOs: often higher (e.g. HL Tau 12%, V376Cass: 21%)

Optical / Near-infrared Polarization

Spatially resolved polarization maps

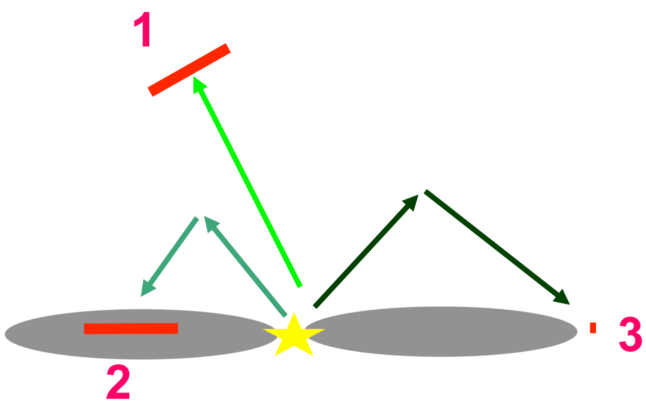

1) Single scattering in optically thin envelope
   => centro-symmetric polarization pattern; high polarization degree

2) Multiple scattering
   => Polarization vectors parallel to disk plane, low pol. degree

3) "Polarization nullpoints"
   Vanishing linear polarization at the edges of the disk

Optical / Near-infrared Polarization

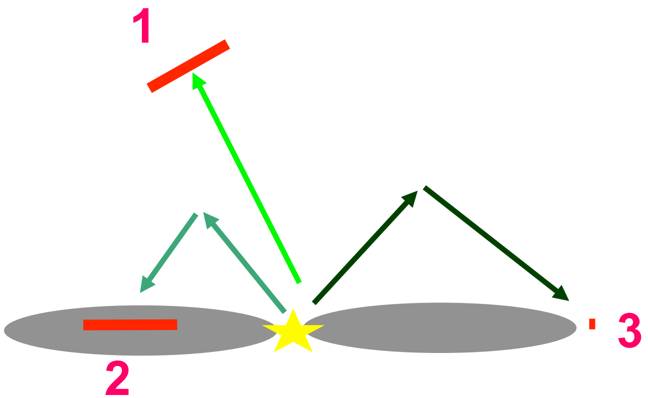

Polarisation degree depends on

- Wavelength
- Size, shape, chemical composition of the dust grains
- Dust density distribution

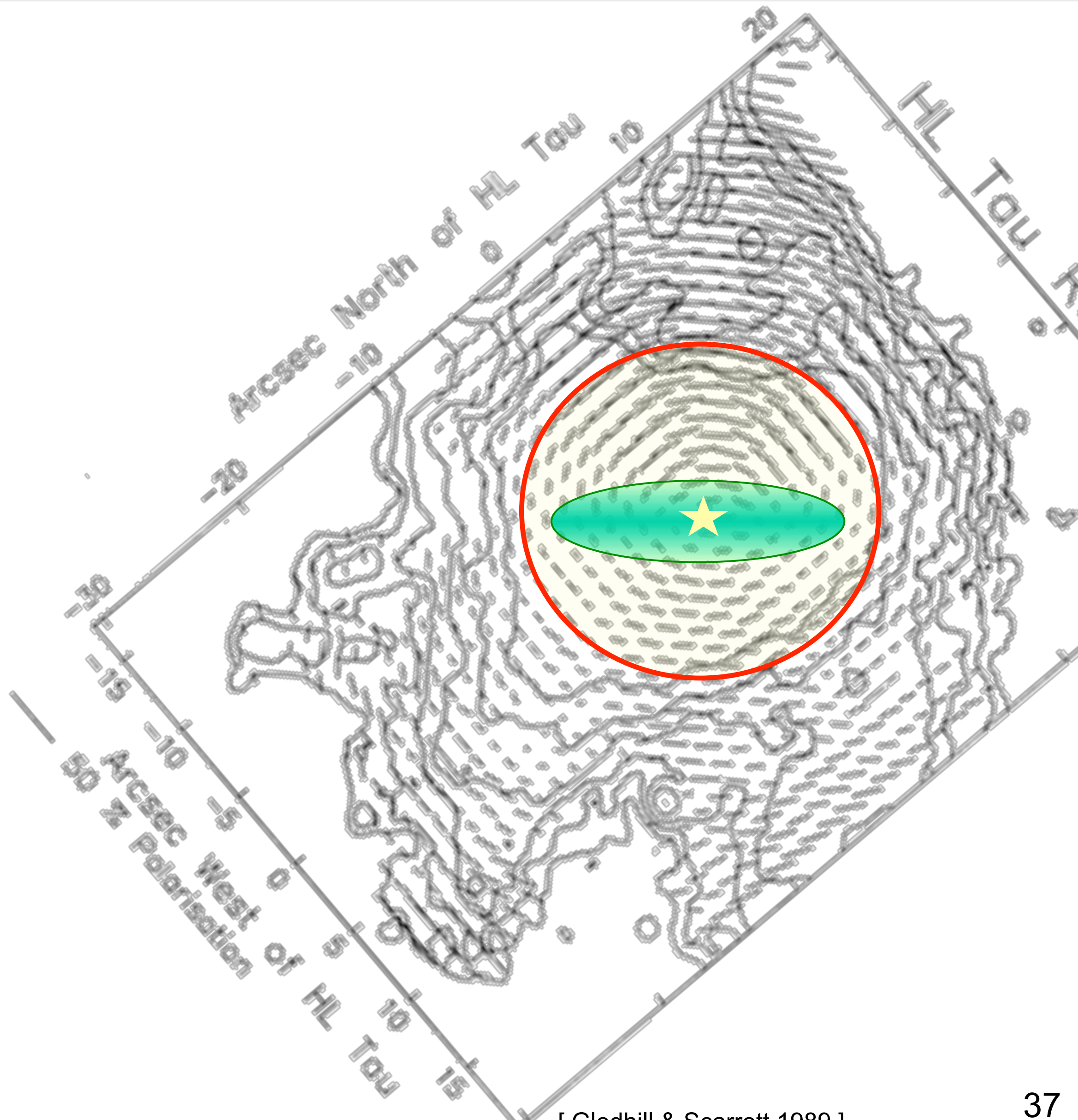

[Gledhill & Scarrott 1989]

High-angular resolution observations:

Spatially resolved images of disks

Edge-On Protoplanetary Disk
Orion Nebula

HST • WFPC2

PRC95-45c • ST ScI OPO • November 20, 1995
M. J. McCaughrean (MPIA), C. R. O'Dell (Rice University), NASA

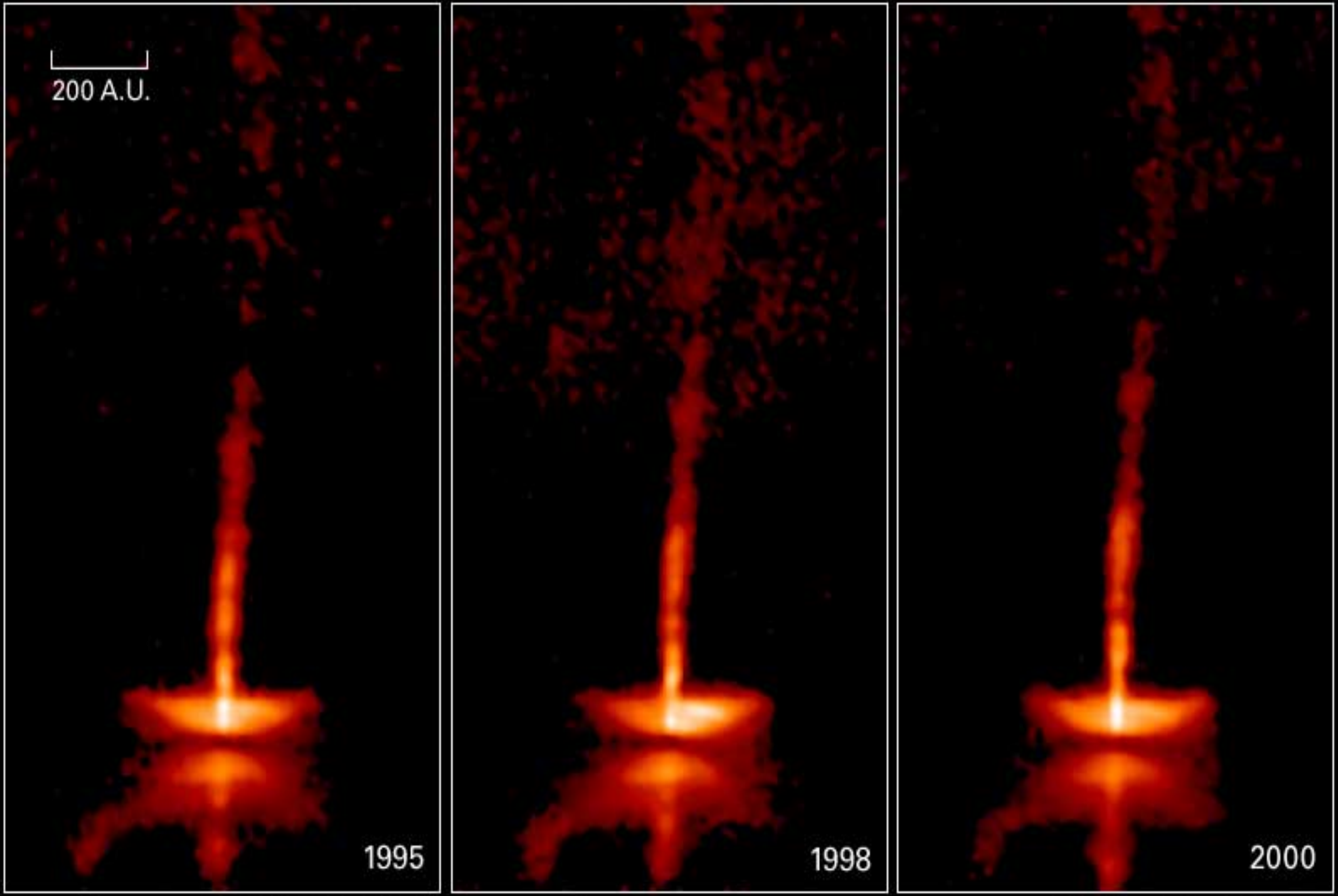

The Dynamic HH 30 Disk and Jet

HST • WFPC2

NASA and A. Watson (Instituto de Astronomía, UNAM, Mexico) • STScI-PRC00-32b

The Dynamic HH 30 Disk and Jet

HST • WFPC2

NASA and A. Watson (Instituto de Astronomía, UNAM, Mexico) • STScI-PRC00-32b

Observations over a wide wavelength range

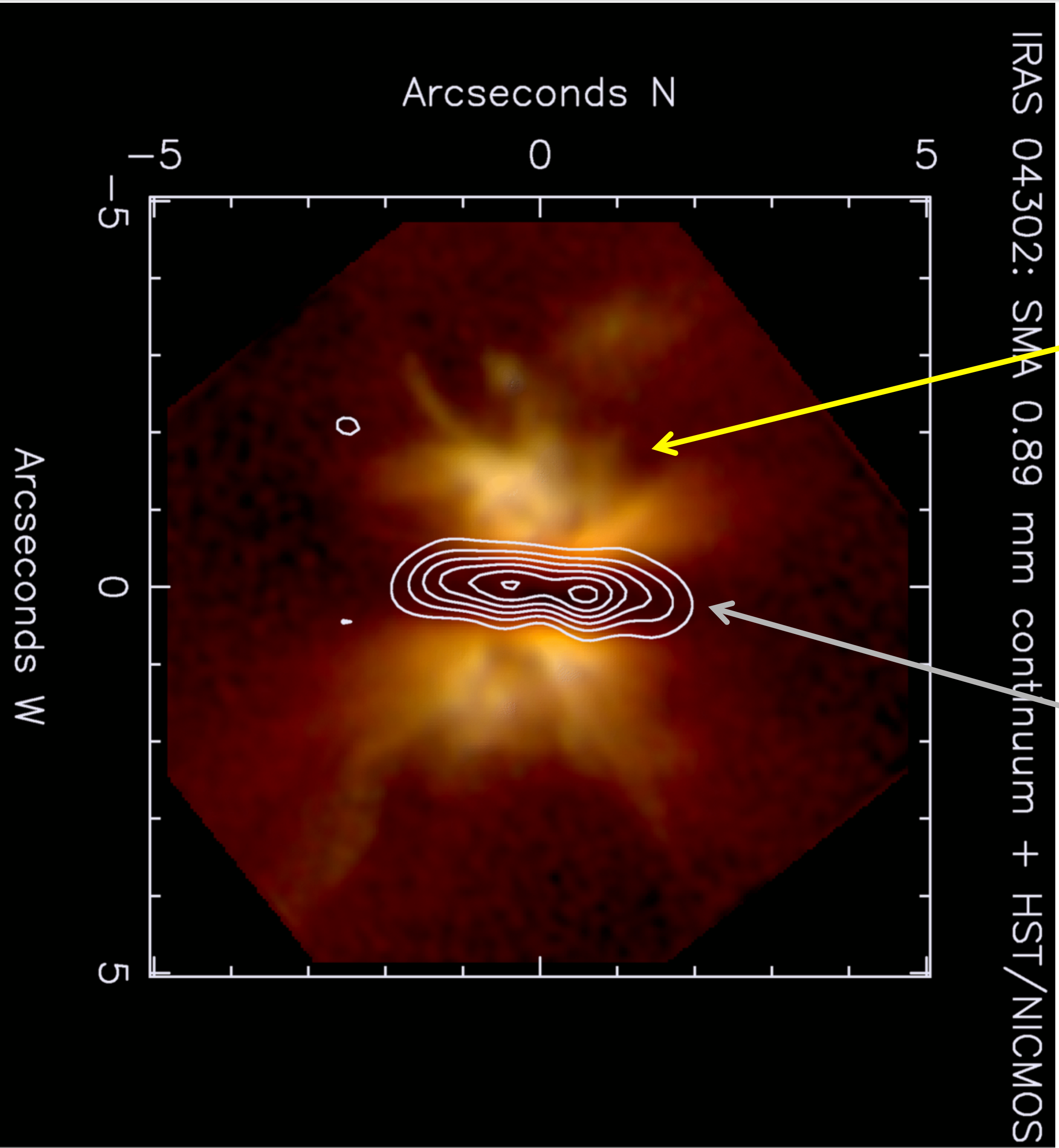

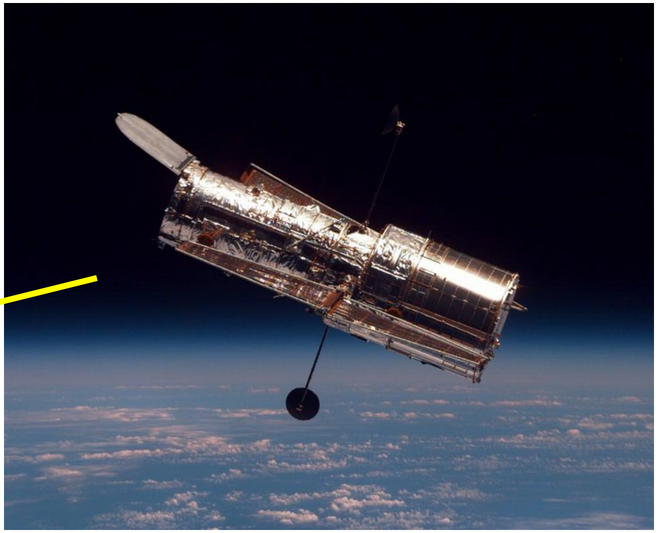

Near-infrared:
Hubble Space Telescope

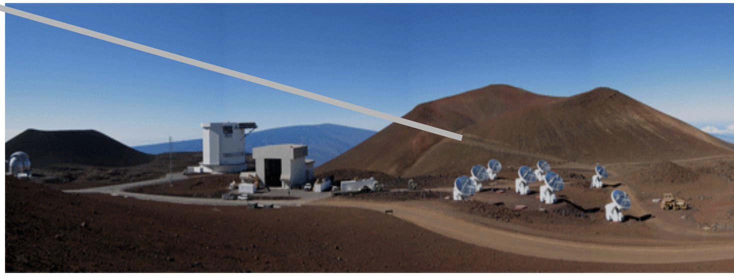

Submillimeter map:
Submillimeter Array (SMA)

[Wolf et al. 2008]

Resolved Circumstellar Disks

circumstellardisks.org

Catalog of Resolved Circumstellar Disks

Last updated: January 16 2007; maintained by Caer McCabe (JPL)

- What's new...
- Description of Catalog
- Contributing to the database

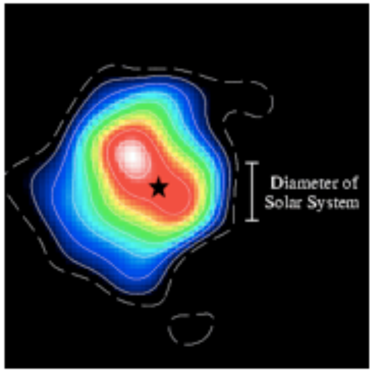

Total number of disks: 92 (Pre-Main Sequence disks: 79, Debris Disks: 13)

Object	SpTy	Category	Distance (pc)	R band (mag)	Disk Diameter (")	Disk Diameter (AU)	Inclination	How well Resolved	At ref. wavelength (micron)
2MASSI1628137-243139		TT	140	17.7	4.3	602	86	10.8	2.1
49 Cet	A1	Hae	61	5.6	0.8	48		3.9	10
AA Tau	M0	TT	140	11.8	1.34	187	75	1.0	2000
AB Aur	A0e	Hae	144	7.1	18	2592	21.5	367.4	0.57
AS 209	K5	TT	140	10.4	3.1	434	56	0.9	1300.39
ASR 41		TT	316		20	6320	80	97.0	2.2

Additional perspective on circumstellar disks:

Planet formation

Planet formation in a nutshell

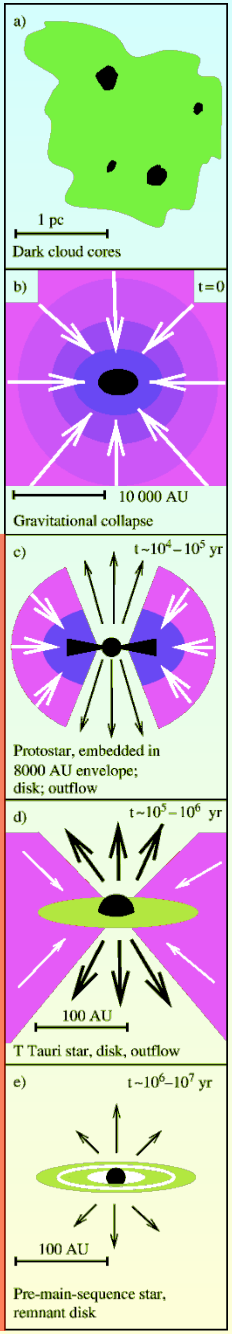

[Waelkens 2001]

Star Formation Process → Circumstellar Disks → Planets

Core Accretion – Gas Capture

(sub)µm particles

↓

cm/dm grains

↓

Planetesimales

↓

Planets (cores)

- Brownian Motion, Sedimentation, Drift
- Inelastic Collision → Coagulation

- Agglomeration;
  Fragmentation

- Gravitational Interaction: Oligarchic Growth

- Gas Accretion

Alternativ: Gravitational Instability → Giant Planet

The first phase of planet formation: The importance of multi-wavelength observations

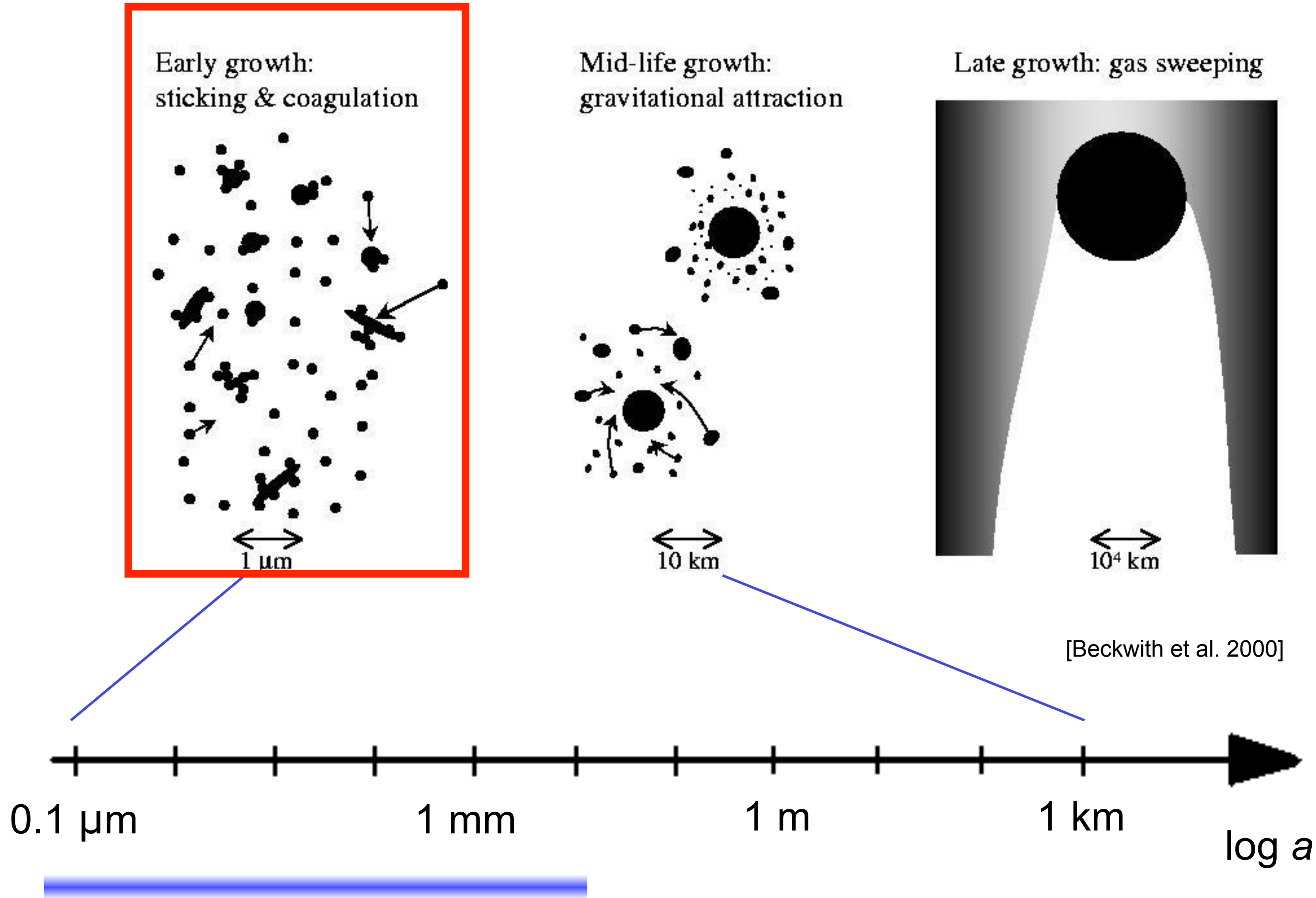

Particle size

$\simeq$

Observing wavelength

The first phase of planet formation: The importance of multi-wavelength observations

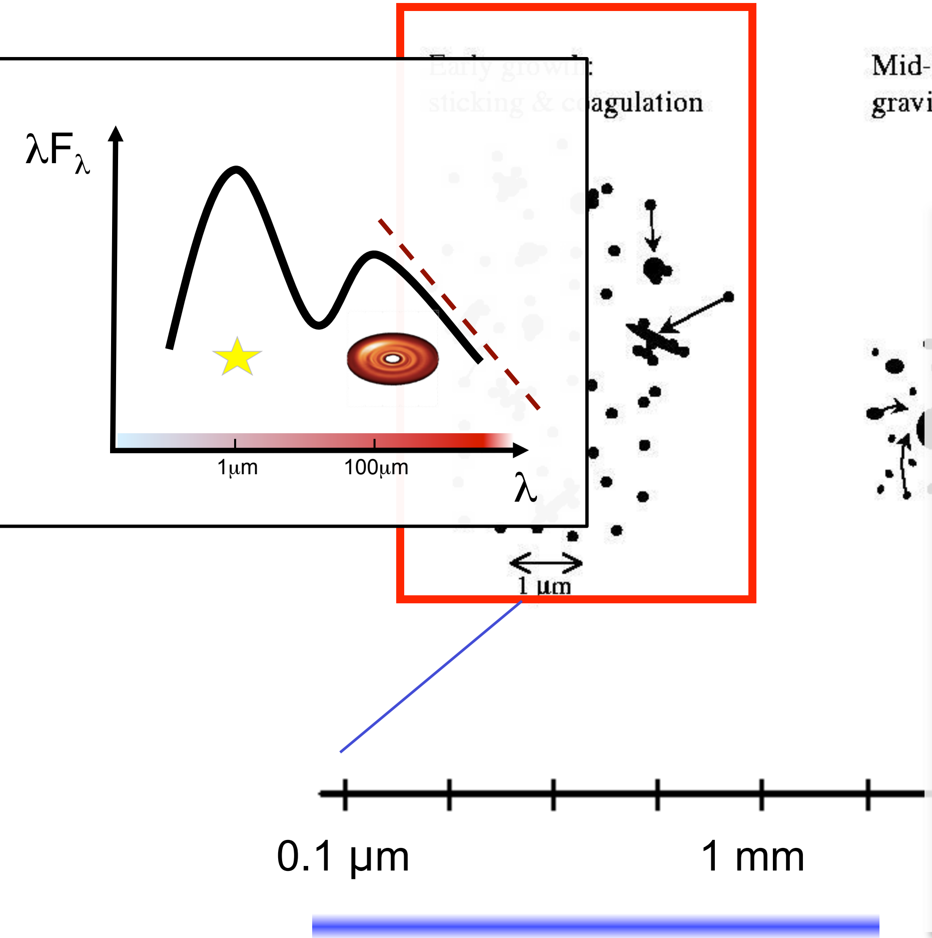

- Spectral Energy Distribution (SED)
  (sub)mm slope:

  $$F_\nu \sim \kappa_\nu \sim \lambda^{-\beta}$$

- Scattered light polarization
- Dust emission/absorption features
- Multi-wavelength imaging

+ Radiative Transfer Modelling

Particle size
≃
Observing wavelength

Interferometry

[Exemplary Telescopes]

VLTI

SMA

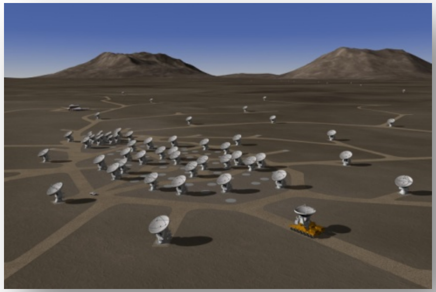

ALMA

IRAM

Keck Interferometer

VLA

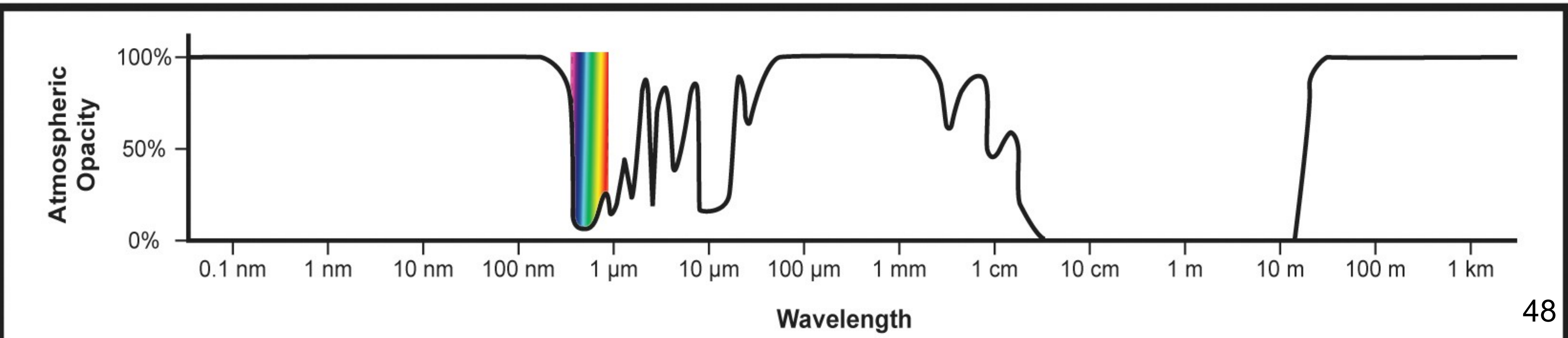

Various wavelengths – Various disk regions

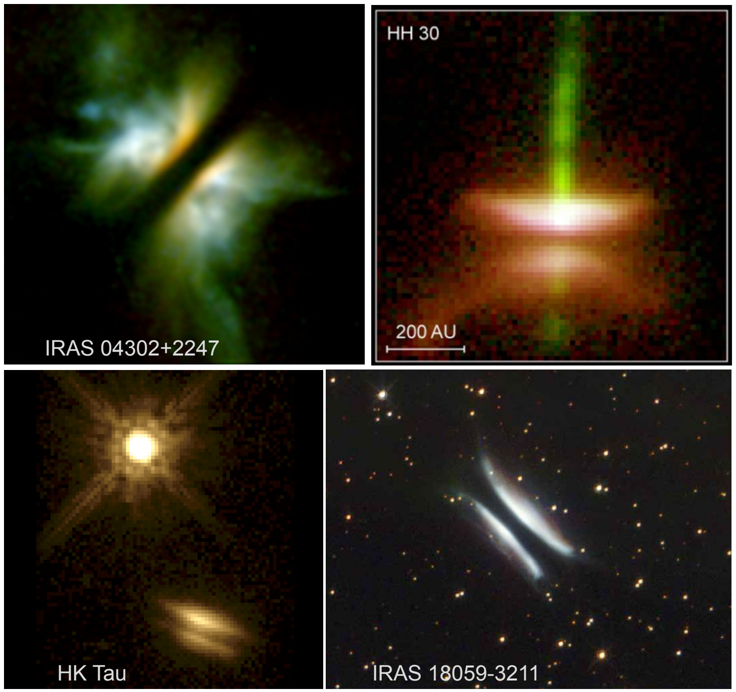

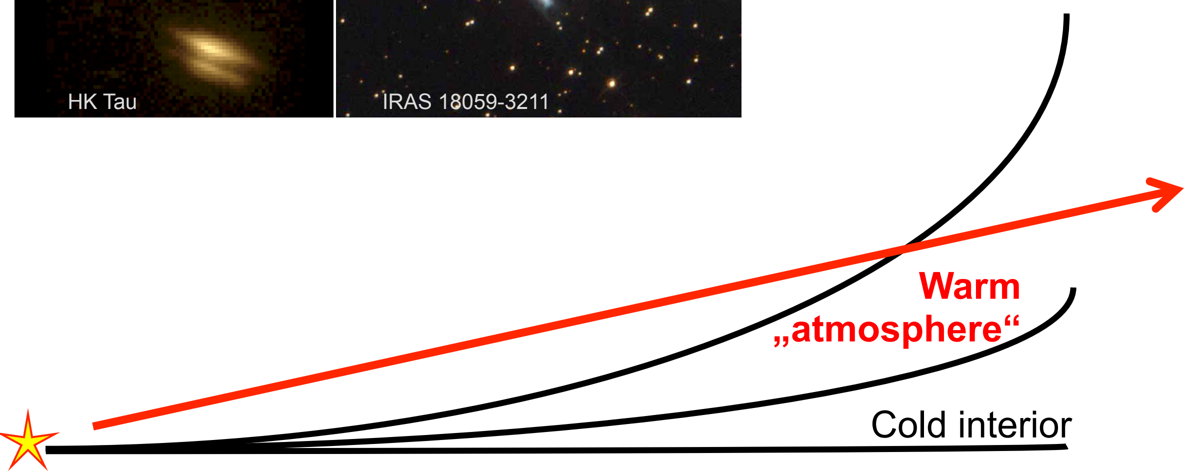

Edge-on disks

Optical / IR

Wavelength-dependence of the apparent *vertical* extent of the disk

⇒ *Vertical opacity structure*

⇒ *Constraints on grain size in upper disk layers (dust settling?)*

Approximate (dust) disk size

Disk flaring

Various wavelengths – Various disk regions

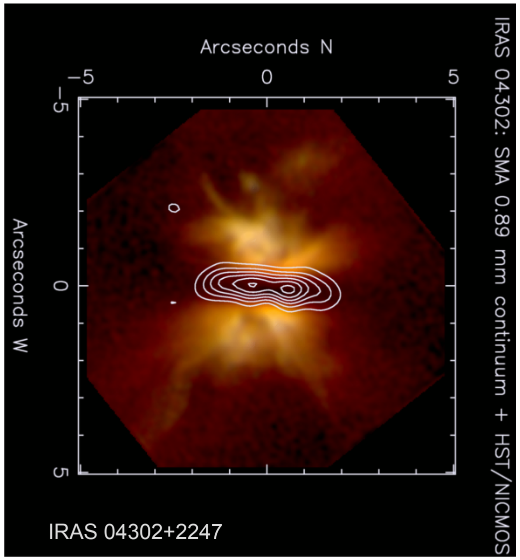

[Wolf et al. 2008]

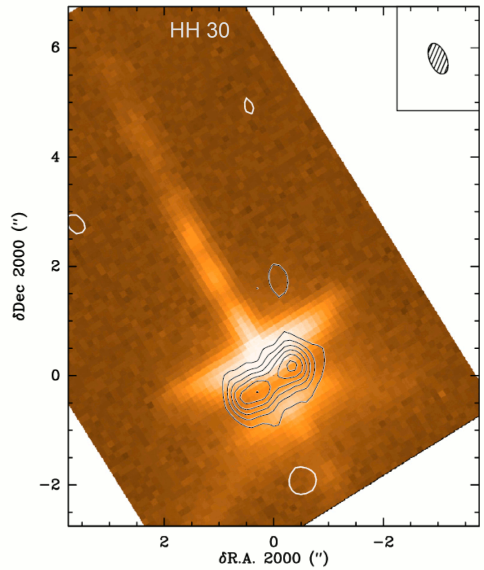

[Guilloteau et al. 2008]

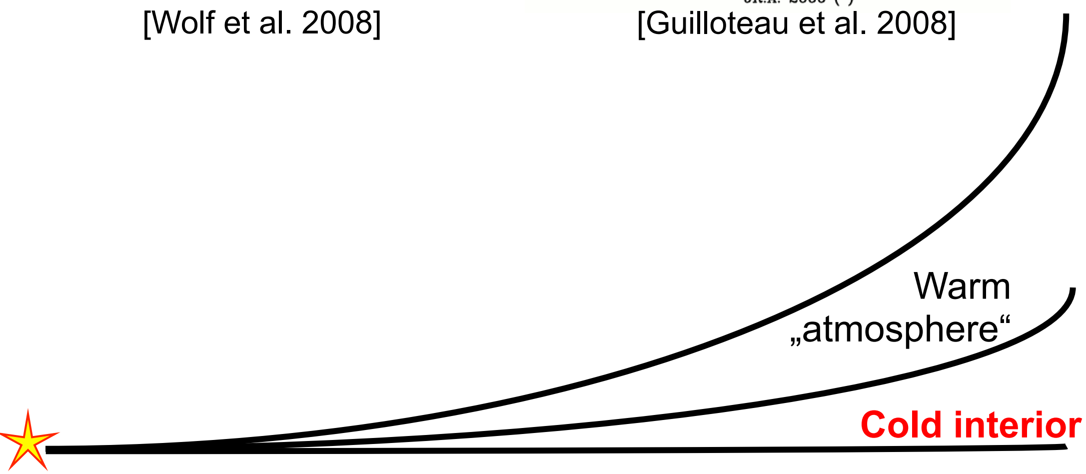

Edge-on disks

(Sub)mm

Wavelength-dependence of the *radial* brightness distribution

⇒ Radial disk structure

⇒ Radial distribution of dust grain properties; Abundance / Excitation conditions of gas species

⇒ Large inner gap?

⇒ Velocity structure (gas)

Various wavelengths – Various disk regions

Face-on disks

Optical / IR

Wavelength-dependence of the *radial* brightness distribution

⇒ Disk: 1) Flaring; 2) Surface structure (local scale height variations)
⇒ Dust: 1) Scattering properties (scattering phase function) in different layers
2) Chemical composition = f (radial position)
(e.g., silicate annealing)

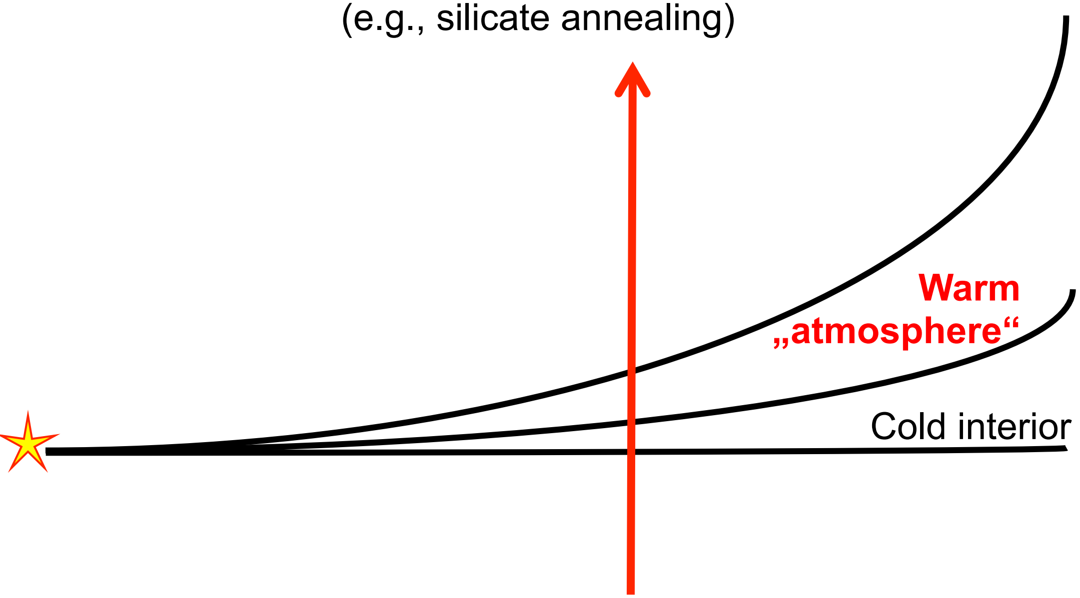

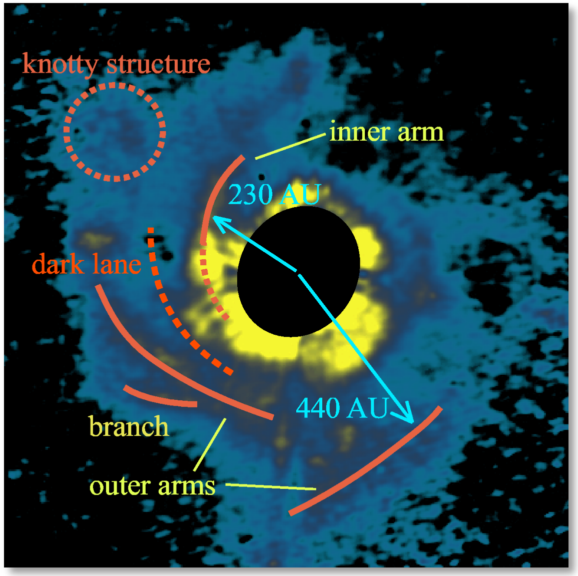

AB Aurigae - Spiral arm structure
(Herbig Ae star; H band; Fukagawa, 2004)

Various wavelengths – Various disk regions

Face-on disks

(Sub)mm

Radial / azimuthal disk structure

⇒ Asymmetries, Local density enhancements
⇒ Gaps, Inner Holes

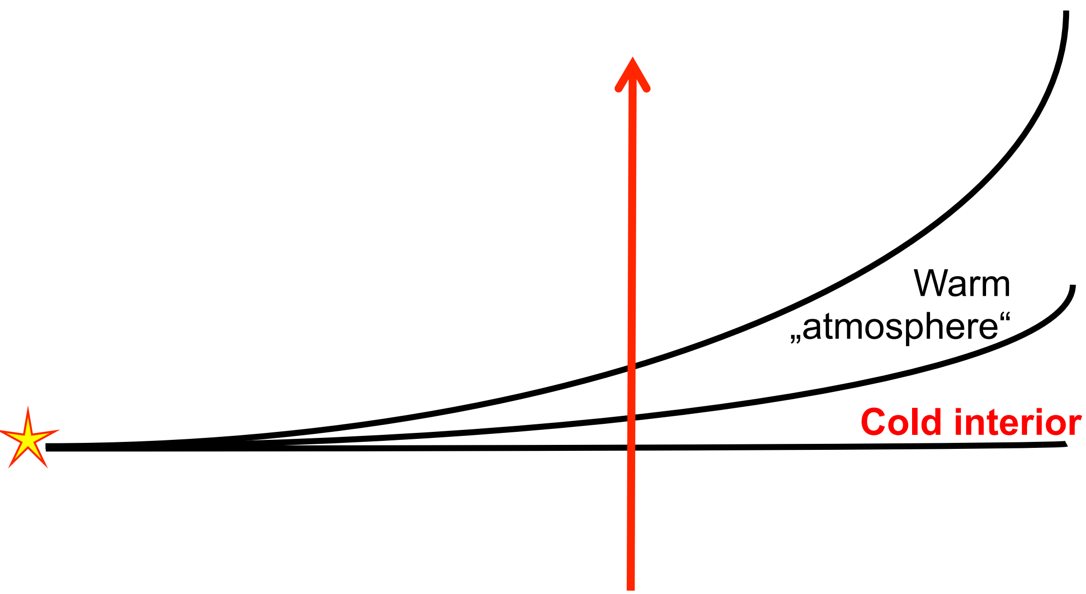

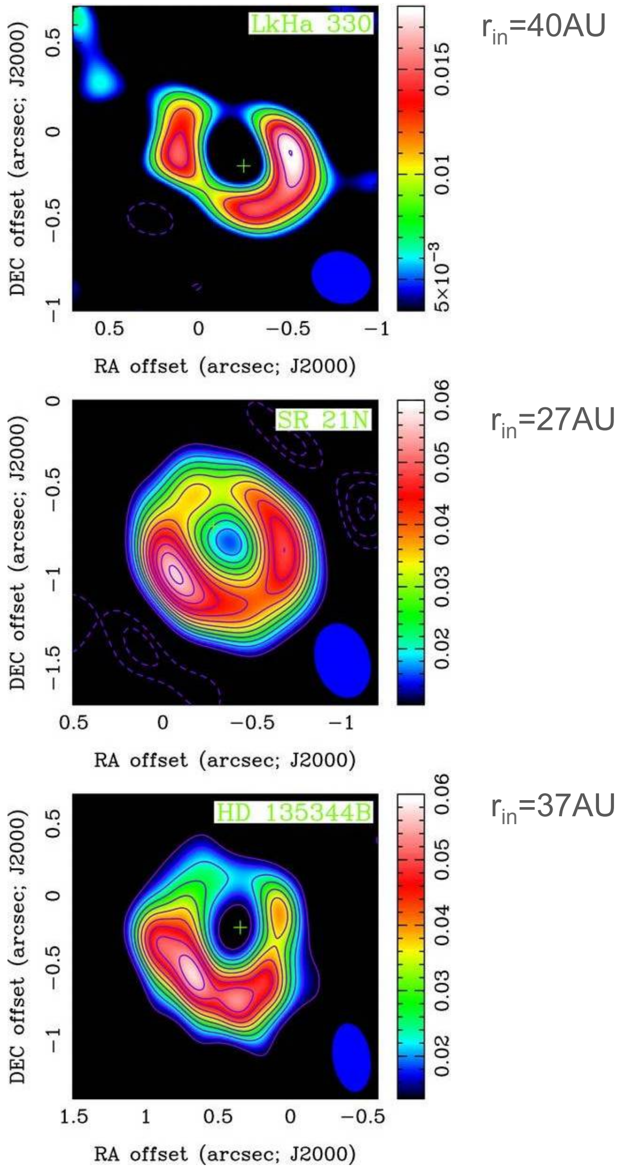

[Brown et al. 2009: 340GHz, continuum]

Radiative transfer

Proper analysis of multi-wavelength observations require

Radiative Transfer Simulations

Detailed numerical modeling taking into account absorption / heating / reemission and scattering processes

+

Sophisticated fitting techniques

<u>Approaches: Radiative Transfer</u>

1. Grid-based algorithms, solving the radiative transfer equation:

$$\begin{aligned} \vec{n}\nabla_{\vec{x}} I_\nu^{tot}(\vec{x},\vec{n}) &= -\kappa^{abs}(\nu,\vec{x})\ I_\nu^{tot}(\vec{x},\vec{n}) - \kappa^{sca}(\nu,\vec{x})\ I_\nu^{tot}(\vec{x},\vec{n}) \\ &+\kappa^{abs}(\nu,\vec{x})\ B_\nu[T(\vec{x})] \\ &+\frac{1}{4\pi}\kappa^{sca}(\nu,\vec{x})\int_\Omega d\Omega' p(\nu,\vec{n},\vec{n}')\ I_\nu^{tot}(\vec{x},\vec{n}') \end{aligned}$$

With:

$I=f(x, y, z, \theta, \phi, \nu)$,

$T=f(x, y, z)$

2. Monte-Carlo Method
   - Very powerful (e.g., wide range of optical depths) + flexible (model)
   - Direct Implementation of Physical Processes (e.g., Photon transport, Scattering, Absorption, Reemission)

Continuum Radiative Transfer

Monte Carlo Radiative Transfer [Illustration]

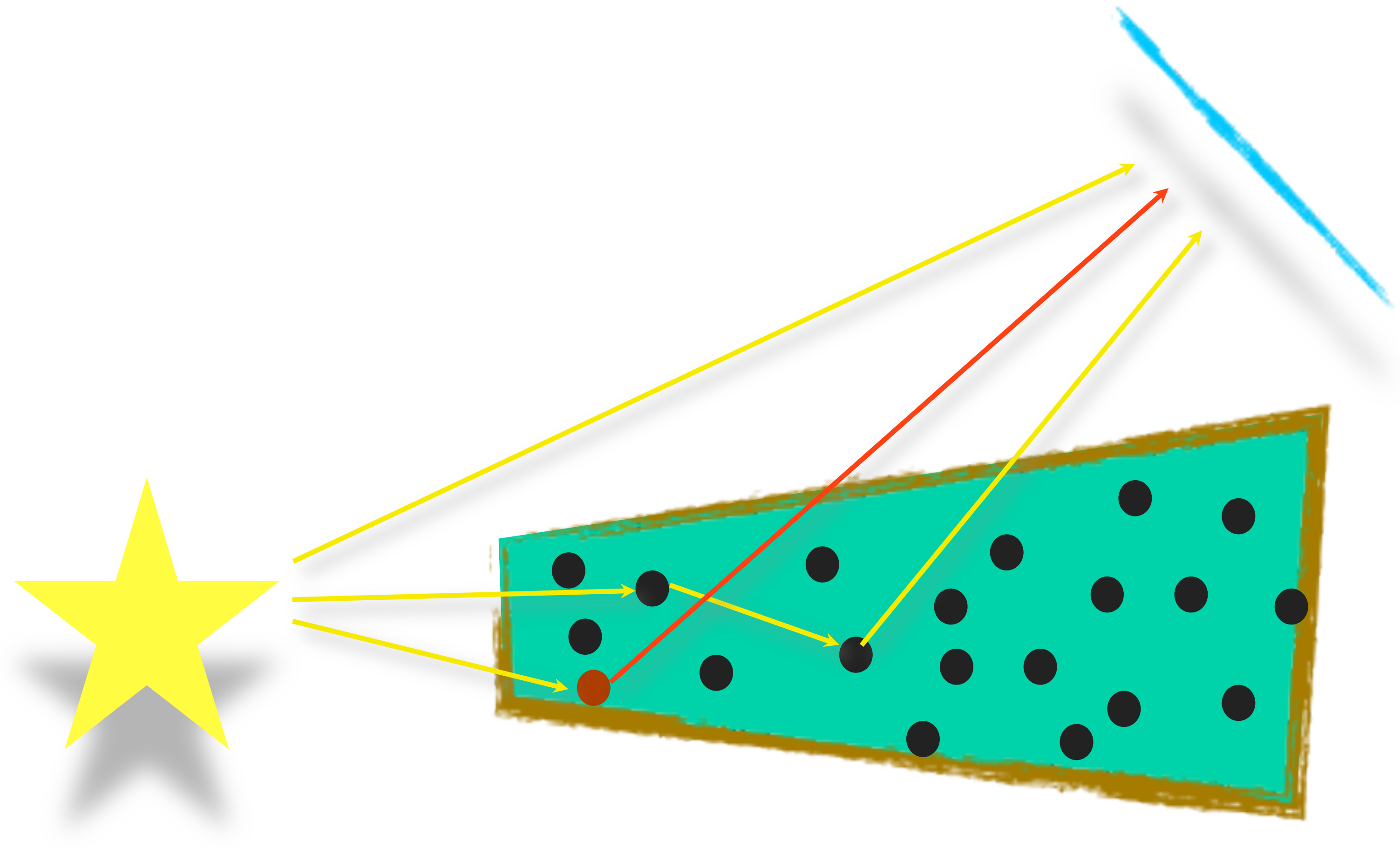

[Courtesy: J. Sauter]

Wolf et al. 1997-2000

Wolf 2003

Continuum Radiative Transfer

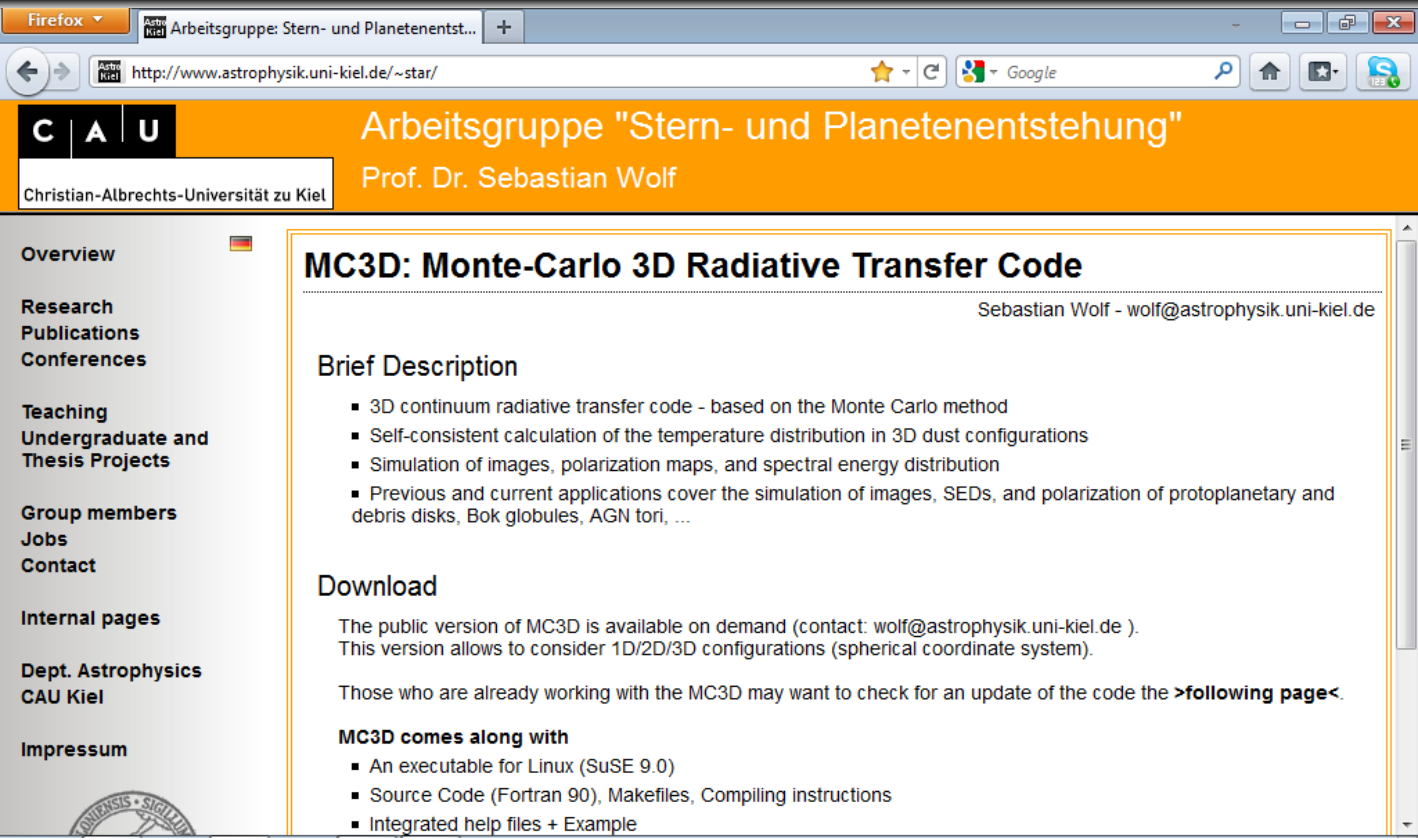
Firefox

Arbeitsgruppe: Stern- und Planetenentst...

http://www.astrophysik.uni-kiel.de/~star/

Google

C A U

Christian-Albrechts-Universität zu Kiel

Arbeitsgruppe "Stern- und Planetenentstehung"

Prof. Dr. Sebastian Wolf

Overview

Research
Publications
Conferences

Teaching
Undergraduate and Thesis Projects

Group members
Jobs
Contact

Internal pages

Dept. Astrophysics
CAU Kiel

Impressum

MC3D: Monte-Carlo 3D Radiative Transfer Code

Sebastian Wolf - wolf@astrophysik.uni-kiel.de

Brief Description

- 3D continuum radiative transfer code - based on the Monte Carlo method
- Self-consistent calculation of the temperature distribution in 3D dust configurations
- Simulation of images, polarization maps, and spectral energy distribution
- Previous and current applications cover the simulation of images, SEDs, and polarization of protoplanetary and debris disks, Bok globules, AGN tori, ...

Download

The public version of MC3D is available on demand (contact: wolf@astrophysik.uni-kiel.de).
This version allows to consider 1D/2D/3D configurations (spherical coordinate system).

Those who are already working with the MC3D may want to check for an update of the code the **>following page<**.

MC3D comes along with

- An executable for Linux (SuSE 9.0)
- Source Code (Fortran 90), Makefiles, Compiling instructions
- Integrated help files + Example

http://www.astrophysik.uni-kiel.de/~star

Wolf & Hillenbrand 2003

Continuum Radiative Transfer

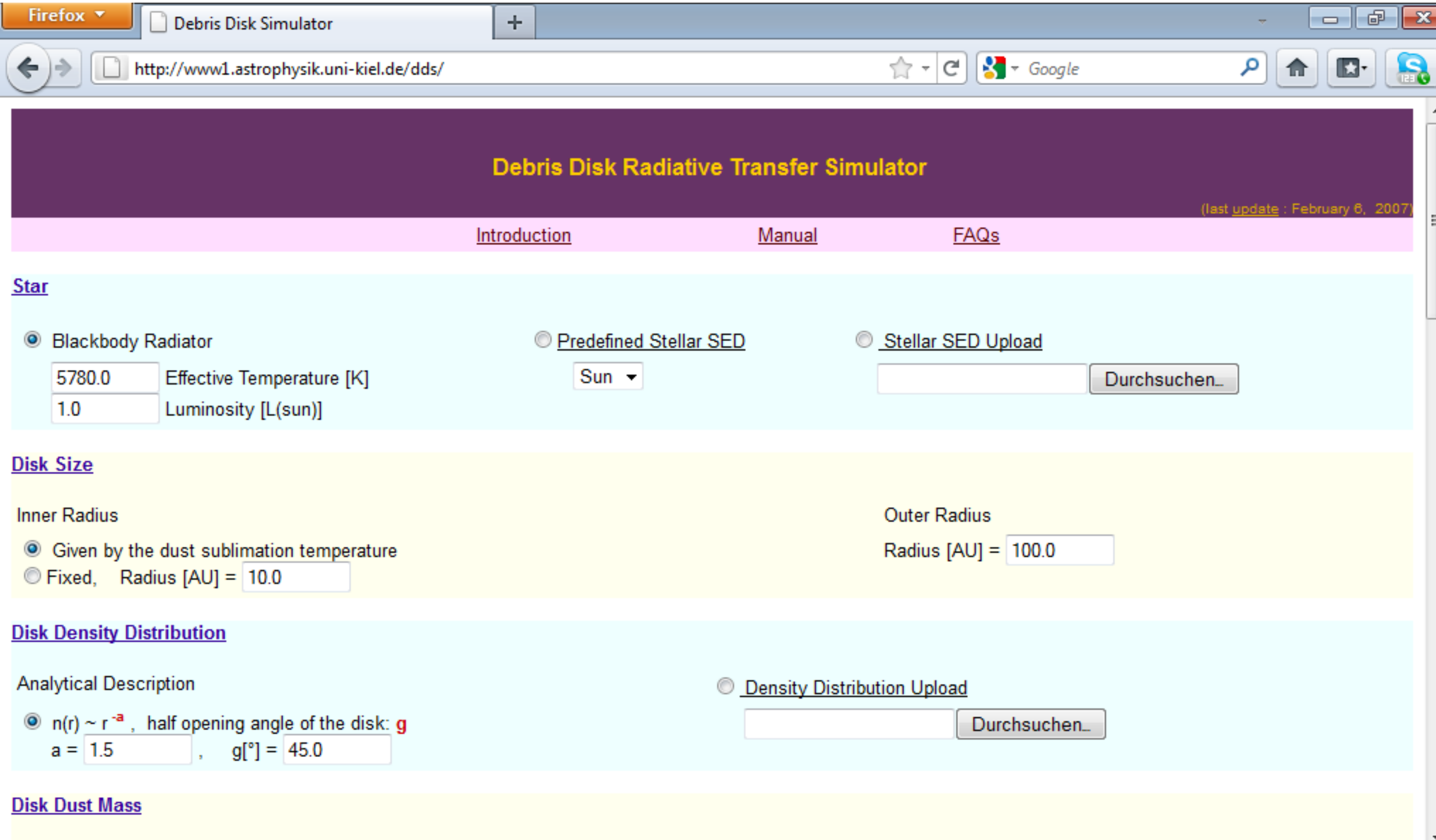

http://www1.astrophysik.uni-kiel.de/dds/

Radiative transfer

Proper analysis of multi-wavelength observations require

Radiative Transfer Simulations

Detailed numerical modeling taking into account
absorption / heating / reemission and scattering processes

+

Sophisticated fitting techniques

Approaches: Fitting (typical)

a. Database fitting (χ^2)

b. Simulated annealing (Kirkpatrick et al. 1983)
   - Modification of Metropolis-Hastings algorithm for optimization
   - Implementation independent of dimensionality of the problem
   - Local optima overcome inherently
   - Easy to implement

“Modeling guidelines”

1. Maximum number of independent constraints from observations
   – Spectral Energy Distribution *(mass, disk structure)*
   – Absorption/Emission Features *(dust properties)*
   – Polarization measurements *(dust properties)*
   – Spatially resolved images in various wavelength ranges *(tracing different physical processes)*
   – Single dish/telescope + Interferometric measurements *(tracing disks on various spatial scales)*
   – Characterize embedded source
   – Possible influence of the environment? (e.g., nearby massive stars?)

2. Set up a disk model with as few parameters as necessary (which are the parameters do you really want/need to constrain?)

3. a) Radiative Transfer Modeling if necessary;
   b) Simple ‘Toy Model Fitting’ if sufficient
      (Problem here: Resulting model/parameters usually not self-consistent)

Example #1: Butterfly star in Taurus

Example #1 The Butterfly Star in Taurus

[Padgett et al. 1999]

μm

μm

μm

μm

- Wavelength-dependence of the dust lane width
- Relative change of the brightness distribution from 1.1μm-2.05μm
- Slight symmetry of the brightest spots

Example #1 The Butterfly Star in Taurus

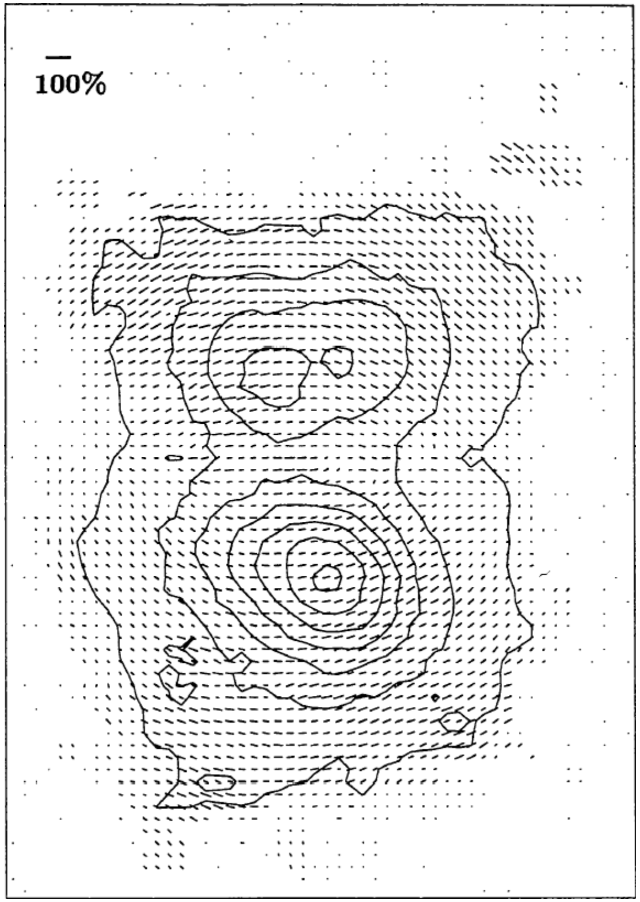

J band polarization map
(Lucas & Roche 1997 – IRCAM-3/UKIRT)

Linear Polarization: up to 80%

Scattering dominated by interstellar-type grains

Disk outer radius:	300 AU
Radial/Vertical density profile:	α=2.37, β=1.29
Disk scale height:	h(100AU) = 15AU
Disk Grain size distribution:	a_{Grain} = (0.005 – **100**) μm
Disk Mass:	7 x 10^{-2} M_{sun}
Envelope Mass:	4.8...6.1 x 10^{-4} M_{sun}

Confirmation of **different dust evolution scenarios** in the circumstellar shell and disk:

1. Interstellar dust (< 1μm) in the shell
2. Dust grains with radii up to ~100μm in the circumstellar disk!

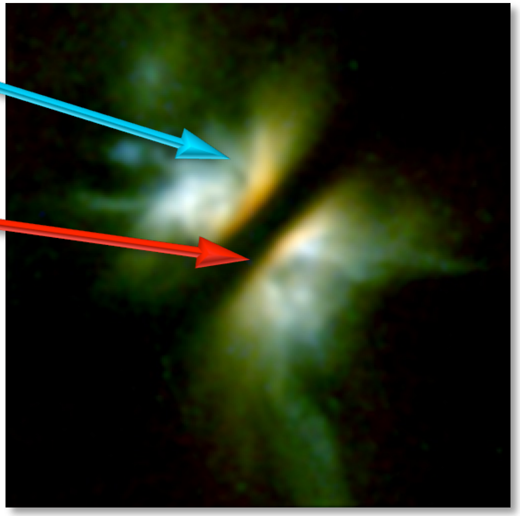

Example #1 The Butterfly Star in Taurus

IRAM / PdBI

Disk outer radius:	300 AU
Radial/Vertical density profile:	α=2.37, β=1.29
Disk scale height:	h(100AU) = 15AU
Disk Grain size distribution:	a_{Grain} = (0.005 – **100**) μm
Disk Mass:	7 x 10^{-2} M_{sun}
Envelope Mass:	4.8...6.1 x 10^{-4} M_{sun}

Confirmation of **different dust evolution scenarios** in the circumstellar shell and disk:

1. Interstellar dust (< 1μm) in the shell
2. Dust grains with radii up to ~100μm in the circumstellar disk!

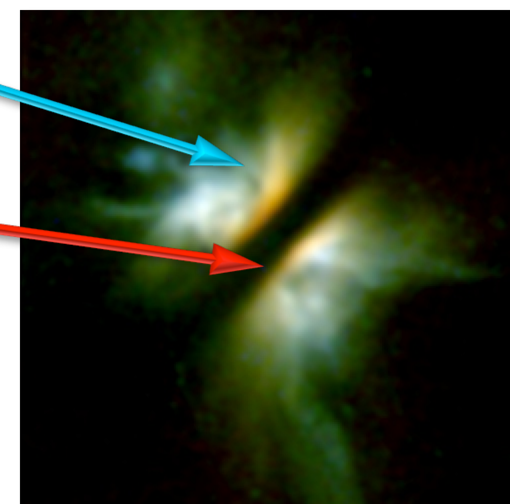

Figure will be added as soon as corresponding article is published

Gräfe et al., in prep.

Example #1 The Butterfly Star in Taurus

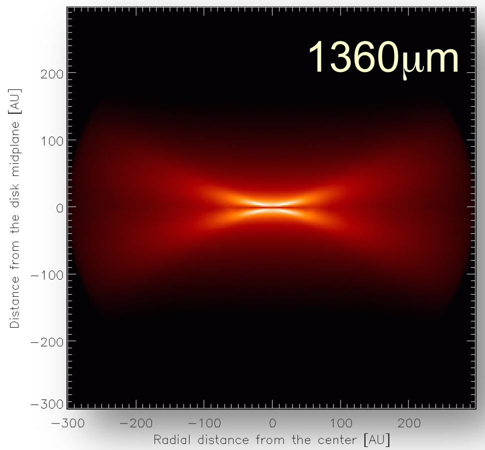

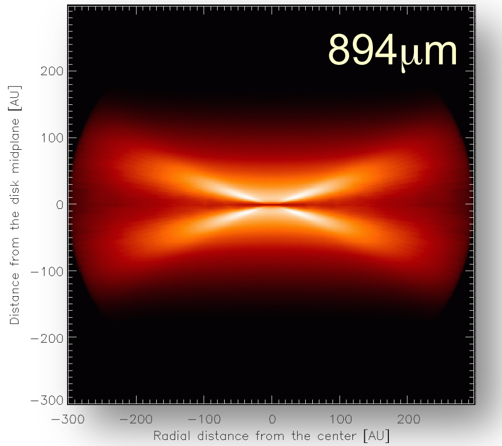

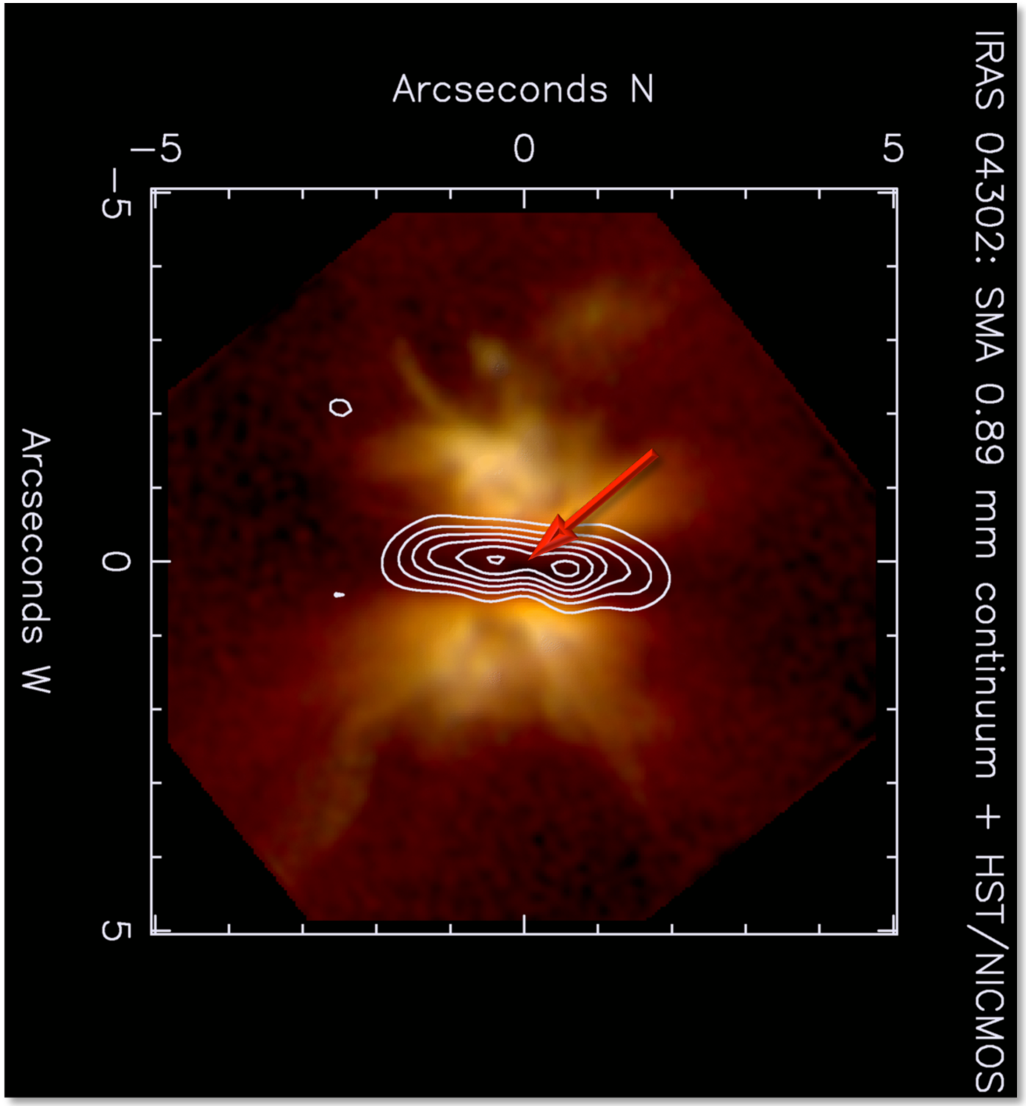

constraints on radial + vertical disk structure
in the potential planet-forming region (r~80-120AU)

[Wolf et al. 2008]

Example #2: CB 26 (Taurus)

Example #2 Disk in the Bok Globule CB26

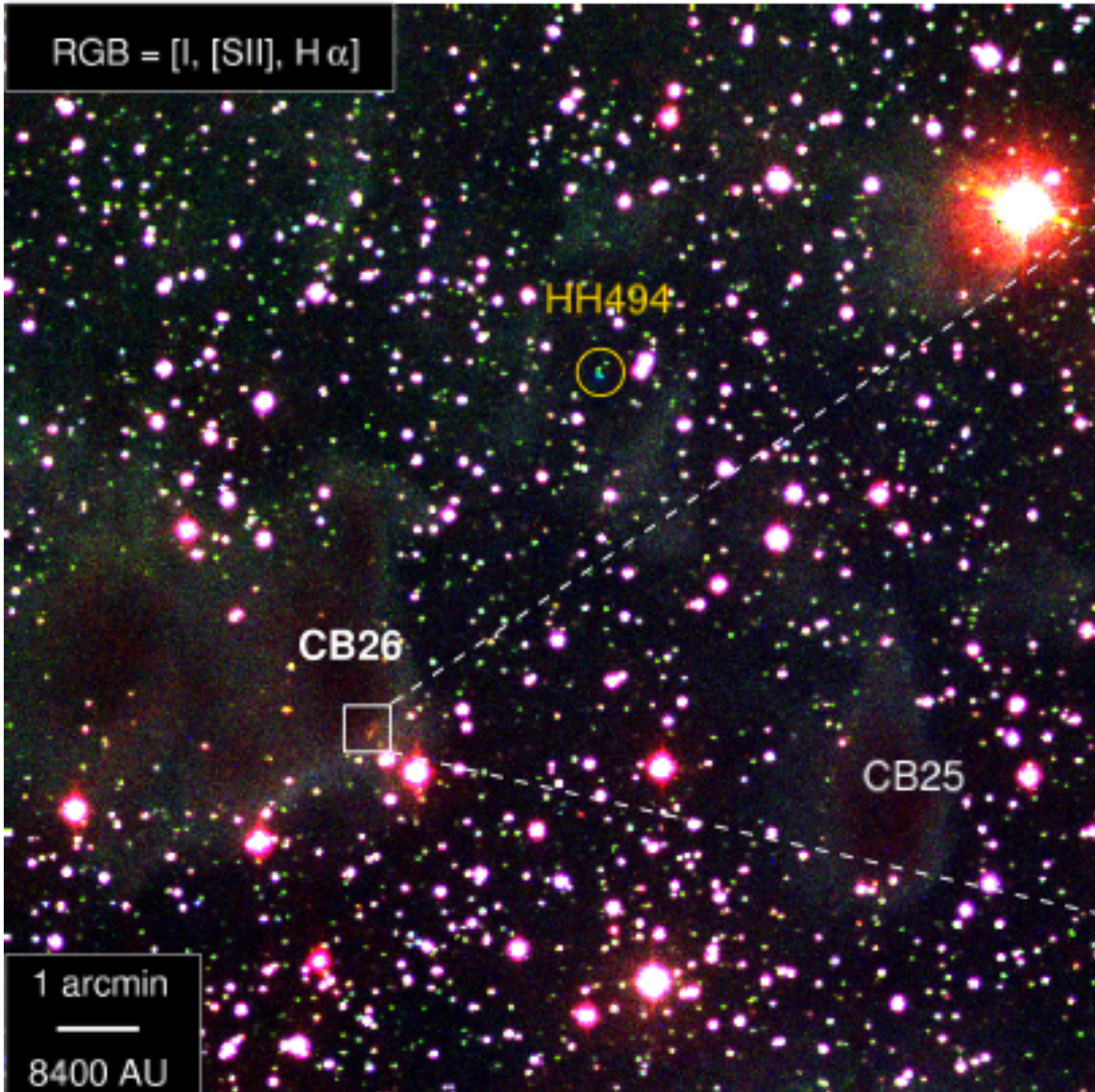

[Courtesy: Launhardt]

Observations considered

- HST NICMOS NIR imaging
- Submm single-dish: SCUBA/ JCMT, IRAM 30m
- Interferometric mm cont. maps: SMA (1.1mm), OVRO (1.3/2.7mm)
- SED, including IRAS, ISO, Spitzer

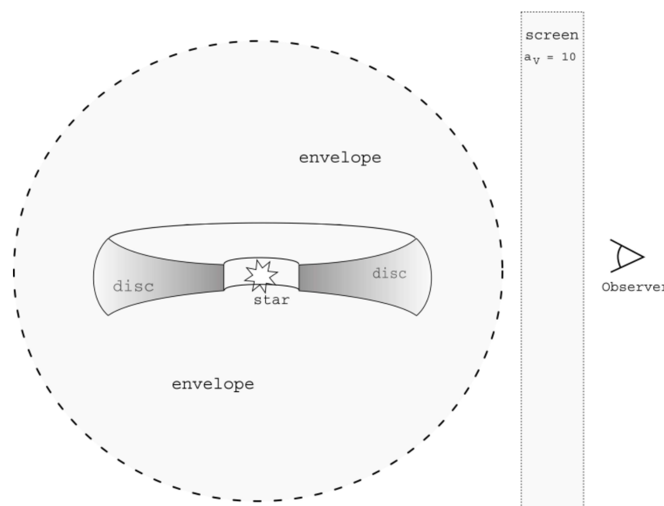

[Sauter et al., 2009]

Example #2 Disk in the Bok Globule CB26

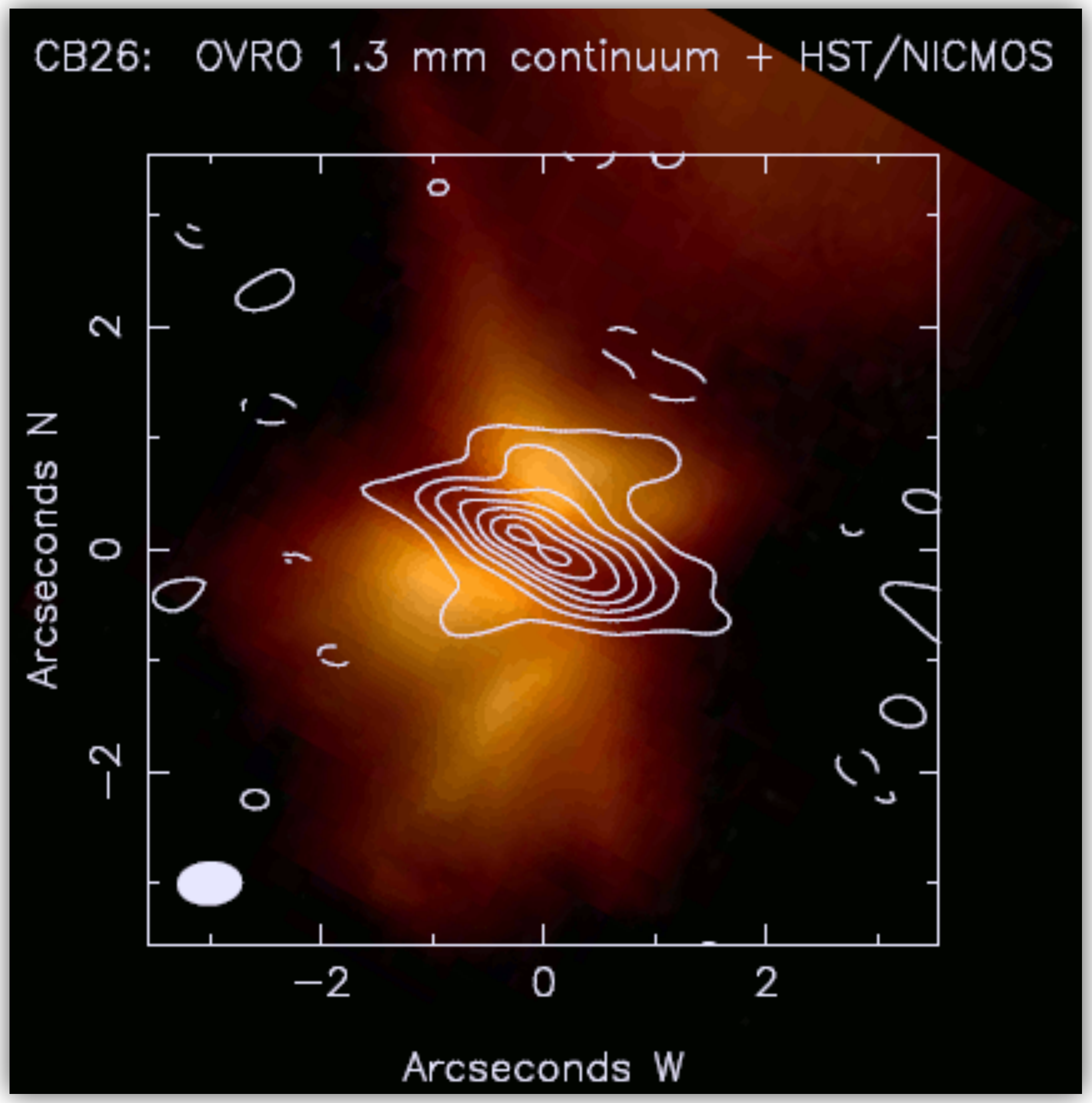

Observations considered

- HST NICMOS NIR imaging
- Submm single-dish: SCUBA/ JCMT, IRAM 30m
- Interferometric mm cont. maps: SMA (1.1mm), OVRO (1.3/2.7mm)
- SED, including IRAS, ISO, Spitzer

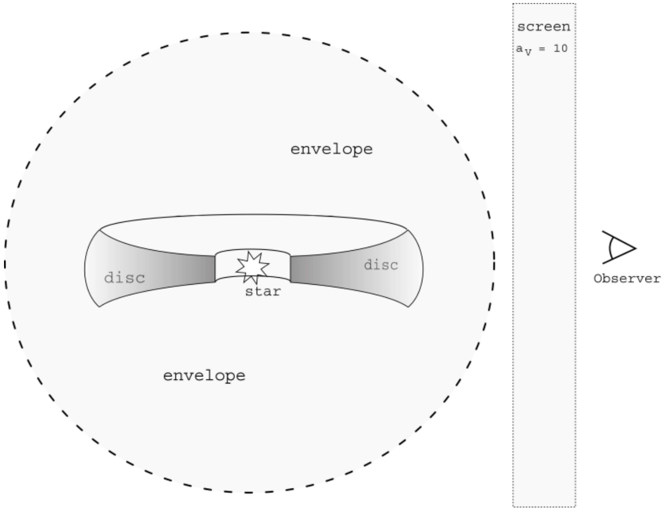

[Sauter et al., 2009]

Example #2 Disk in the Bok Globule CB26

$$\rho_{\rm disc}(\vec{r}) = \rho_0 \left(\frac{R_*}{r_{\rm cyl}}\right)^{\alpha} \exp\left(-\frac{1}{2}\left[\frac{z}{h}\right]^2\right)$$

$$h(r_{\rm cyl}) = h_0 \left(\frac{r_{\rm cyl}}{R_*}\right)^{\beta}$$

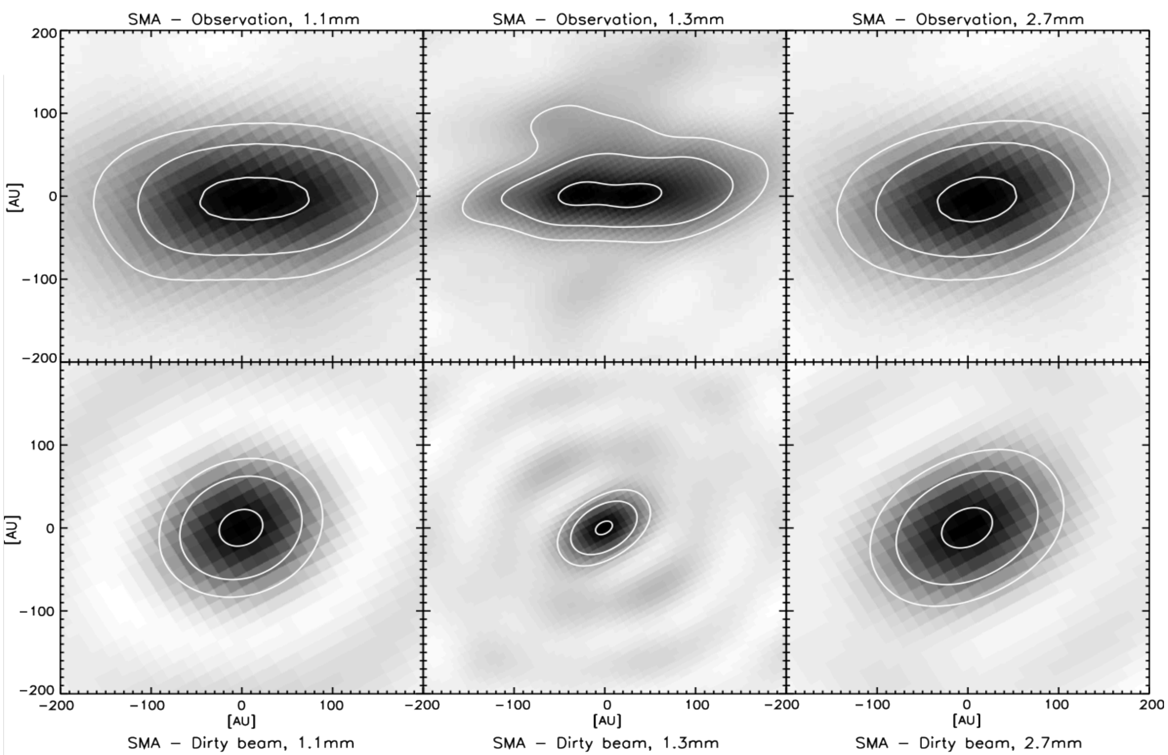

<u>Parameters</u>

- Surface density
- Flaring
- Scale height @ 100AU
- Inner/Outer radius
- Chemical composition, and size distribution of dust (Spherical grains)
- Stellar luminosity and effective temperature
- Distance

[Sauter et al., 2009]

Example #2   Disk in the Bok Globule CB26

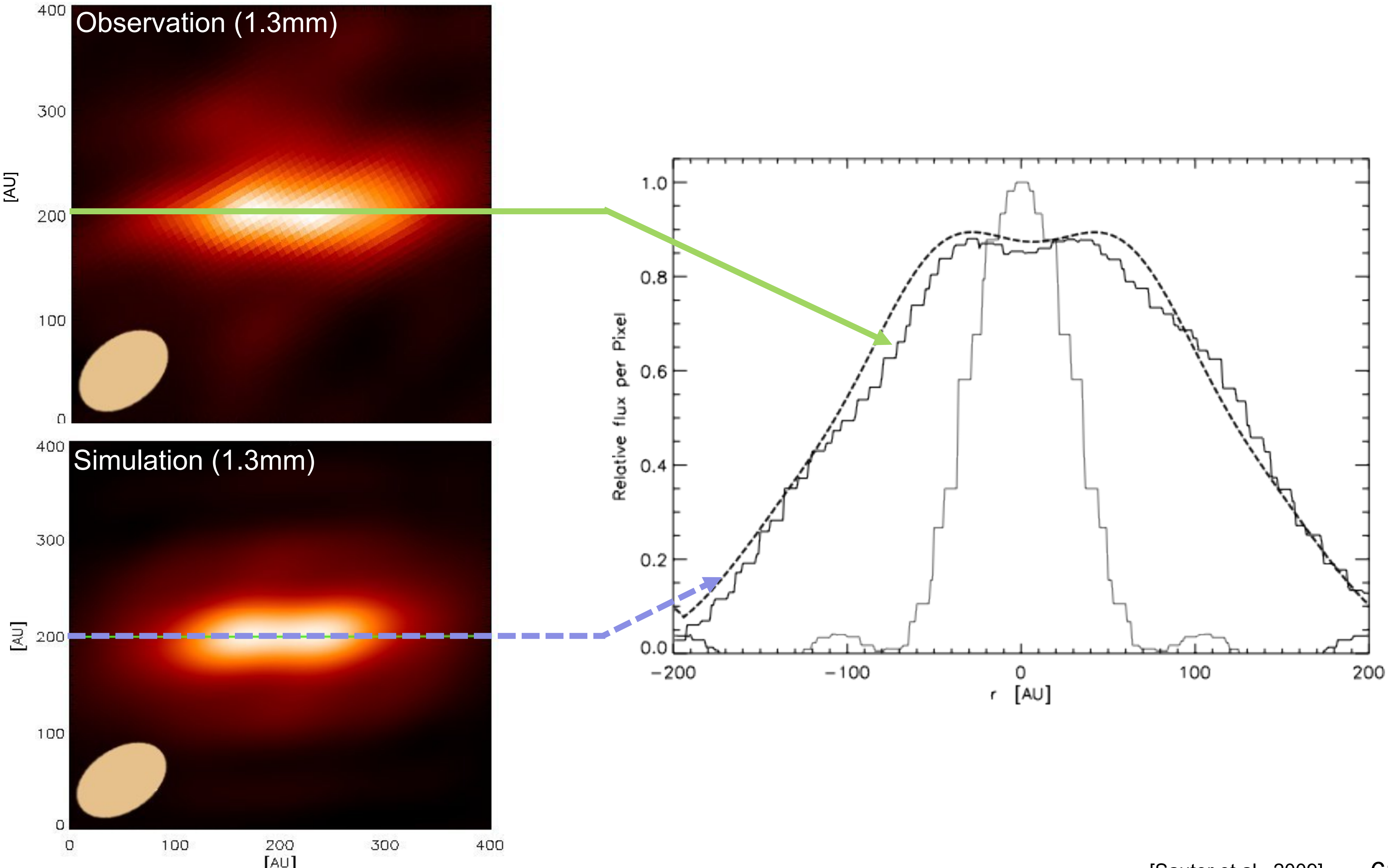

[Sauter et al., 2009]

Example #2 Disk in the Bok Globule CB26

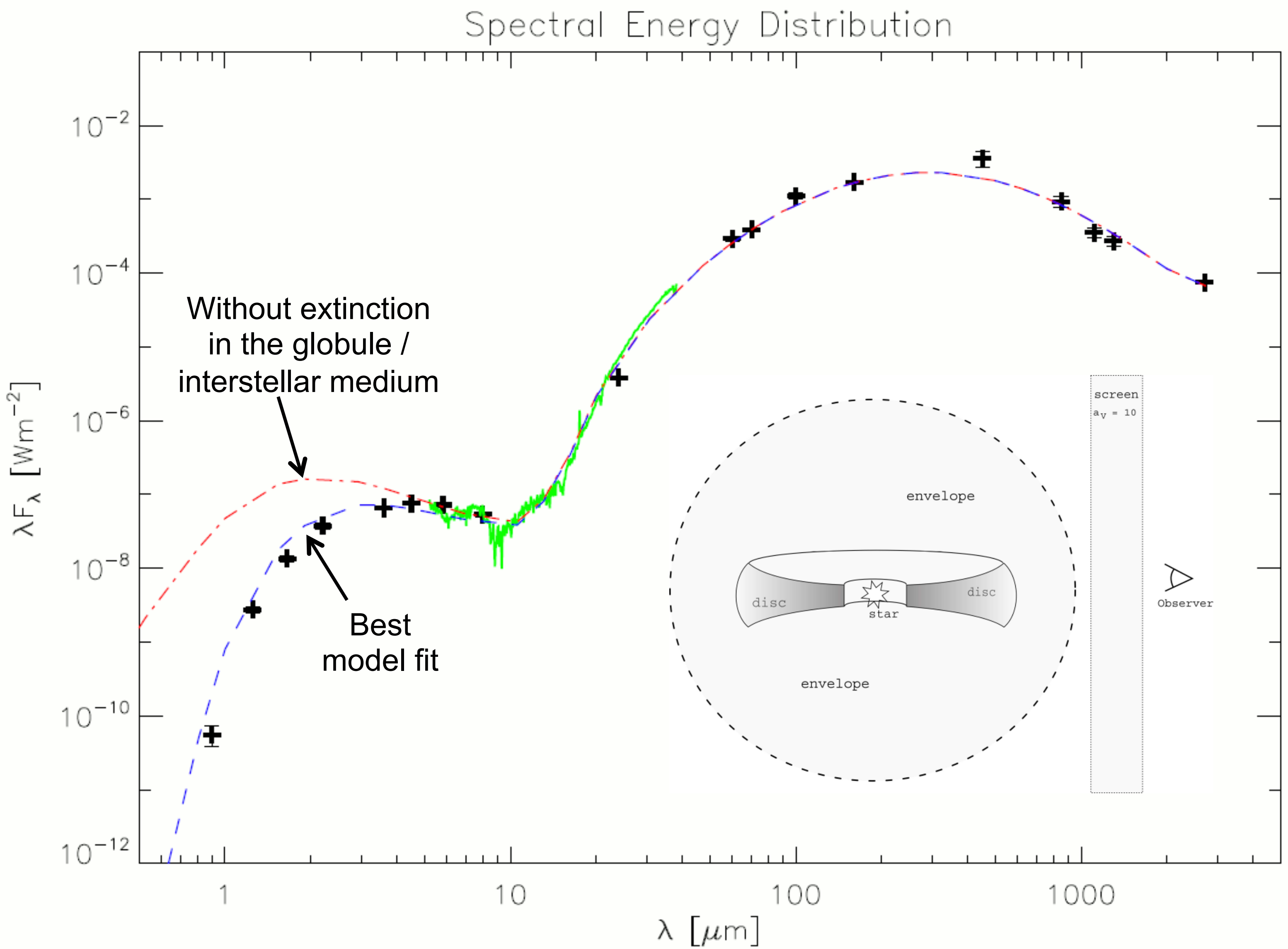

[Sauter et al., 2009]

Example #2 Disk in the Bok Globule CB26

Main Conclusions

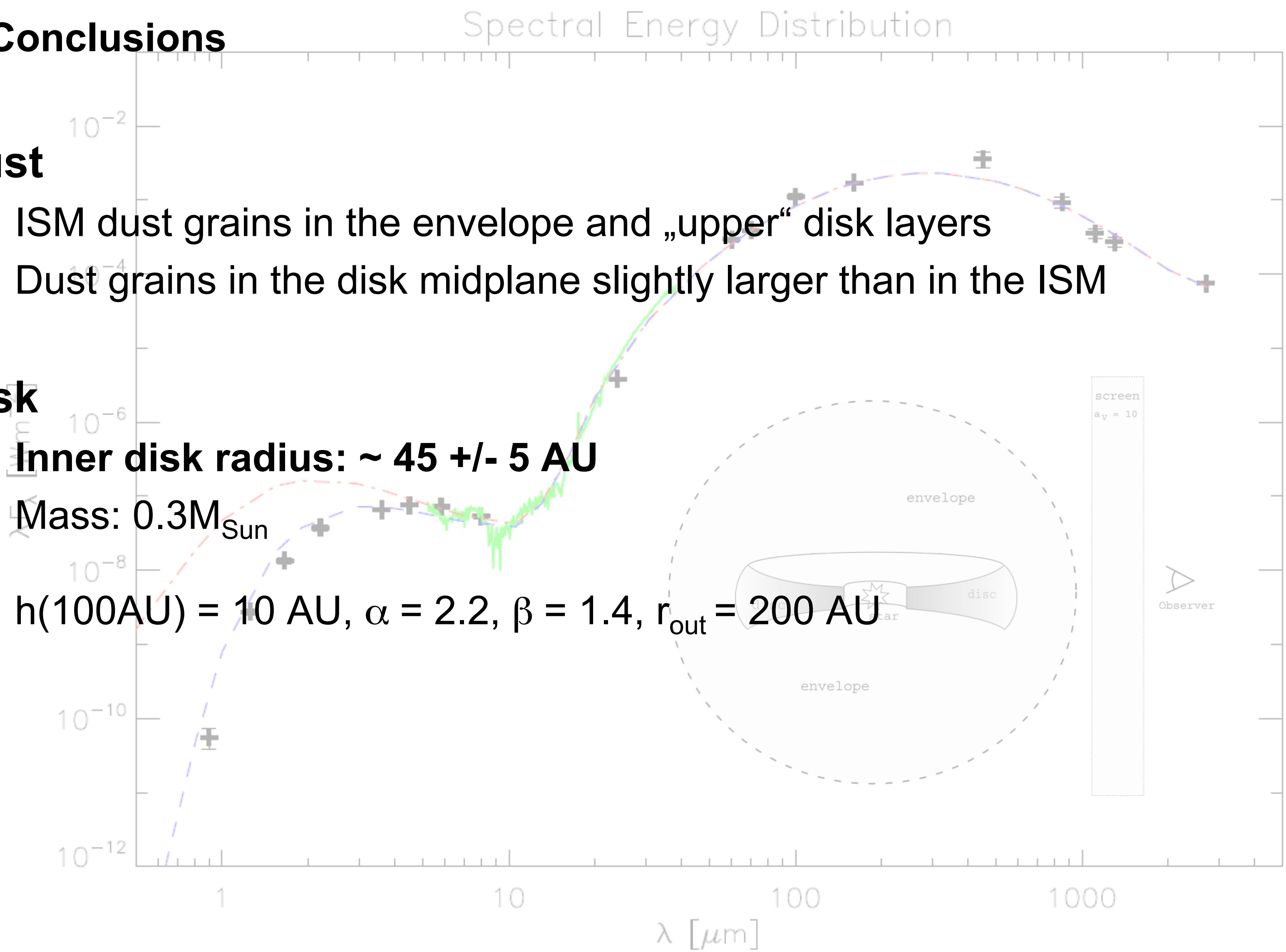

- **Dust**
  - ISM dust grains in the envelope and „upper“ disk layers
  - Dust grains in the disk midplane slightly larger than in the ISM
- **Disk**
  - **Inner disk radius: ~ 45 +/- 5 AU**
  - Mass: $0.3M_{Sun}$
  - $h(100AU) = 10$ AU, $\alpha = 2.2$, $\beta = 1.4$, $r_{out} = 200$ AU

[Sauter et al., 2009]

Example #3: HH30

Example #3 HH30

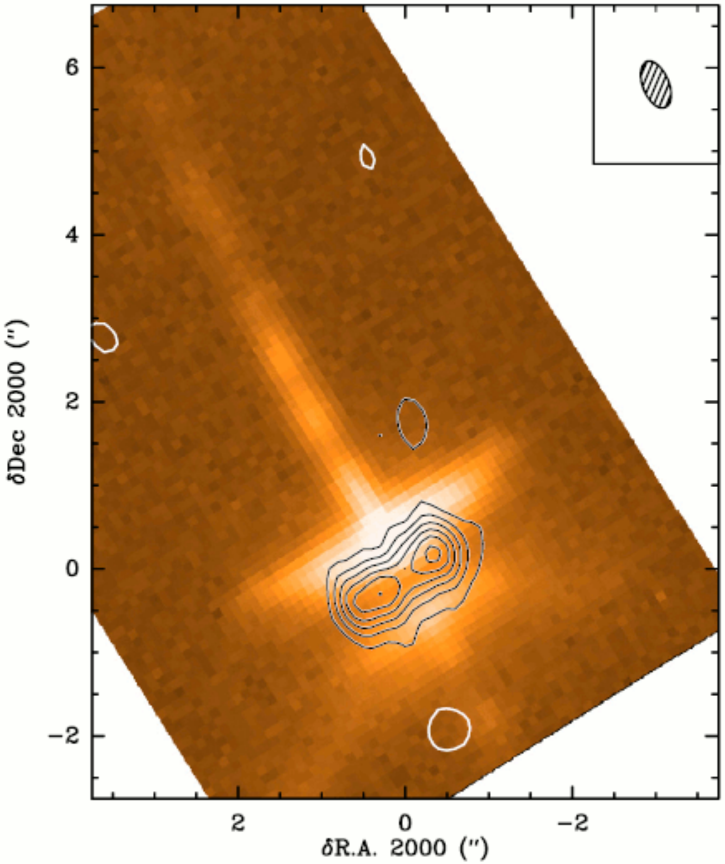

Fig. 1. Superimposition of the PdBI 1.30 mm continuum map on the HST data. The spatial resolution is 0.59 × 0.32″ at PA 22°. The center of projection is RA = $04^h31^m37^s.469$ and Dec = 18°12′24″.22 in J2000. Contour levels start at and are spaced by 3σ = 0.56 mJy/beam, corresponding to 68 mK. The registration of the HST image is approximate, as the positions given by Anglada et al. (2007) and Cotera et al. (2001) differ by 1″.

[Guilloteau et al. 2008]

Observation

- IRAM interferometer, 1.3mm, beam size ~0.4”

Results

- Disk of HH30 is truncated at an inner radius 37 ± 4 AU.

Interpretation

- Tidally truncated disk surrounding a binary system (two stars on a low eccentricity, 15 AU semi-major axis orbit)

- Additional support for this interpretation: Jet wiggling due to orbital motion

- The dust opacity index, β ≈ 0.4, indicates the presence of cm size grains (assuming that the disk is optically thin at 1.3mm)

“… In this domain, ALMA will likely change our observational vision of these objects.“

Example #3 HH30

Further material will be added as soon as corresponding article is published

[Madlener et al., subm.]

Short interlude:

The gas phase

Jet rotation: DG Tau

Co-rotation of Disk and Jet

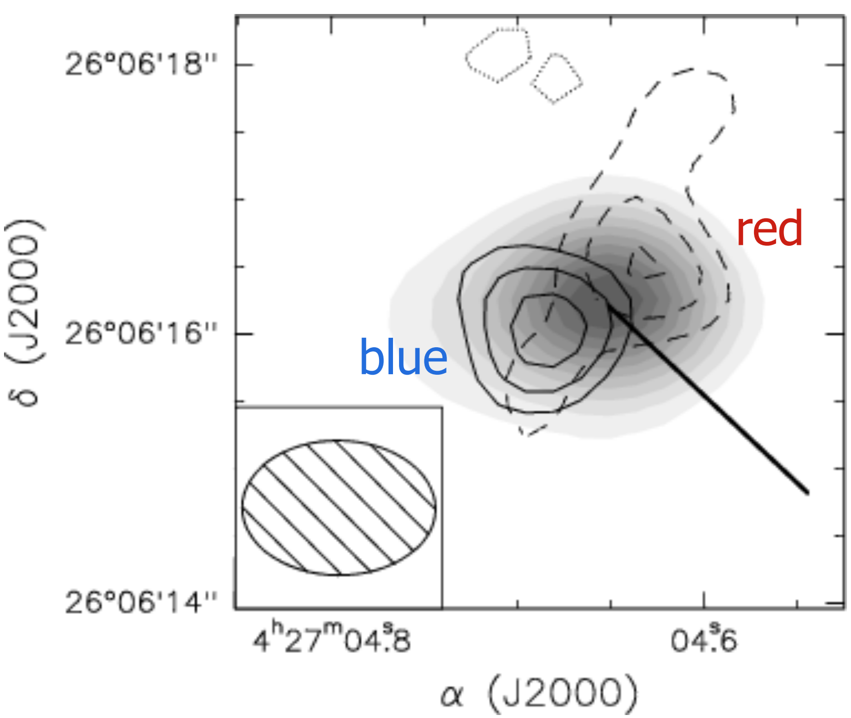

[Testi et al. 2002]

Observed Radial Velocity Shift

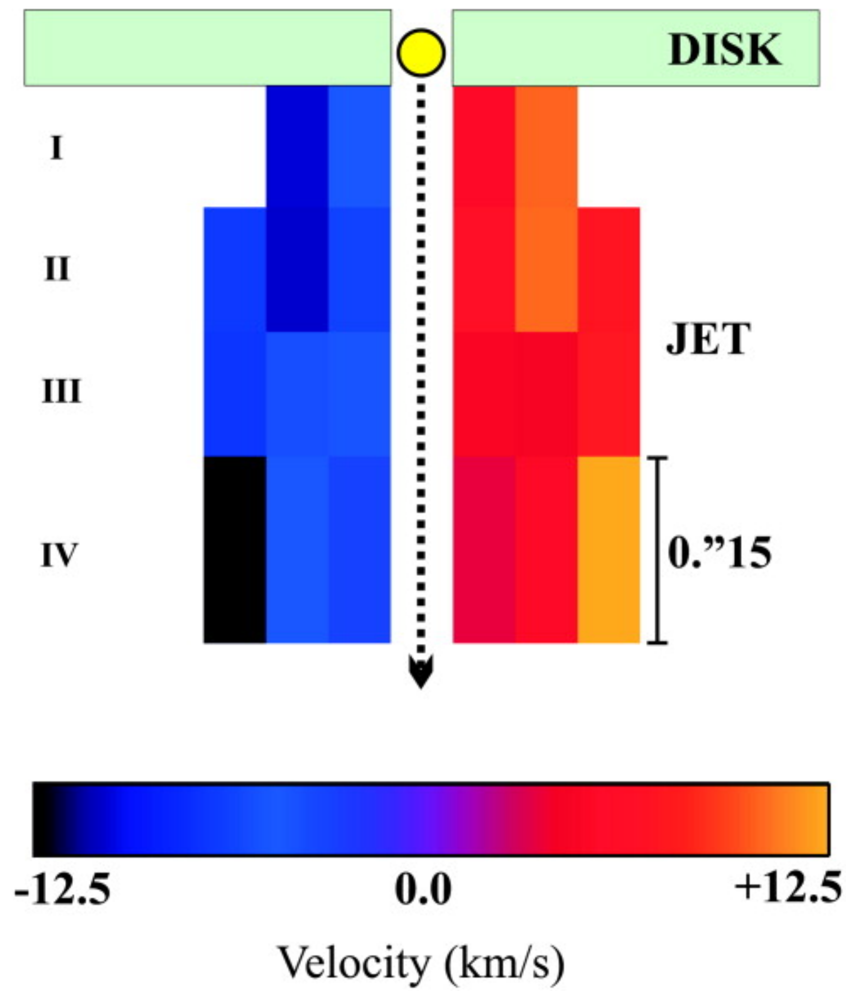

[Bacciotti et al. 2002]

Gas phase

- **Complex interplay**
  between various gas species, gas and dust phase, and the radiation field

- **Processes**
  - Gas phase chemistry
  - Dust-Gas interaction (freeze-out)
  - Dust / surface reactions (e.g., chemical reactions)
  - Photo-chemical reactions (surface)

  Radial and vertical temperature gradient

- Density and temperature often not sufficiently high to achieve chemical equilibrium

=> Time-dependent chemical networks

Comparison: Dust- vs. Gas distribution

Dust distribution

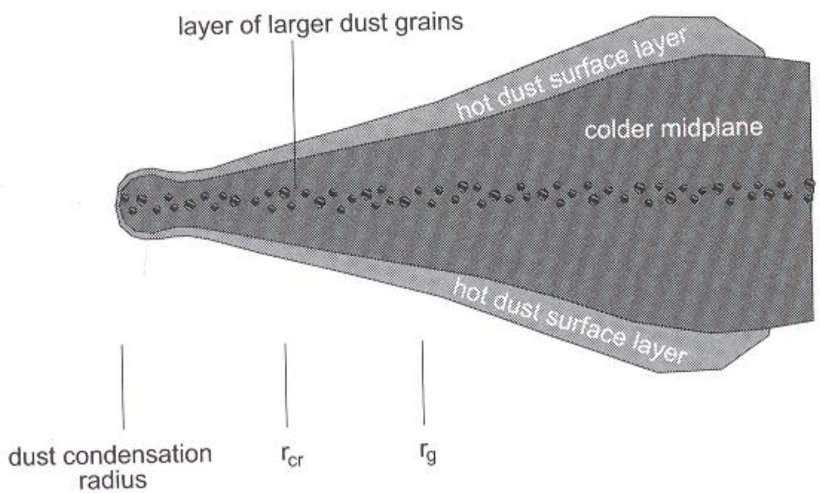

Gas distribution

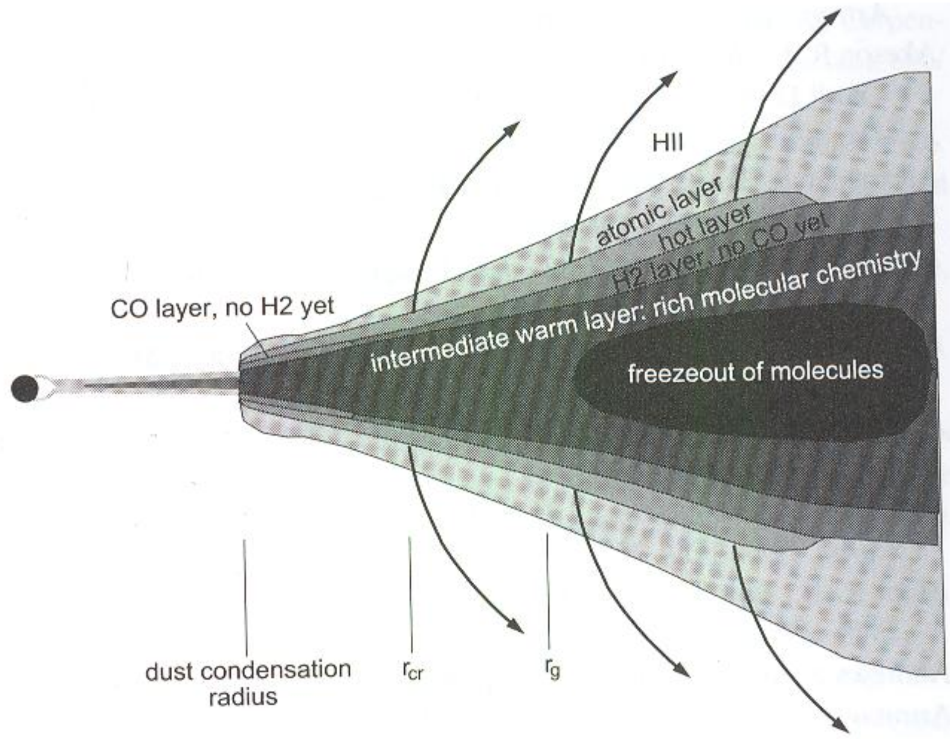

[from Protostars & Planets V, 2008]

Gas

Gas in disks: Observation

To be considered in the analysis of line observation:

- Observations at different lines allow to trace different disk layers

  (Reasons: different optical depths and excitation conditions for different lines)

  Example:

  DM Tau at 100AU (Dartois et al. 2003):

  ^{13}CO J=1-0: Disk midplane

  ^{13}CO J=2-1: One scale height

- *Isotopes:* $\boldsymbol{^{12}C^{16}O}$ *(most abundant),* $\boldsymbol{^{13}C^{16}O}$*,* $^{12}C^{18}O$*,* $^{12}C^{17}O$*,* $^{13}C^{18}O$

  (^{16}O: most abundant: 99,762%)

- *Molecules with less abundant isotopes are (consequently) less abundant (in first approximation)*

  => Lines of these molecules become optically thick at higher masses

- Temperature / Density structure:

  Line emission from different disk regions (radial / vertical distrib. of molecular abundances)

- Temperature structure: In agreement with flared disk model
- Indication of vertical temperature gradient (cold disk midplane)
- Disks around low-mass stars: T(r>150AU) < 17K => Freeze-out of CO on dust grains

Gas

Inner regions of circumstellar disks

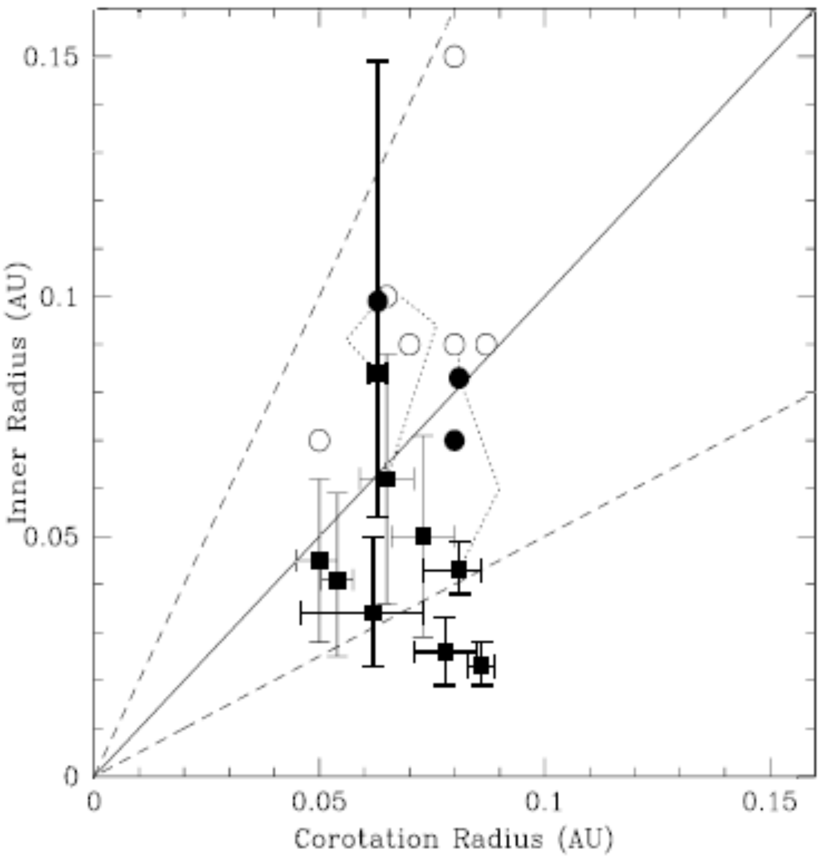

[Najita et al. 2007]

Squares:
Inner radius of gas disks
(from vibrational transitions
of CO @ 4,6μm; T_{Gas} > 1000K)

Underlying assumption:
Gas rotates with Keplerian velocity
=> Line width
=> Inner disk radius

Circles: Inner radius of dust disk
(Interferometry: filled circles;
SEDs: open circles)

Radius of the gas disk

– Inside the sublimation radius of the dust
– Near co-rotation radius

radius(angular velocity of the disk = angular velocity of the star)
=> indicated coupling between stellar magnetic field and disk

10AU – 1000AU

↓

0.1AU – 10AU

Inner disks – Open questions

Hypotheses / Theoretical model to be tested

- Accretion: Viscosity, Angular momentum transfer, Accretion geometry on star(s)
- Snow-line (location / surface density profile)
- Planets: Luminosity, induced gaps
- Puffed-up inner rim and associated shadowed region
- Gas within the inner rim
- Gas-to-dust mass ratio; Empty(?) holes in transition disks

The general context (exemplary questions):

- How do inner and outer disk relate to each other?
- Where and when do planets form?

Required

Empirically-based input to improve our general understanding and thus to better constrain planet formation / disk evolution models

Approach

Imaging the inner disk

Dust evolution in the planet forming region

Herbig Ae/Be Stars

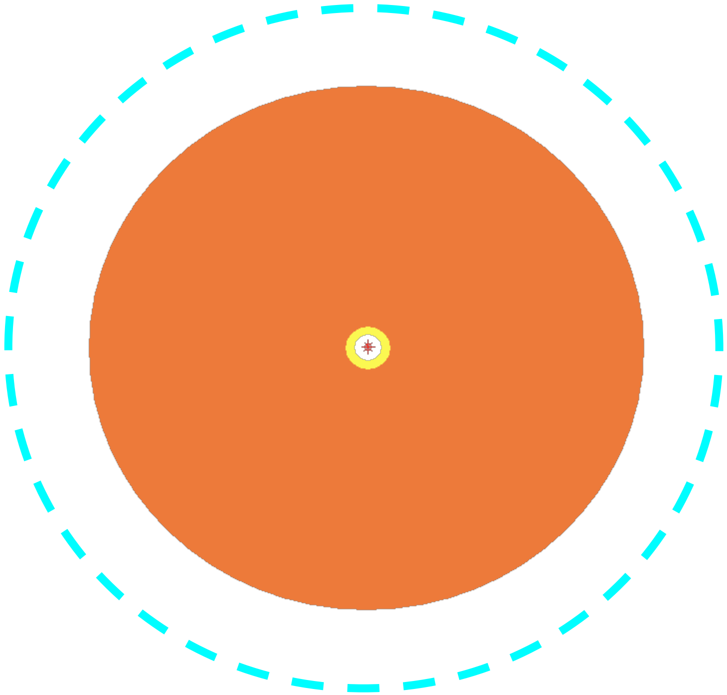

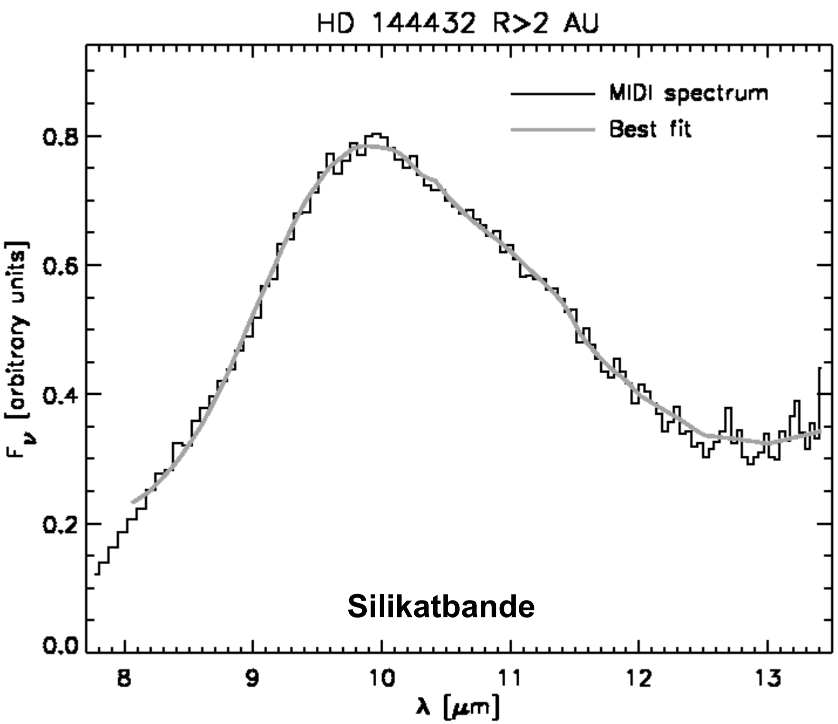

[Leinert et al. 2004, van Boekel et al. 2004]

Dust evolution in the planet forming region

Herbig Ae/Be Stars

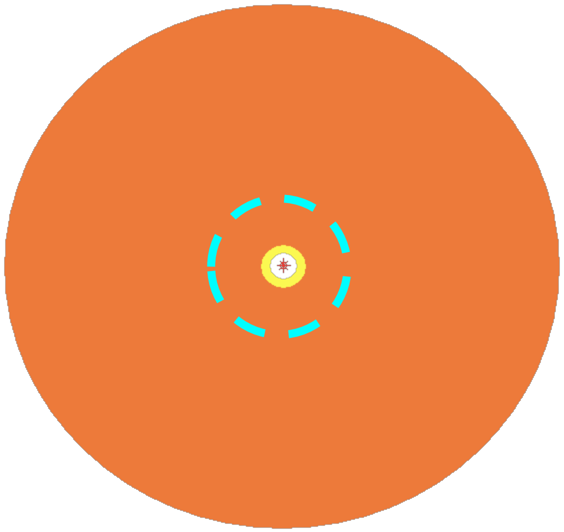

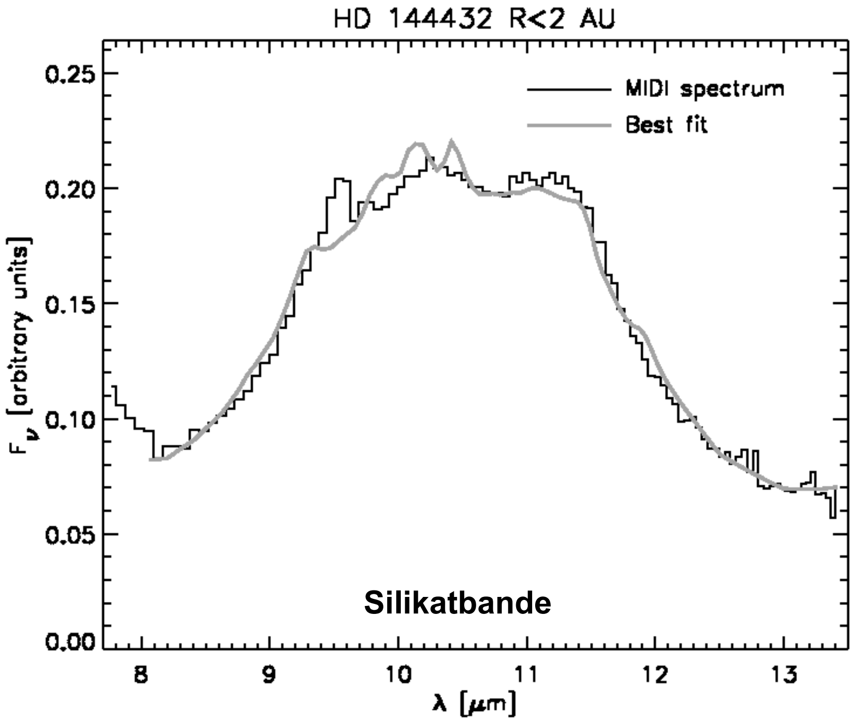

[Leinert et al. 2004, van Boekel et al. 2004]

Example #4 Mid-IR Interferometry

Schegerer, Wolf, et al., 2008, 478, 779
„The T Tauri star RY Tauri as a case study of the inner regions of circumstellar dust disks "

Schegerer, Wolf, et al. 2009, A&A, 502, 367
„Tracing the potential planet-forming region around seven pre-main sequence stars"

The VLT Array on the Paranal Mountain

Mid-Infrared Interferometric Instrument (MIDI)

Spatial resolution: $\lambda/B \geq$ 1AU @ 140pc with B ≤ 130m

Spectrally resolved (R=30) data in N band:
- Silicate feature + (relative) radial distribution
- Inner disk region ≤ 40 AU

General results

(1) **SED** (global appearance of the disk) + spectrally resolved **visibilities** can be fitted **simultaneously**
(2) Best-fit achieved in most cases with an **active accretion disk and/or envelope**
(3) Decompositional analysis of the 10μm feature confirms effect of **Silicate Annealing** in the inner disk (~ few AU)

Limitation of 2-beam interferometers
[Example]

True surface brightness profile in circumstellar disks around TTauri / HAe/Be stars

Two-telescope interferometers: “Mean” disk size & approximate inclination of the disk
Assumption: Iso-brightness contours are centered on the location of the central star

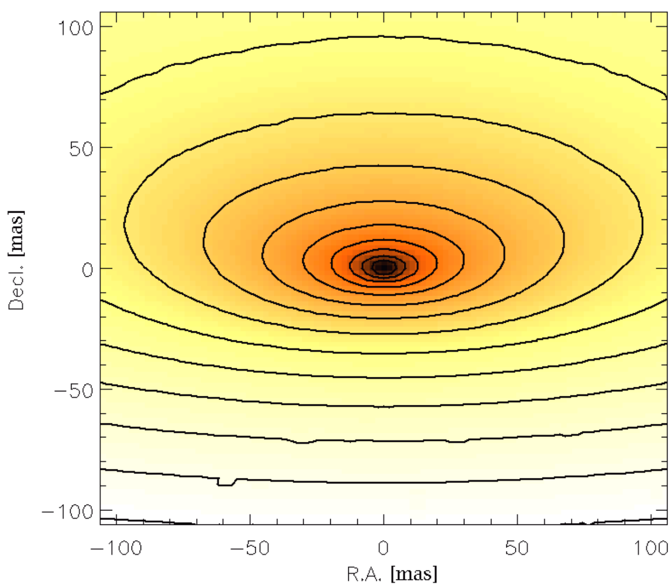

Simulated 10μm intensity map of the inner 30AU×30AU region of a circumstellar T Tauri disk at an assumed distance of 140 pc; inclination angle: 60°.

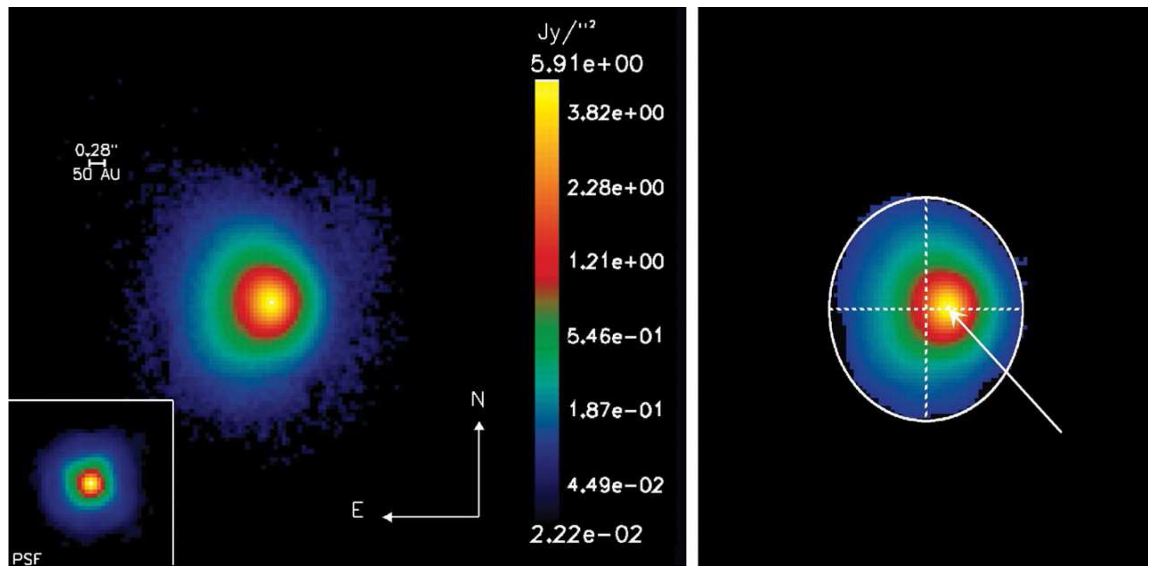

Left: VISIR false-color image of the emission from the circumstellar material surrounding the HAe star HD97048. The emission is widely extended, as compared with the point spread function (inset) obtained from the observation of a pointlike reference star.
Right: Same image as in the middle, but with a cut at the brightness level and a fit of the edge of the image by an ellipse (Lagage et al. 2006).

Planet-Disk Interaction

Size scales

IRAS 04302+2247
„Butterfly Star“

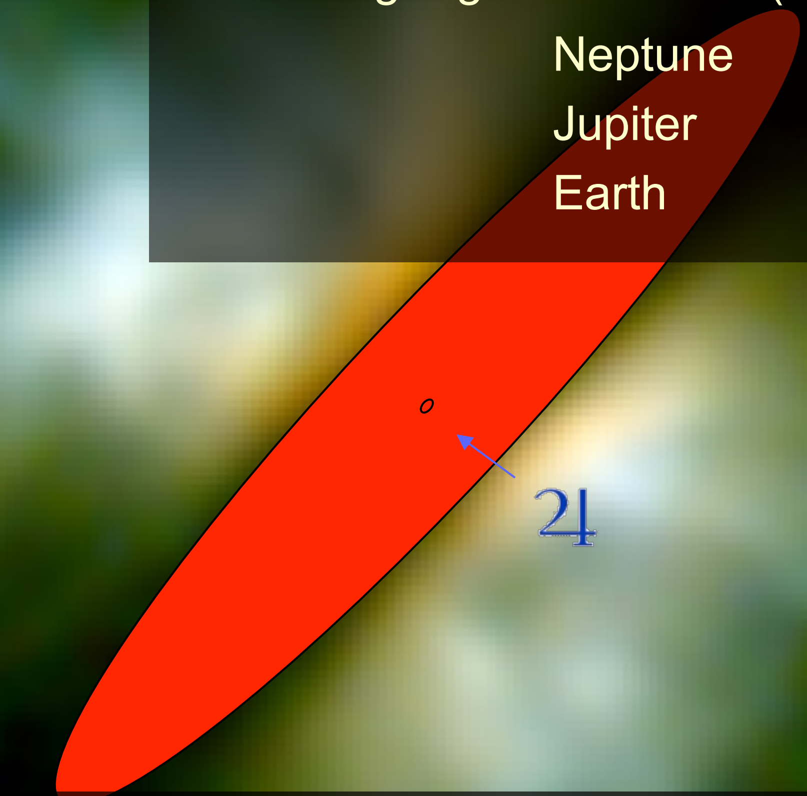

Solar System

Angular diameter of the orbits of selected Solar System planets as seen from the distance of the nearby star-forming region in Taurus (140pc) :

Neptune	-	0.43”
Jupiter	-	0.074”
Earth	-	0.014”

What is possible? – TODAY

AMBER / VLTI	~ a few mas	[near-IR]
MIDI / VLTI	~ 10 – 20 mas	[N band: ~8-13μm]
SMA	~ 0.3” (goal: 0.1”)	[~submm]

Size scales

IRAS 04302+2247
„Butterfly Star“

Solar System

Angular diameter of the orbits of selected Solar System planets as seen from the distance of the nearby star-forming region in Taurus (140pc) :

Neptune	-	0.43”
Jupiter	-	0.074”
Earth	-	0.014”

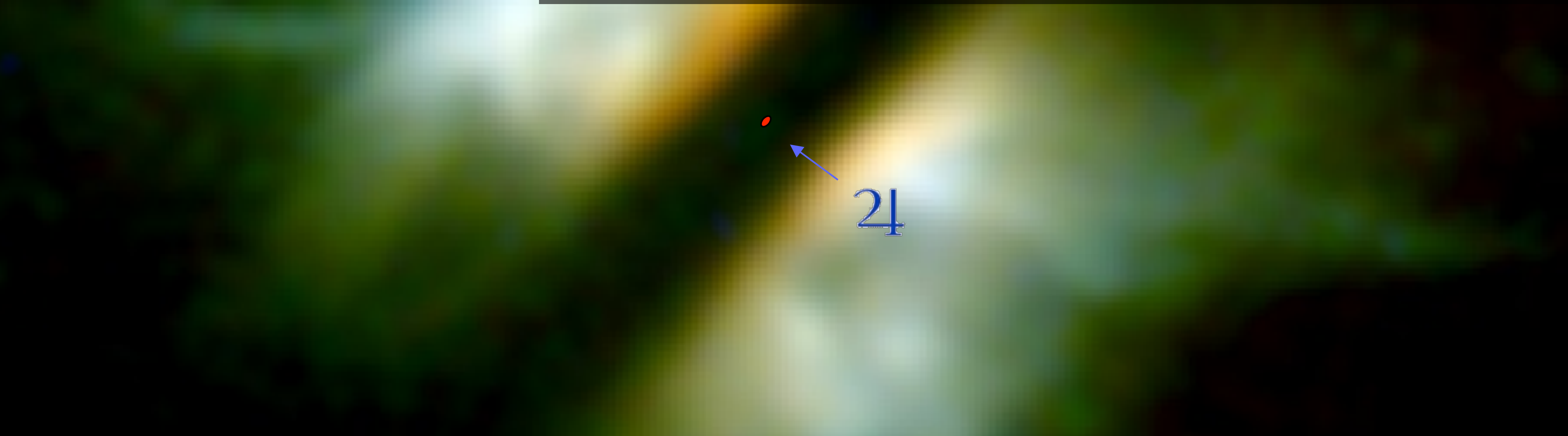

What is possible? – WITHIN THE NEXT DECADE (examples)

VSI / VLTI	~ a few mas	[near-IR]	4-6 telescopes; image reconstruction
MATISSE / VLTI	~ 3 – 20 mas	[L/M/N bands: ~3-13μm]	
ALMA	~ 20 mas	[~submm]	

Tracing Planets in young, gas-rich disks

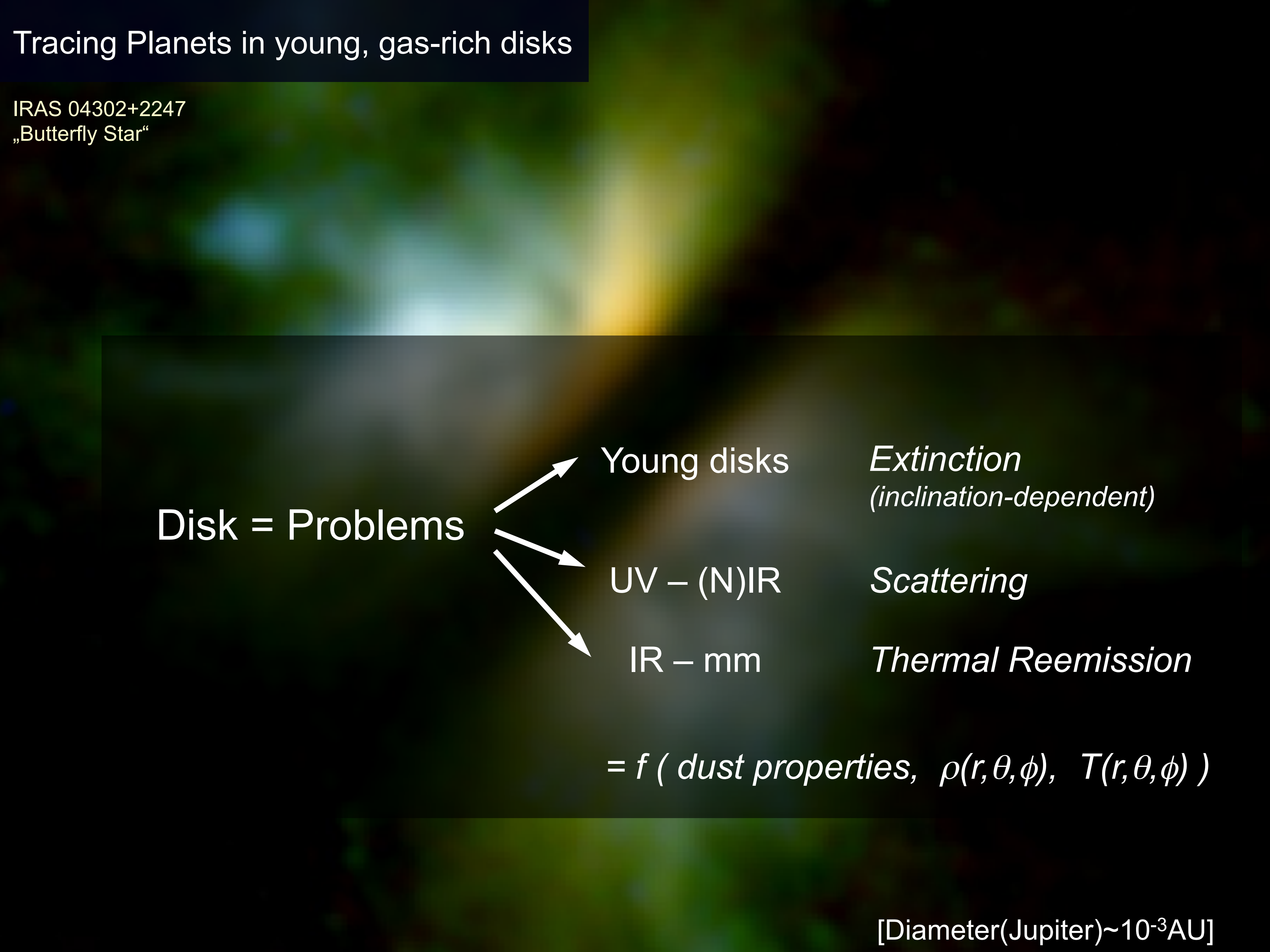

IRAS 04302+2247
„Butterfly Star“

Disk = Problems

→	Young disks	*Extinction* *(inclination-dependent)*
→	UV – (N)IR	*Scattering*
→	IR – mm	*Thermal Reemission*

$= f\,(\text{ dust properties},\ \rho(r,\theta,\phi),\ T(r,\theta,\phi)\ )$

[Diameter(Jupiter)~10^{-3}AU]

Disk-Planet Interaction

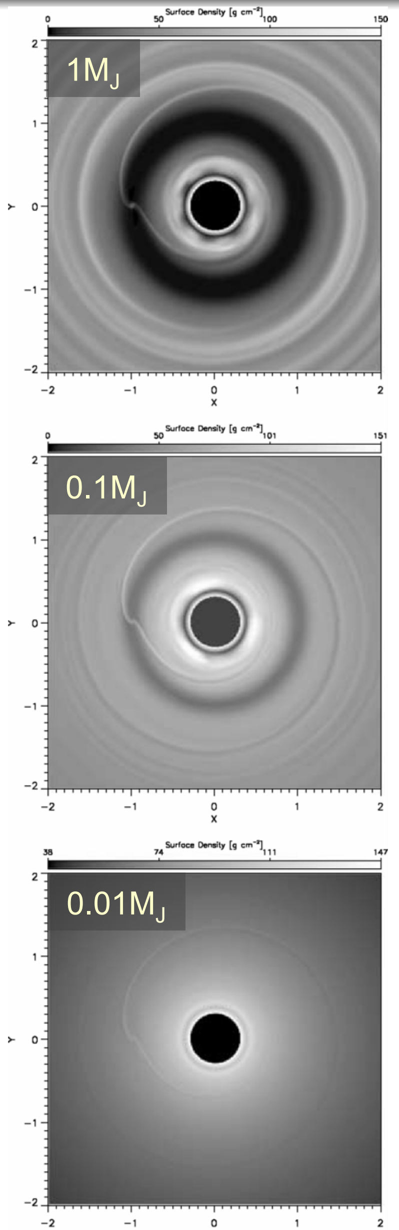

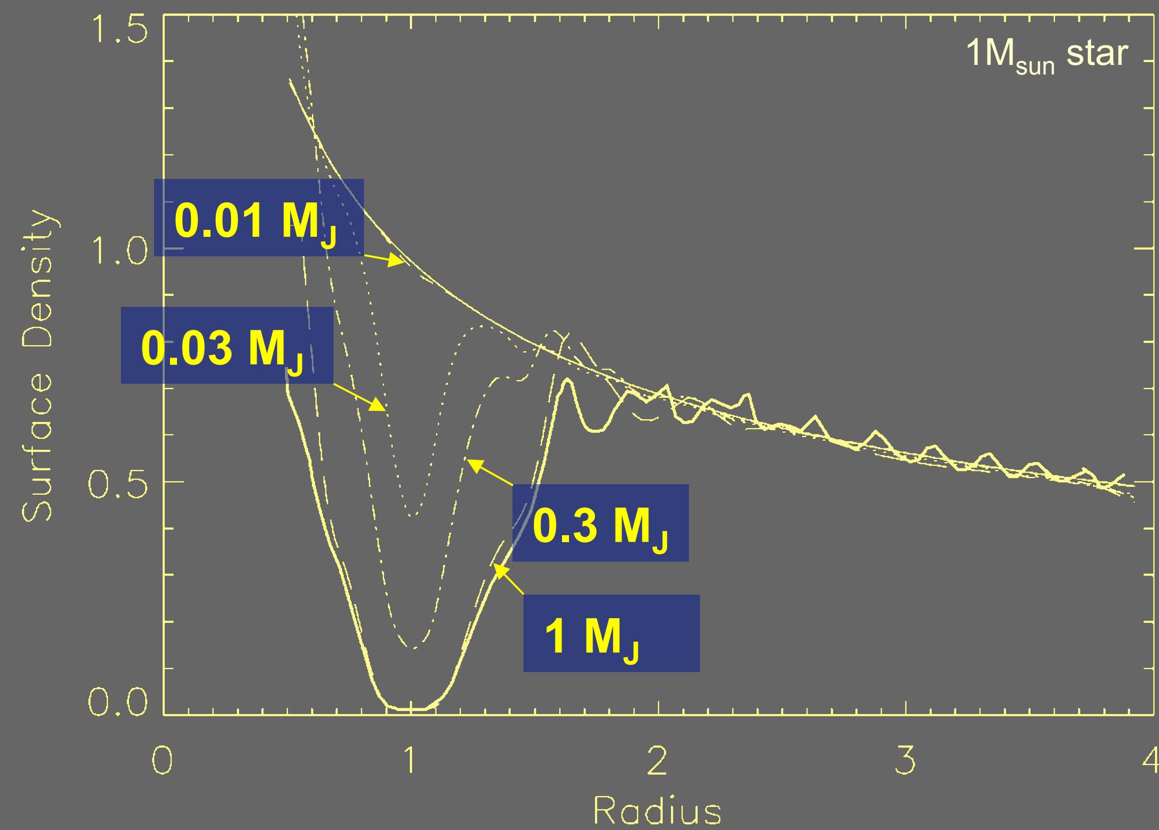

Figure 2. The final azimuthally averaged disc surface density for planets with masses of 1 (long-dashed), 0.3 (dot-dashed), 0.1 (dotted), 0.03 (short-dashed) and 0.01 (thin solid) M_J. Only planets with masses $M_p \gtrsim 0.1\ M_J$ ($M_p \gtrsim 30\ M_\oplus$) produce significant perturbations. The thick solid line gives the result for a 1-M_J planet from the two-dimensional calculations of Lubow et al. (1999).

[Bate et al. 2003]

ALMA: Gaps

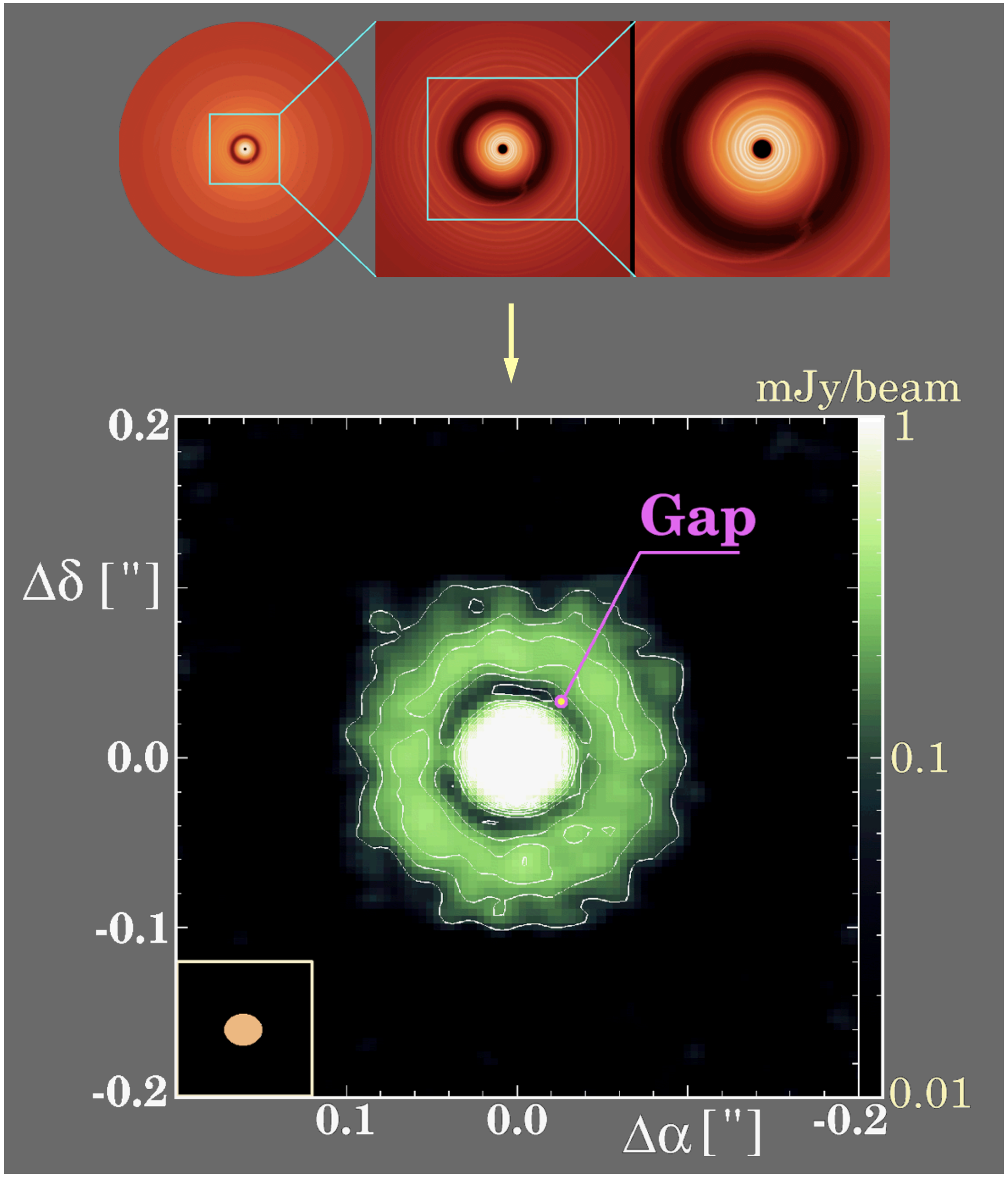

Jupiter
in a 0.05 M_{sun} disk
around
a solar-mass star
as seen with ALMA

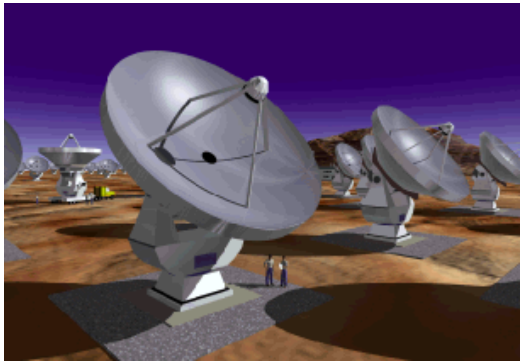

d=140pc

Baseline: 10km

λ=700μm, t_{int}=4h

[Wolf et al. 2002]

Planetary Accretion Region

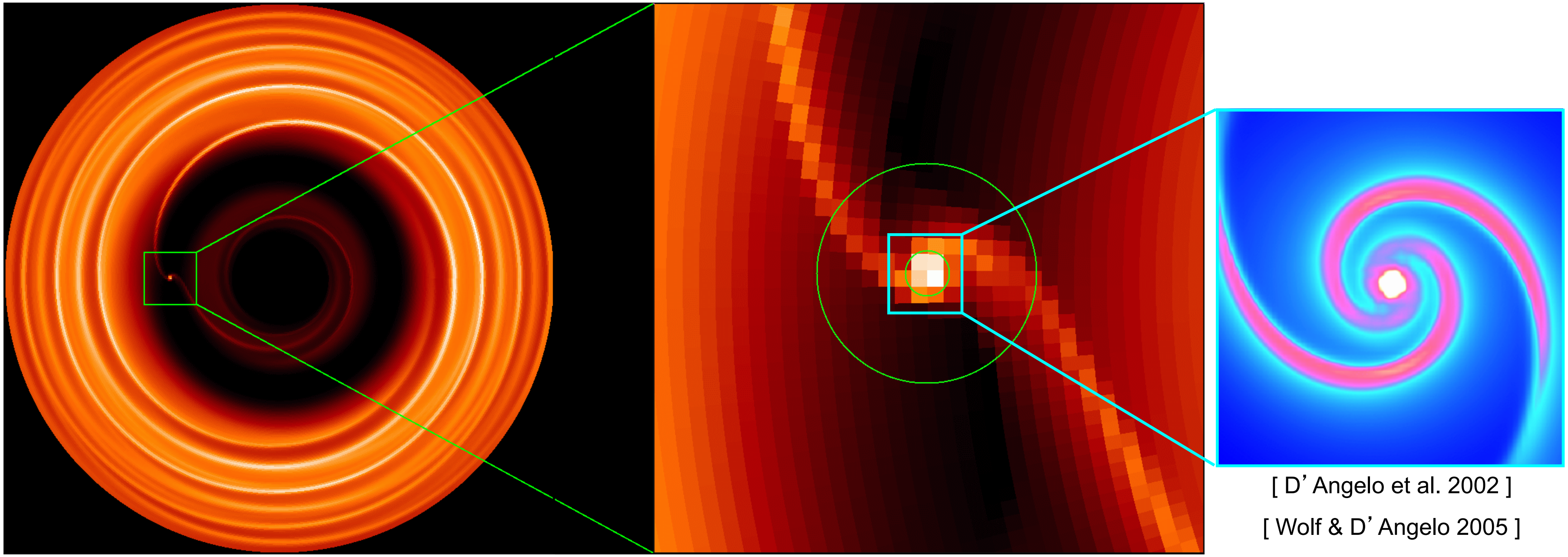

[D’Angelo et al. 2002]

[Wolf & D’Angelo 2005]

Procedure

Density Structure

↓

Stellar heating

↓

Planetary heating

↓

Prediction of Observation

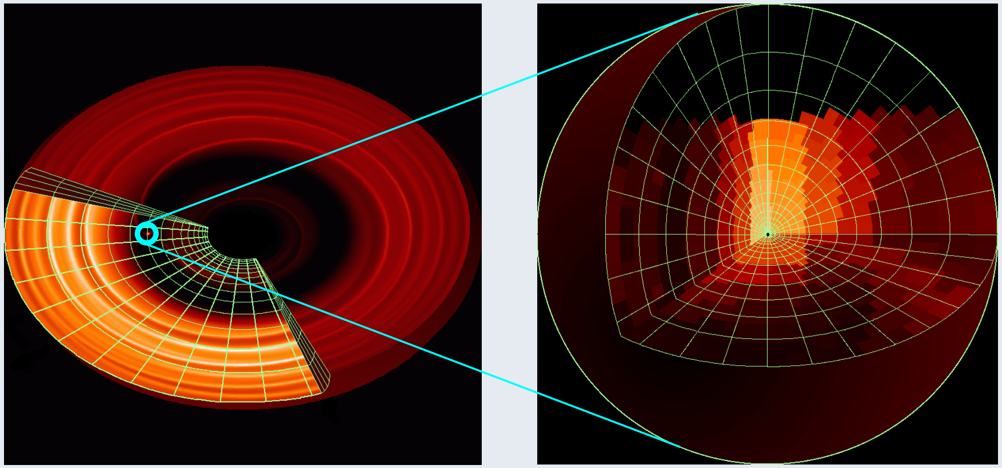

Close-up view: Planetary Region

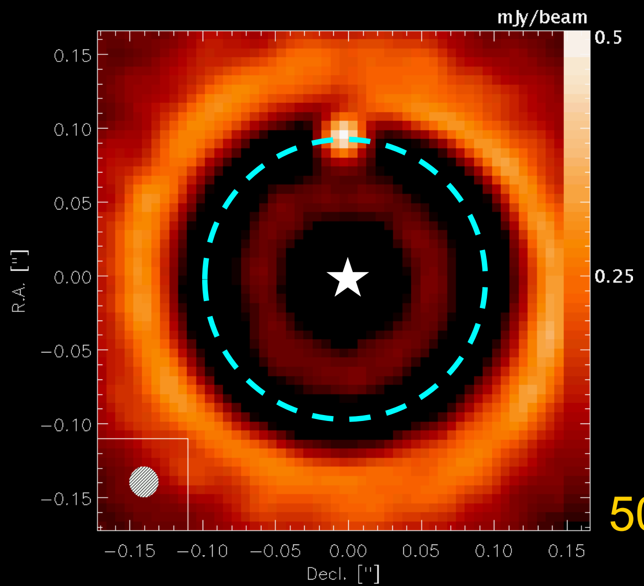

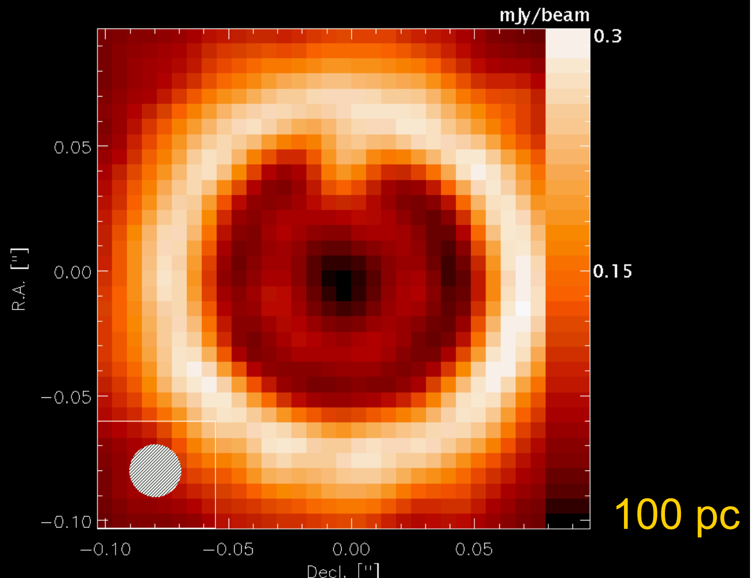

[Wolf & D' Angelo 2005]

$M_{planet} / M_{star} = 1 M_{Jup} / 0.5\ M_{sun}$

Orbital radius: 5 AU

Disk mass as in the circumstellar disk around the Butterfly Star in Taurus

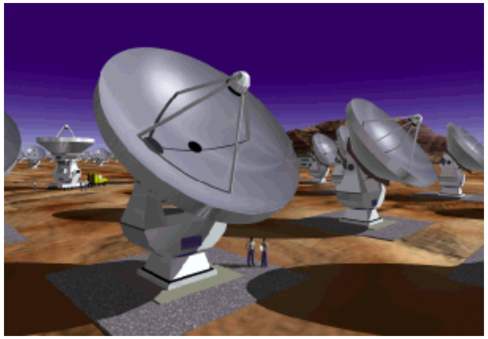

Maximum baseline: 10km, 900GHz, t_{int}=8h

Random pointing error during the observation: (max. 0.6"); Amplitude error, "Anomalous" refraction; Continuous observations centered on the meridian transit; Zenith (opacity: 0.15); 30° phase noise; Bandwidth: 8 GHz

Shocks & MRI

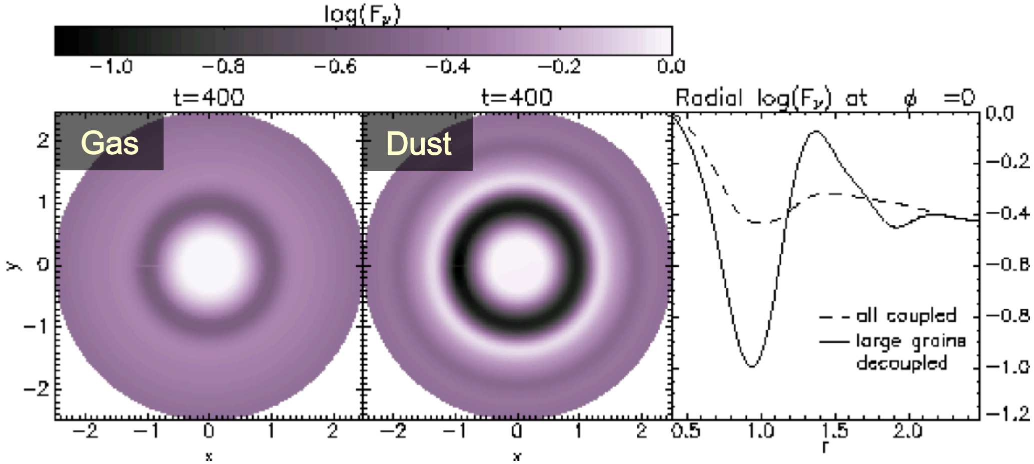

Fig. 3. Logarithm of flux densities at 1 mm, normalized by the maximum and convolved with a Gaussian of FWHM 2.5 AU, corresponding to a resolution of 12 mas at 140 pc. Left panel: all particles follow the gas exactly (static dust evolution). Middle panel: particles larger than the critical size decouple from the gas (dynamic dust evolution). Right panel: the corresponding radial flux densities.

[PaardeKooper & Mellema 2004]

Strong spiral shocks near the planet are able to decouple the larger particles (>0.1mm) from the gas

→ **Formation of an annular gap in the dust, even if there is no gap in the gas density.**

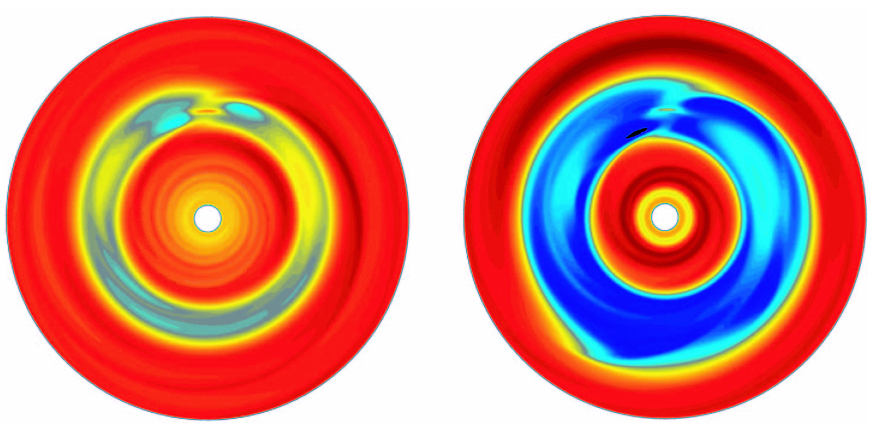

Log Density in MHD simulations after 100 planet orbits for planets with relative masses of $q=1\times10^{-3}$ and 5×10^{-3} [Winters et al. 2003]

MHD simulations - Magnetorotational instability

- gaps are *shallower* and *asymmetrically wider*
- rate of gap formation is *slowed*

→ Observations of gaps will allow to constrain the physical conditions in circumstellar disks

Complementary Observations: Mid-IR

Hot Accretion Region around the Planet

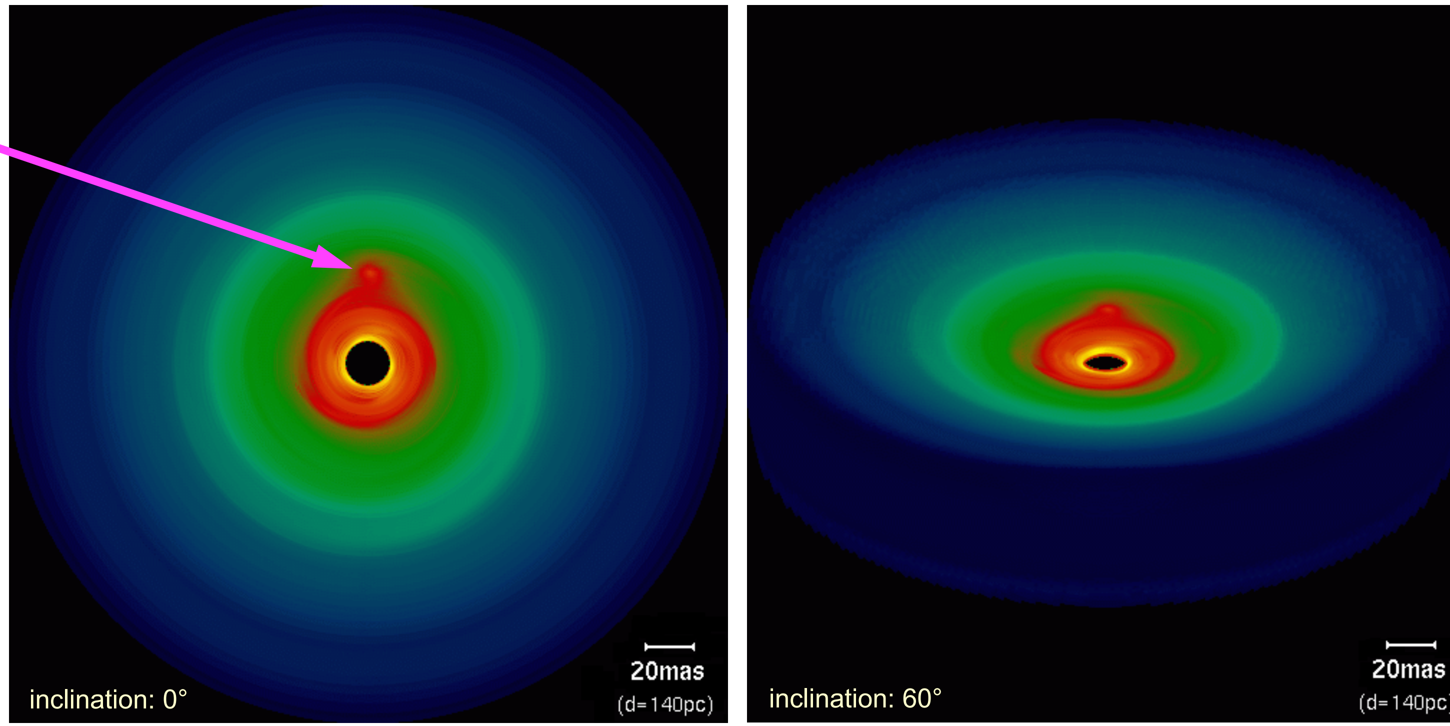

10µm surface brightness profile of a T Tauri disk with an embedded planet (inner 40AUx40AU, distance: 140pc)

[Wolf et al. 2007]

MATISSE @ Very Large Telescope Interferometer

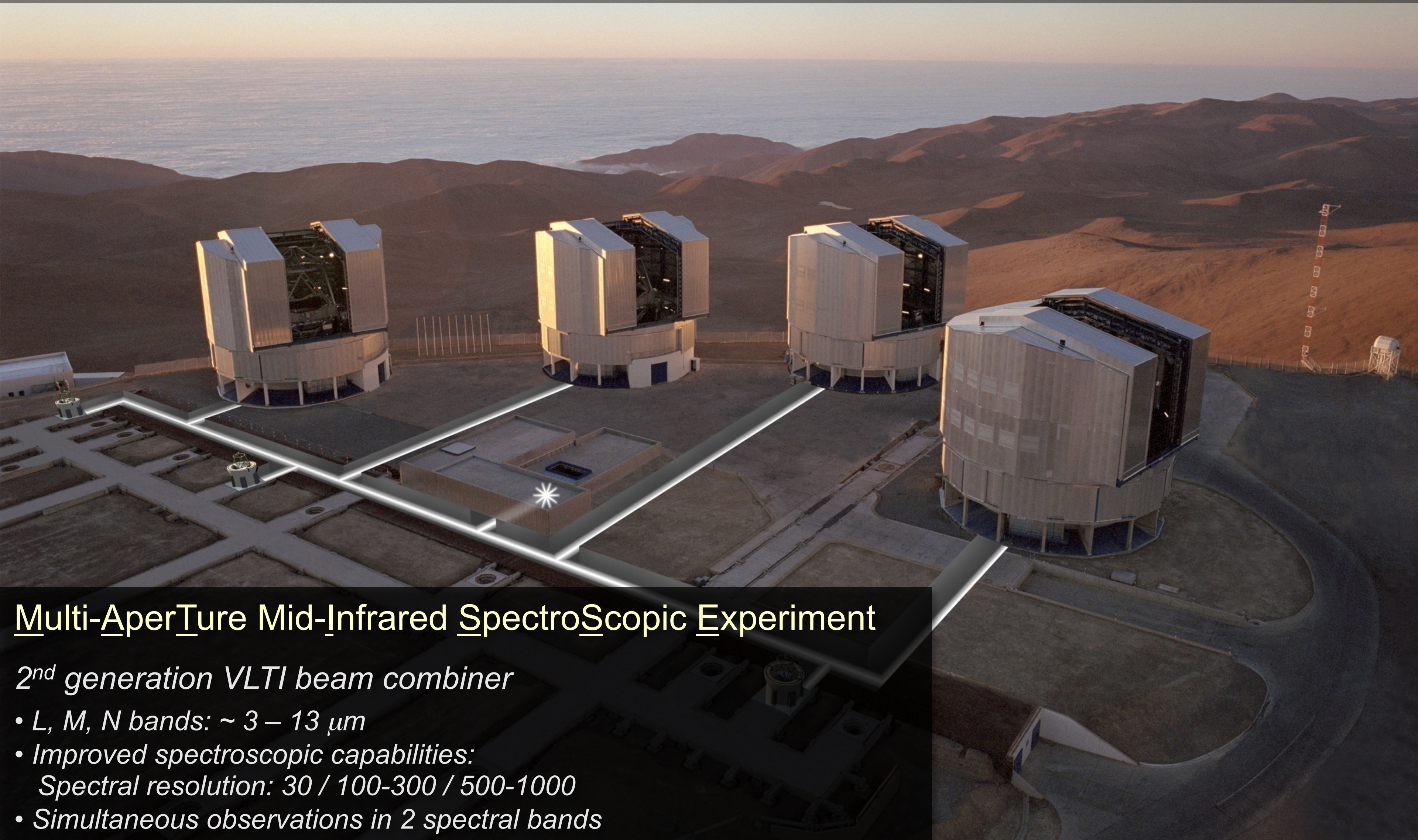

Multi-AperTure Mid-Infrared SpectroScopic Experiment

2nd generation VLTI beam combiner

- *L, M, N bands: ~ 3 – 13 μm*
- *Improved spectroscopic capabilities:*
  Spectral resolution: 30 / 100-300 / 500-1000
- *Simultaneous observations in 2 spectral bands*

MATISSE

Goal: Thermal reemission images with an angular resolution of 0.003“

ESO

MATISSE – Planets

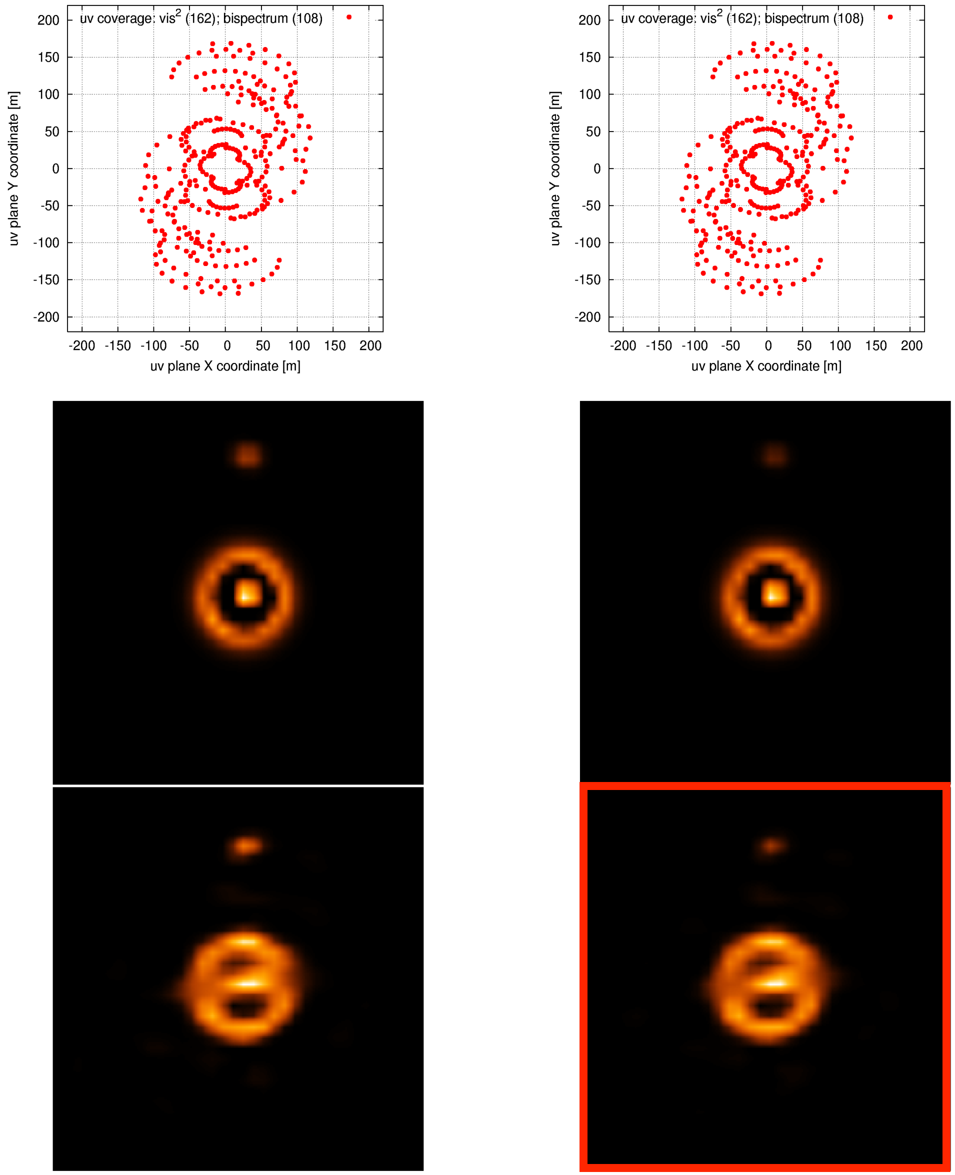

Figure 6: Reconstructed N band images (3x4ATs; ∼ 150 m) of a protoplanetary disk with an embedded planet (see Fig. 5[right]). Left: Brighter planet: intensity ratio star/planet=100/1; Right: Fainter planet: intensity ratio star/planet=200/1. First row: uv coverages Second and third row: originals and reconstructions, respectively. The images are not convolved (2x super resolution). Simulation parameter: modelled YSO with planet (declination -30°; observing wavelength 9.5 μm; FOV = 104 mas; 1000 simulated interferograms per snap shot with photon and 10 μm sky background noise (average SNR of visibilities: 20). See Doc. No. VLT-TRE-MAT-15860-5001 for details.

Hot Accretion Region around the Planet

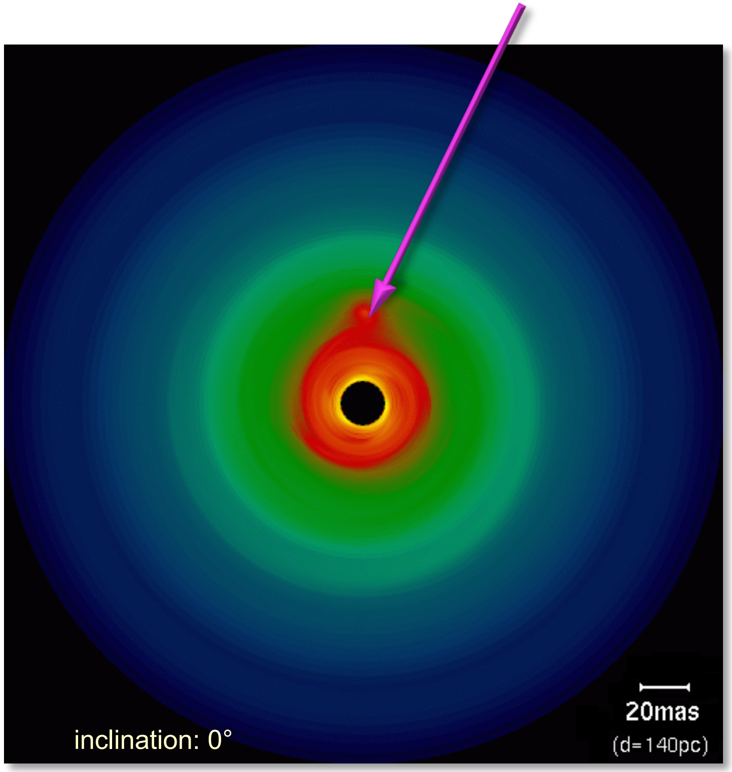

[Wolf et al. 2005-2007]

Scattered light images (II): Surface Structure

[Wolf & Klahr]

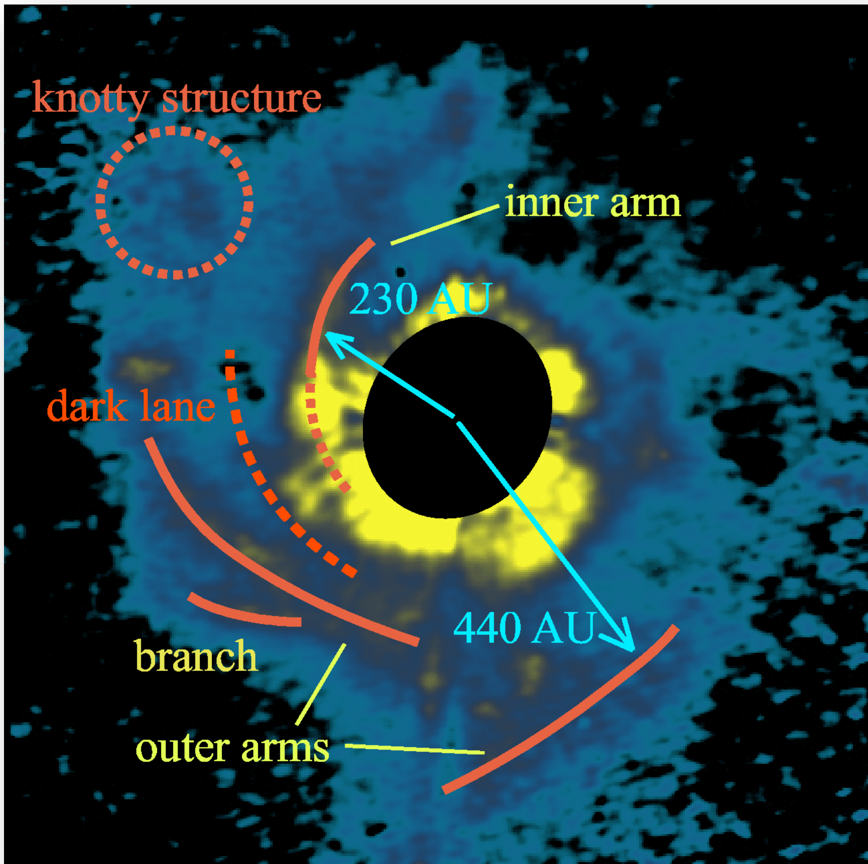

AB Aurigae

Spiral arm structure: H band

(Herbig Ae star; Fukagawa et al. 2004; SUBARU)

Distance: ~140 pc

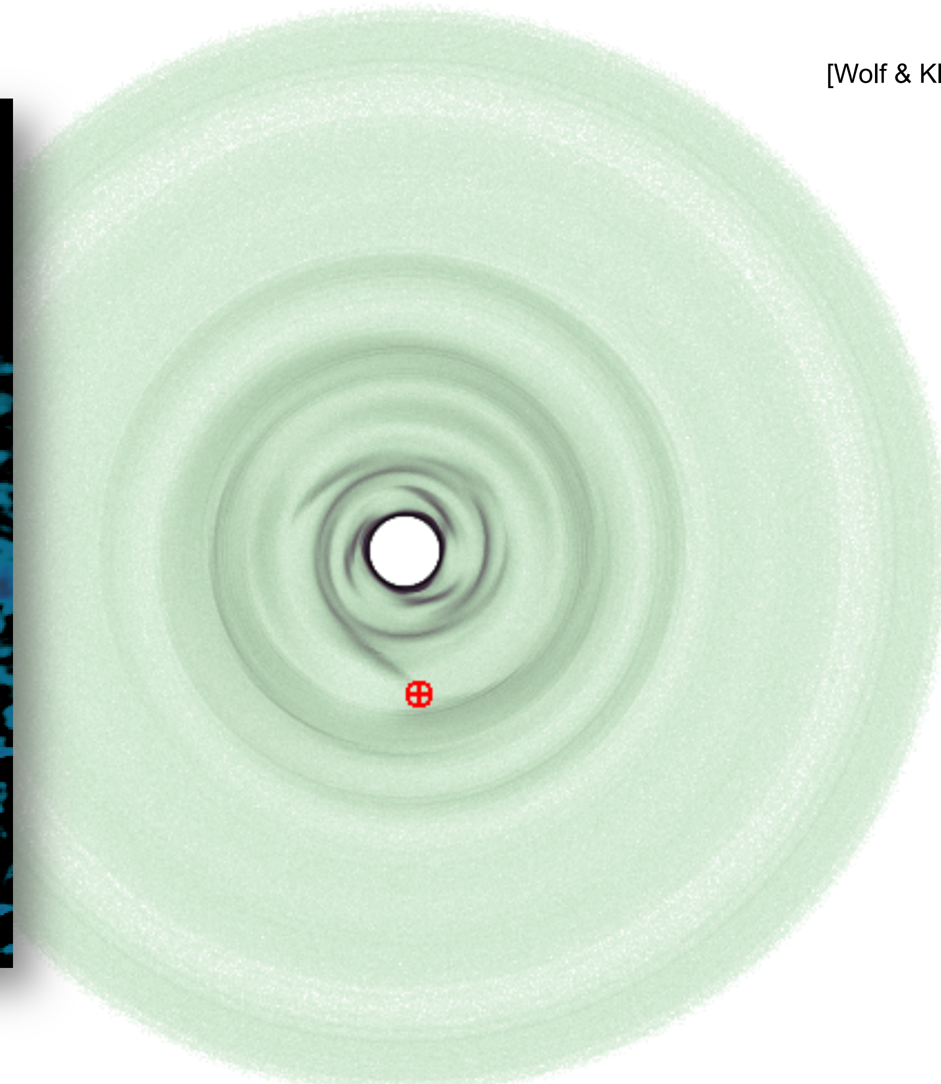

K band scattered light image (Jupiter/Sun + Disk)
[Disk radius: 20AU]

Scattered light images (II): Surface Structure

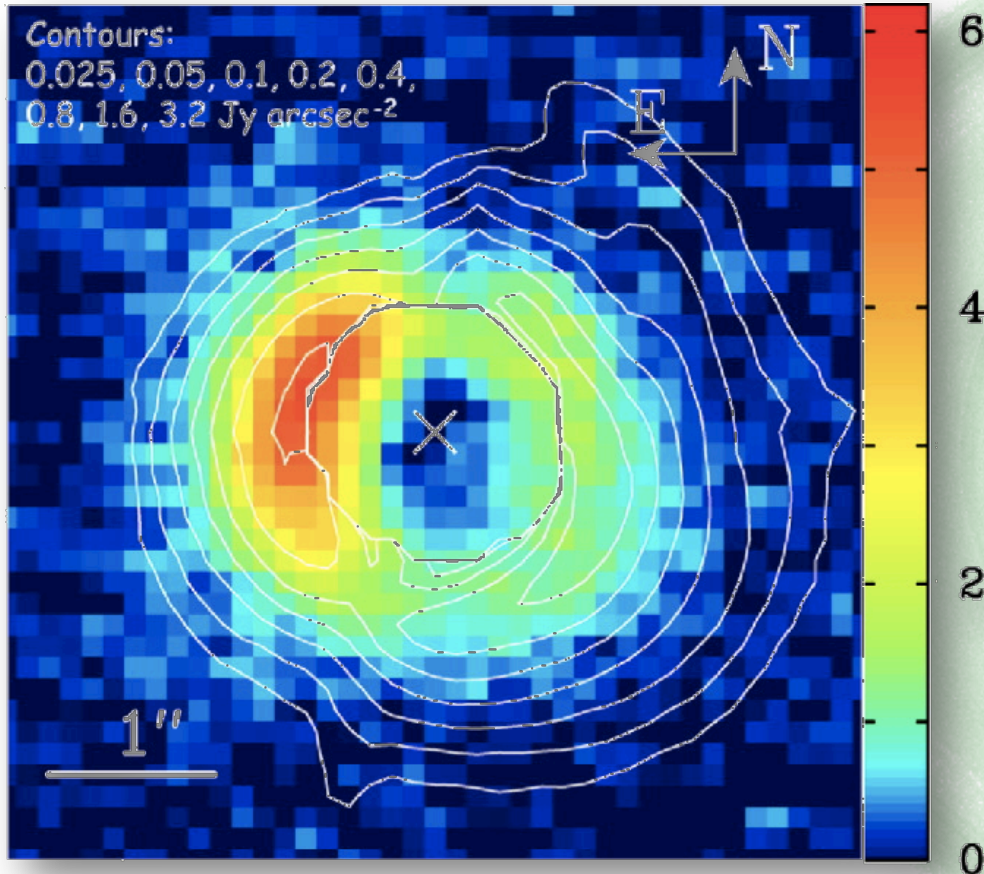

AB Aurigae

Asymmetry (Color: 24.5μm, Contours: H Band)

(Herbig Ae star; Fujiwara et al., 2006, SUBARU)

Distance: ~140 pc

[Wolf & Klahr]

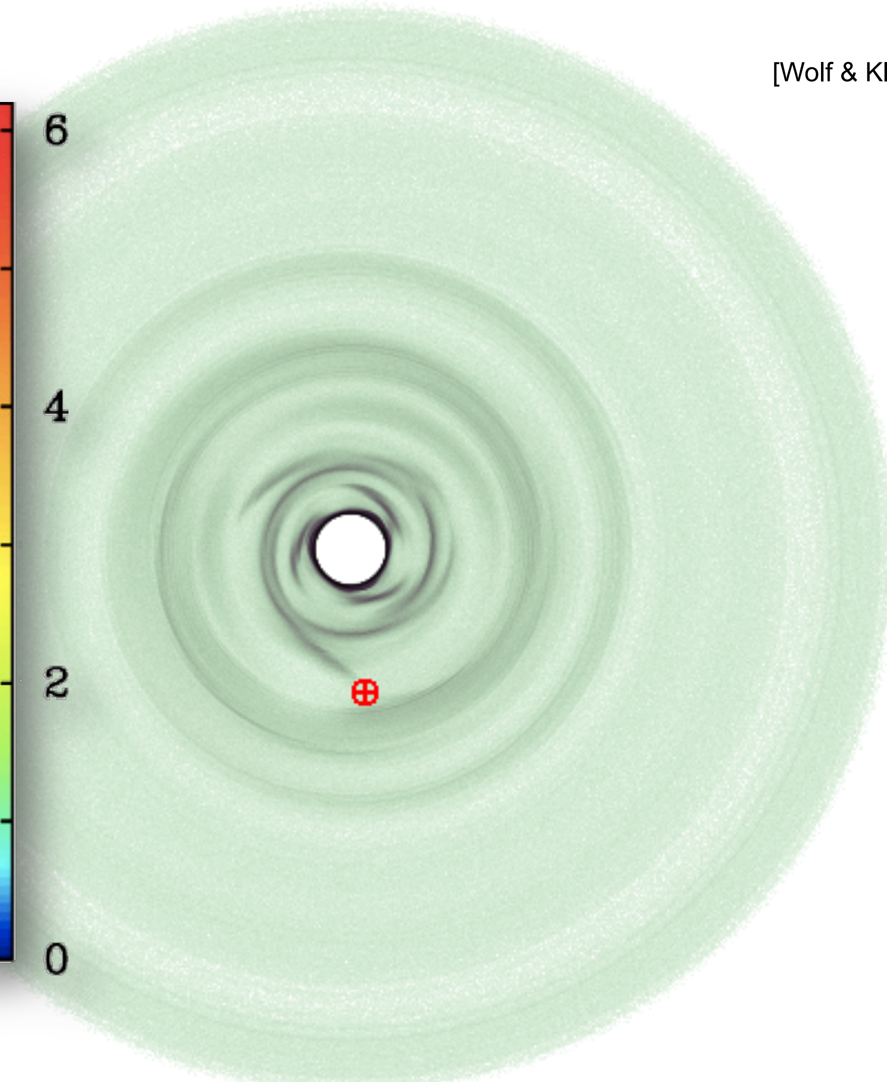

K band scattered light image (Jupiter/Sun + Disk)
[Disk radius: 20AU]

Scattered light images (II): Surface Structure

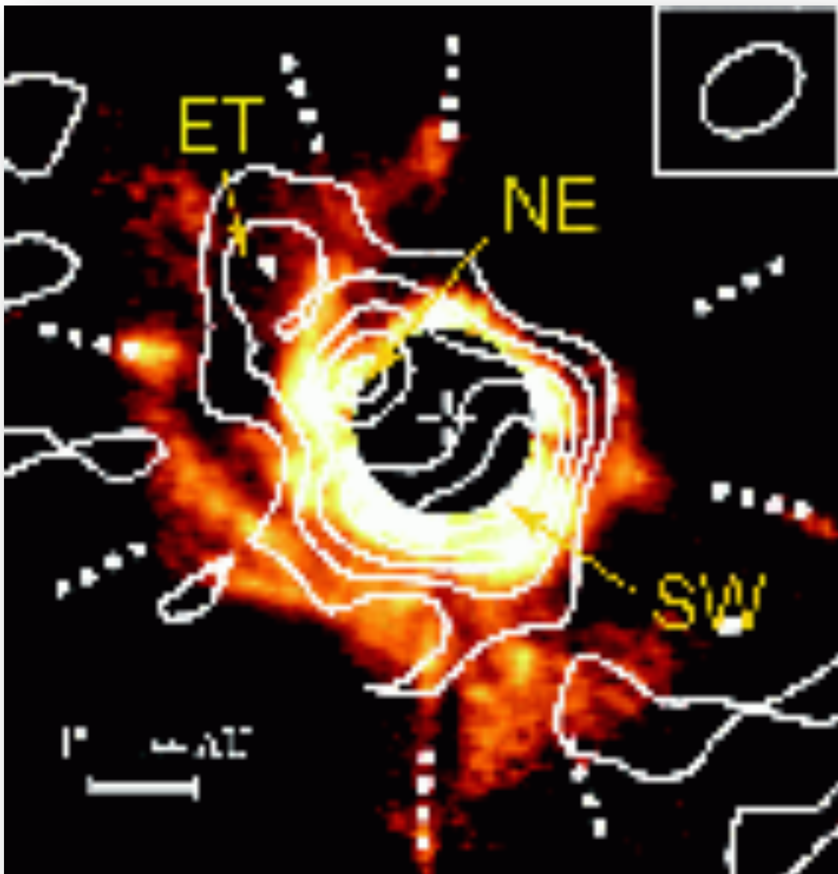

AB Aurigae

Spiral (345 GHz, continuum)

(Herbig Ae star; Lin et al., 2006, SMA)

Distance: ~140 pc

[Wolf & Klahr]

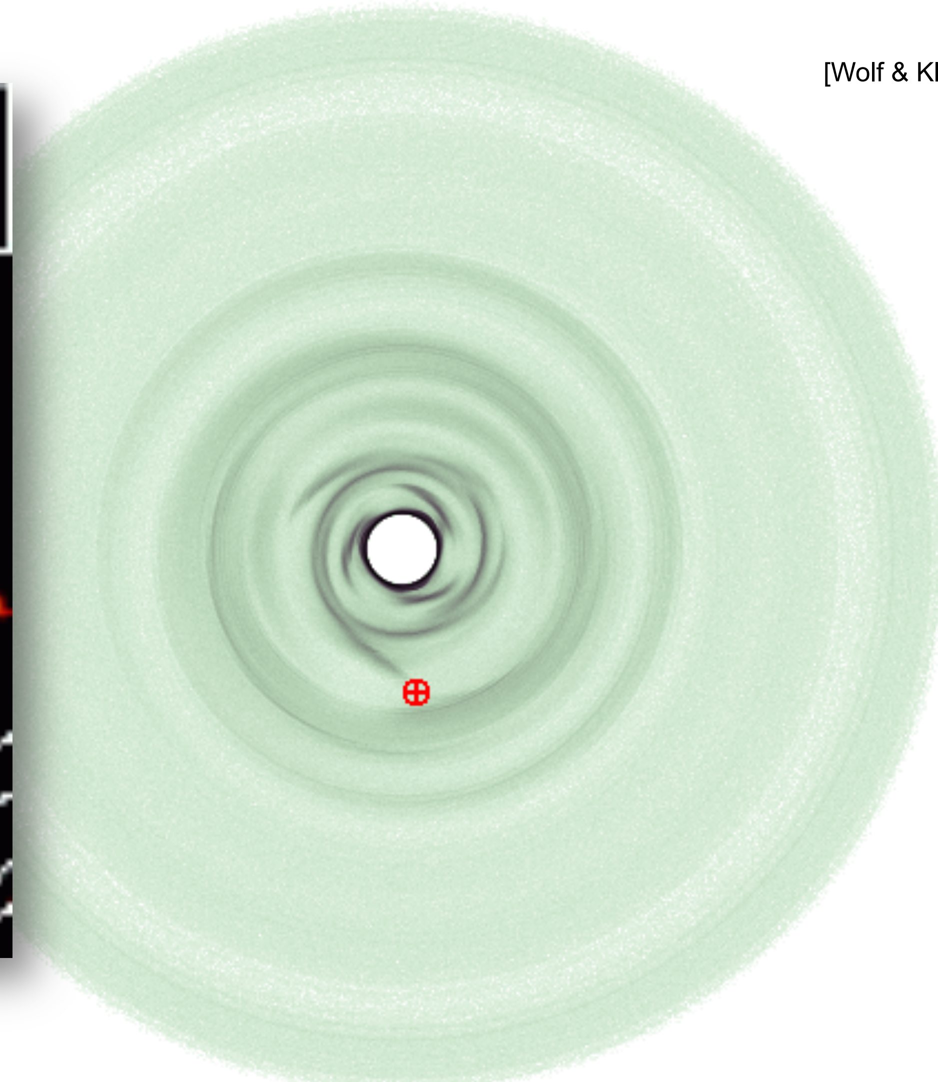

K band scattered light image (Jupiter/Sun + Disk)
[Disk radius: 20AU]

Shadow – Astrometry

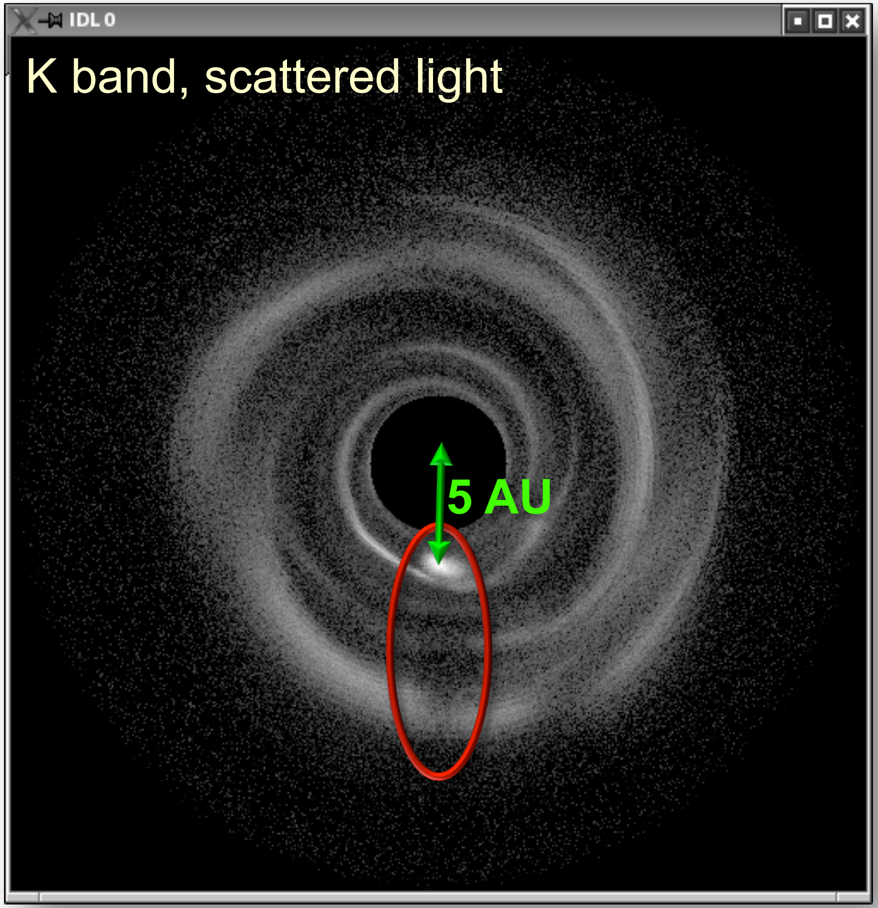

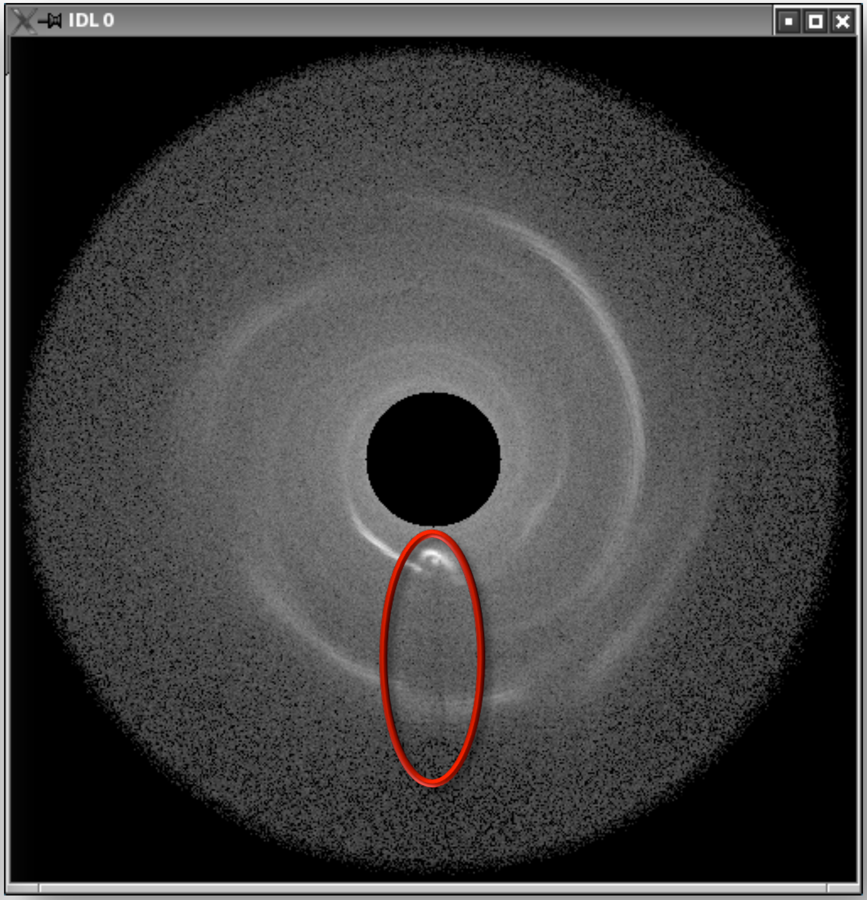

[Wolf & Klahr]

Conditions for the occurrence of a significantly large / strong shadow still have to be investigated

Planetary signatures in the near-IR?

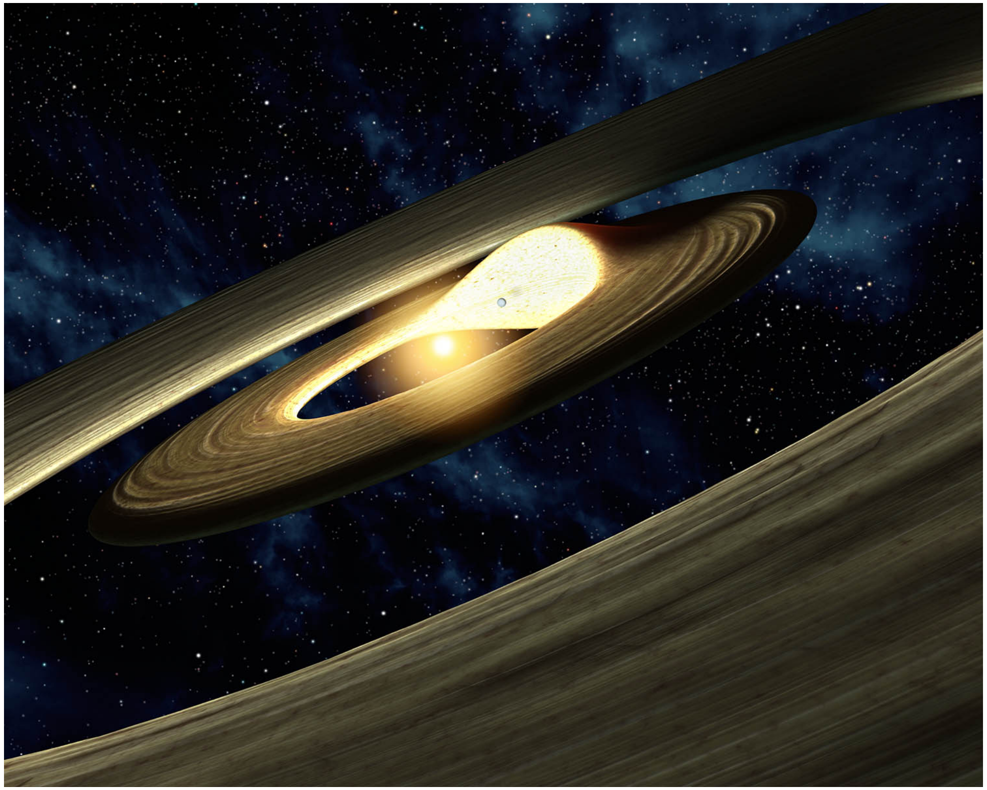

Artist impression of the disk around LRLL 31. A planet in the innermost region influences the disk to cast a large shadow on the outer region. The orbit of the planet, and thus the shadow, causes the disk to be variable in the near infrared on timescales on the order of one week. Picture credits: NASA.

Observation
Variability of T Tauri stars
on time scales < 1 year

Various interpretations

- Clumpy inner circumstellar shell/disk structure
- Variable stellar accretion rate
  ⇒ variable net luminosity
  ⇒ variable inner disk structure / disk illumination
- Embedded stellar or planetary companion
  => dynamical perturbation (short-term)

Example
Transitional disk LRLL 31 in the 2-3Myr old star-forming region IC 348:
Variations of the near-IR and N band spectra on a few months timescale
[Muzerolle et al. 2009]

Observational basis: Spitzer/IRS 5-40μm observations, 6 months (Houck et al. 2004); further Spitzer/MIPS observations (Muzerolle et al. 2009) + SpeX/IRTF, SPOL (Spectro-polarimeter; Steward observatory) spectroscopic measurements

Differential Polarimetry

Goal

High-resolution, high-contrast (large dynamic range) imaging of disks, seen face-on (problem: star dominates)

Technique

Based on high contrast between polarized and unpolarized fraction of scattered radiation (disk) and unscattered radiation (direct stellar radiation)

- Scattered radiation: $P_l > 0$
- Direct stellar radiation: $P_l = 0$
- Differential images (Q, U):
  - show only scattering medium (dust disk);
  - the otherwise dominating stellar light is canceled out

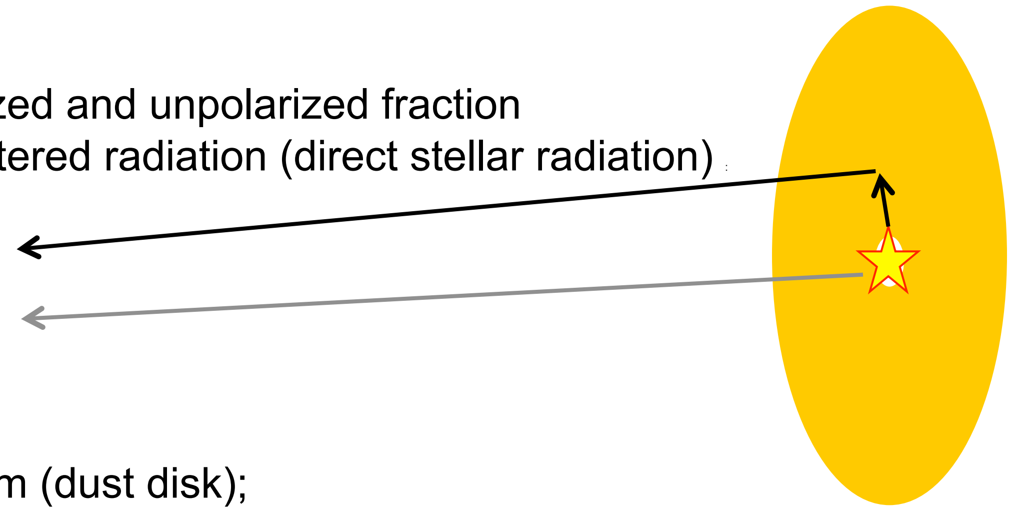

Example

Apai et al. 2004: Circumstellar Disk of TW Hya:

Radial density profil as close as 0.1" to the central star

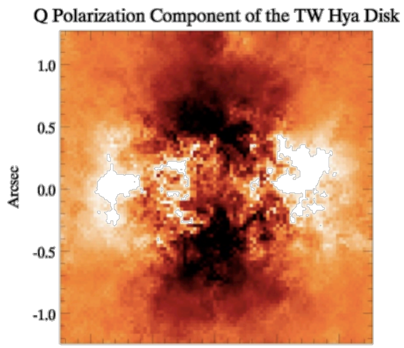

Differential Polarimetry

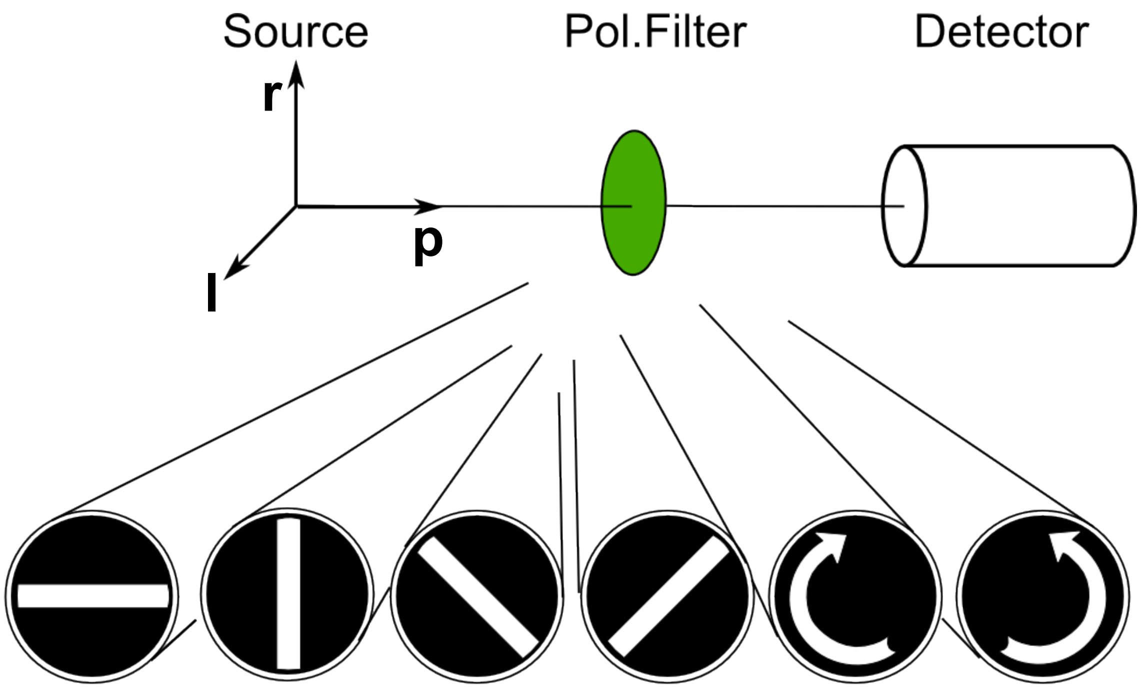

$I_\perp$ $I_\parallel$ I_+ I_- I_R I_L

$I = I_\perp + I_\parallel$ $Q = I_\perp - I_\parallel$ $U = I_+ - I_-$ $V = I_R - I_L$

[based on figure by G. Bertrang]

Degree of linear polarization

$$P_{\text{lin}} = \sqrt{\frac{Q^2 + U^2}{I^2}}$$

Degree of circular polarization

$$P_{\text{zirk}} = \frac{V}{I}$$

Orientation:

$$\tan 2\gamma = \frac{U}{Q}$$

$$(0^\circ \le \gamma \le 180^\circ)$$

Differential Polarimetry

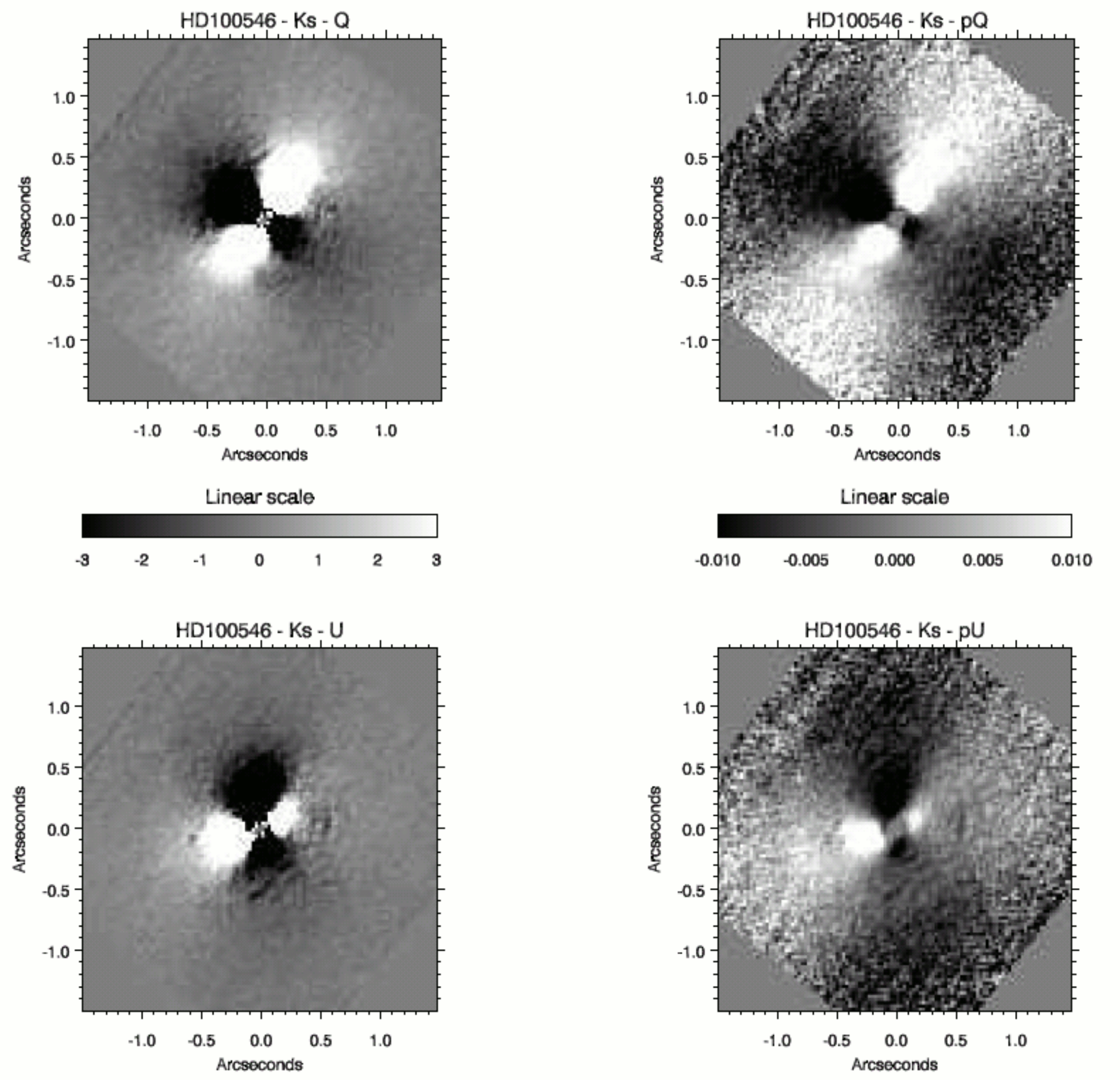

Example:

NACO PDI observations of the disk around HD100546 (Quanz et al. 2011)

Final Stokes Q and U images (count rates in arbitrary units, left column) and fractional polarization pQ and pU (right column) of HD100546 in the H filter. The core of the PSF, where the count rate was no longer in the linear detector regime in at least one of the individual raw images before they were combined, has been masked out.

[Quanz et al., 2009]

Differential Polarimetry

- Possible problems:
  - Instrumental Polarization

    (Solution: Observation of polarization standard stars)

  - Interstellar Polarization
    - Measured polarization may be dominated by polarized light of the star forming region
    - For spatially resolved polarization maps: less of a problem, since local polarisation degree usually >> P_{ISM}
    - Important for net polarization (low / comparable to degree of interstellar polarization)

- Data analysis:

  Careful interpretation of structures in the derived maps, i.e., polarized intensity:

$$P \cdot I = \sqrt{Q^2 + U^2}$$

Polarization (P) and Net Intensity (I) of the scattered light depend on optical properties of the dust

=> Structures seen in polarized intensity are not necessarily caused by structures in the density profile (traced by the intensity)

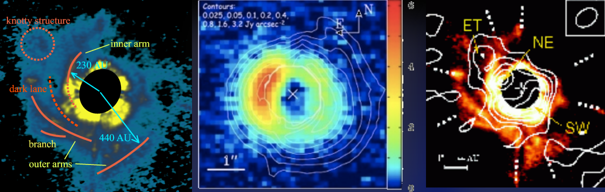

2008: Planet in the disk of AB Aurigae?

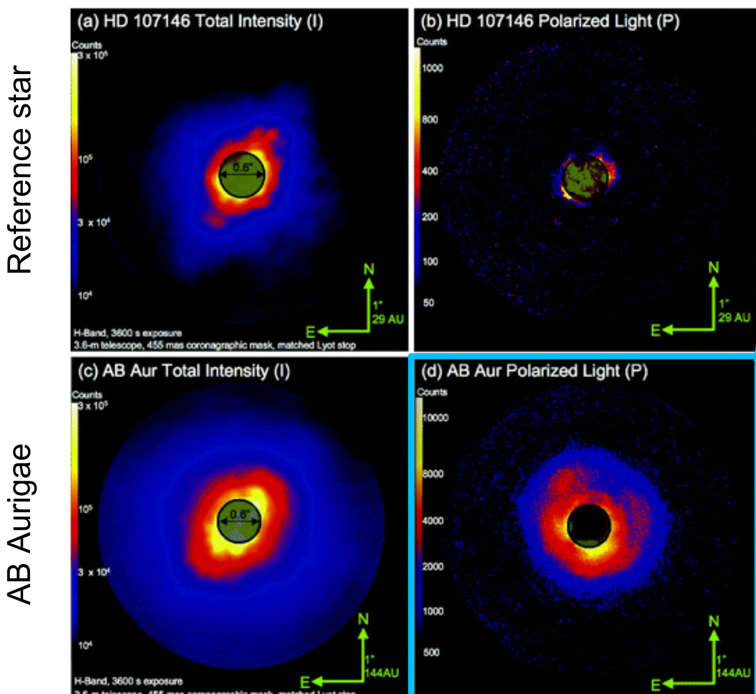

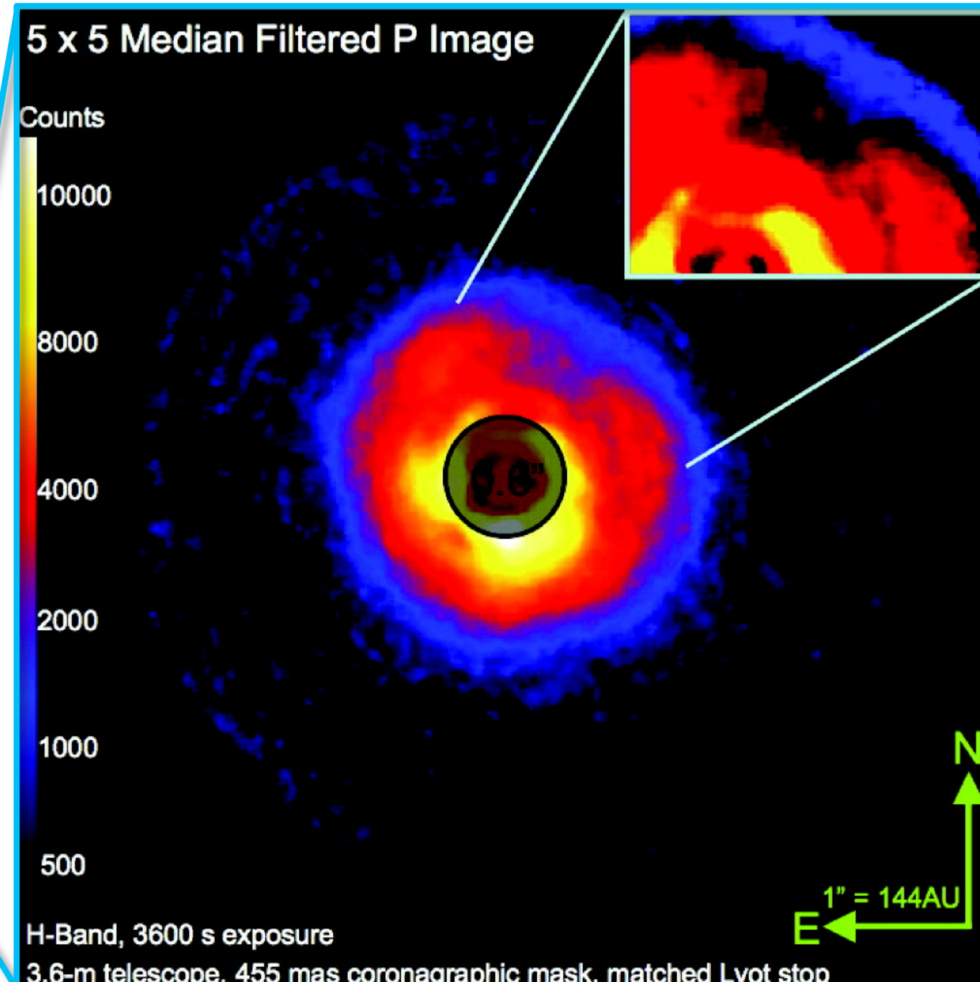

Polarized intensity: (color-coded) $P \cdot I = \sqrt{Q^2 + U^2}$

[Oppenheimer et al. 2008]

H band (3.63m AEOS telescope, Maui)

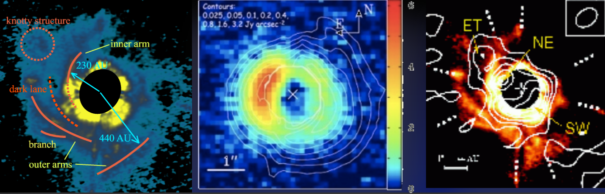

2008: Planet in the disk of AB Aurigae?

Observation

Polarized and total intensity measurements:
NICMOS: 2.0 μm imaging polarimetry and 1.1 μm imaging on angular scales of 0.3"–3" (40–550 AU)

Analysis

1. Polarized intensity map: Reproduces morphology seen by Oppenheimer et al.
2. Total intensity map: *no* evidence for a gap in either our 1.1 or 2.0 μm images
3. Region of apparent gap has lower polarization fraction, *without* a significant decrease in total scattered light

Explanation

Apparent gap (in polarized intensity): consistent with expectations for back-scattered light on the far side of an inclined disk (i.e., geometrical scattering effect)

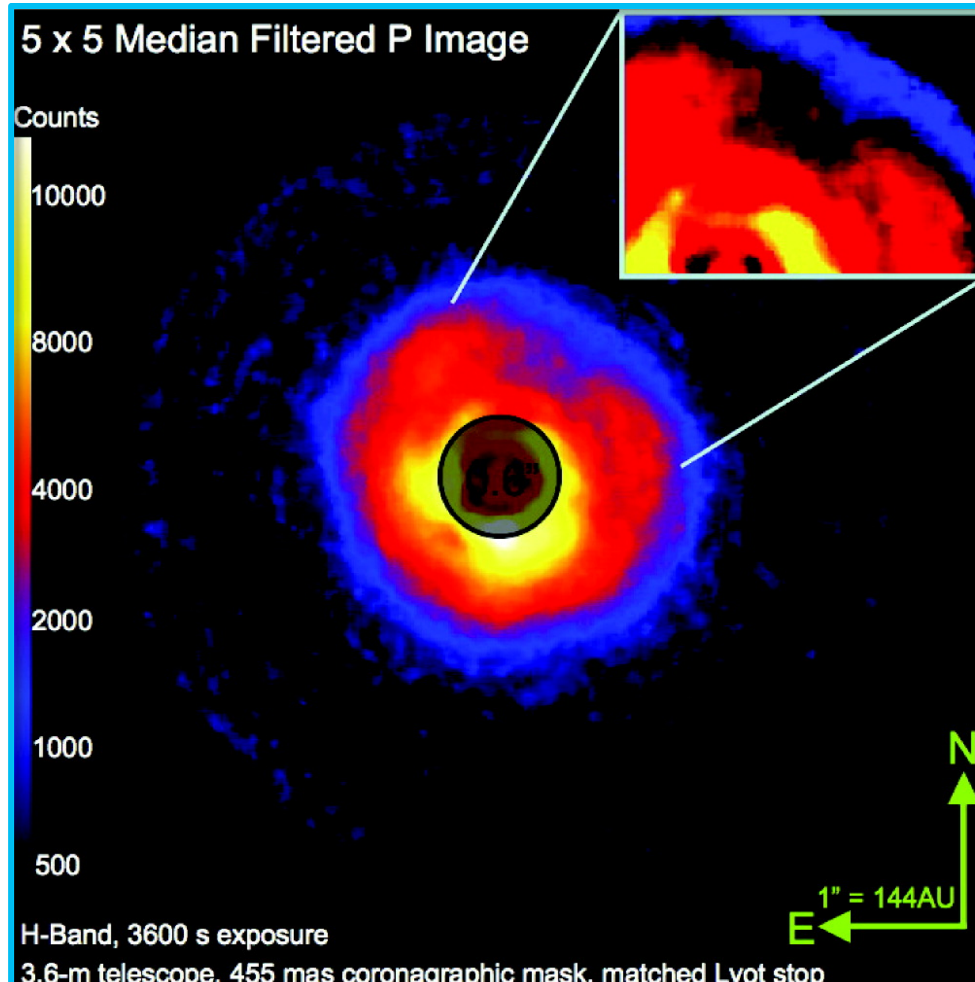

Polarized intensity: $P \cdot I = \sqrt{Q^2 + U^2}$
(color-coded)

[Oppenheimer et al. 2008]

[Perrin et al. 2009]

H band (3.63m AEOS telescope, Maui)

Not only giant planets leave their footprints …

- Potential YSO binary systems?

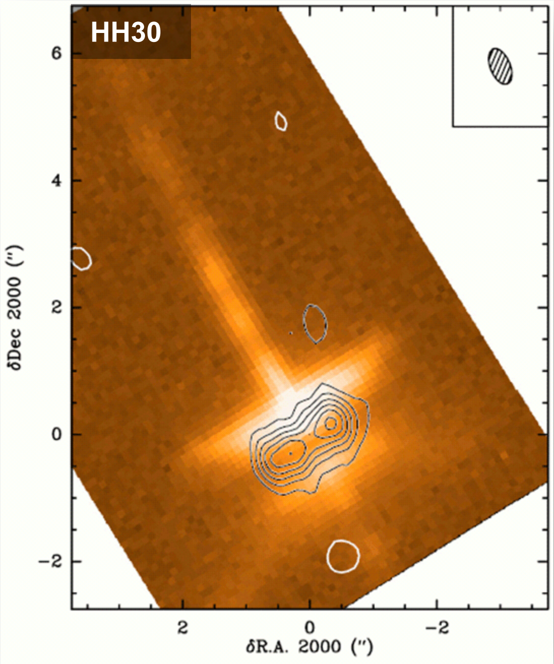

[Guilloteau et al. 2008]

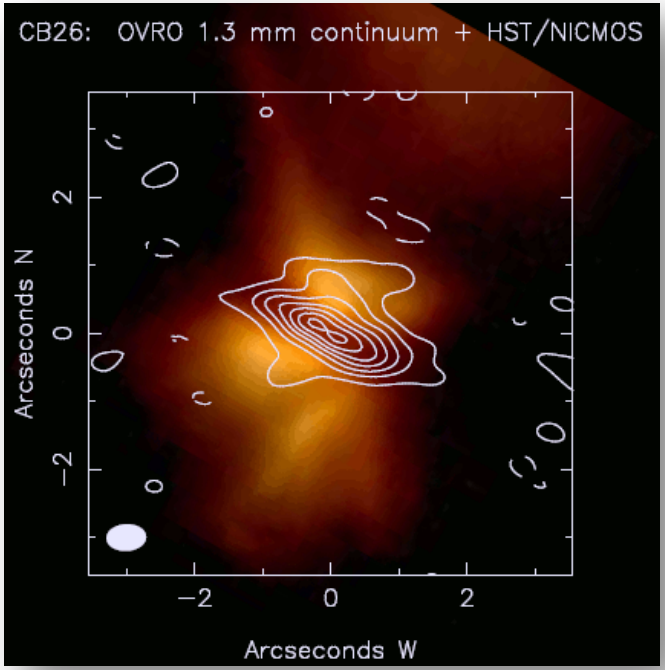

[Sauter et al. 2009]

<u>Motivation</u>
Young solar-type stars are preferentially found in multiple systems

Taurus-Auriga star forming region: 80-100% (Ghez et al. 1993, Leinert et al. 1993, Reipurth & Zinnecker 1993)

<u>Possible Indicators:</u>
Jet / Outflow wobbling

- Disk evolution:
  – Evolution of the disk structure due to the planet formation process: e.g., Grain growth, settling, radial drift
    => Changing opacity/temperature structure
    => Modified gas phase structure and chemistry
  – Disk dispersal

Life span of disks: The inner region

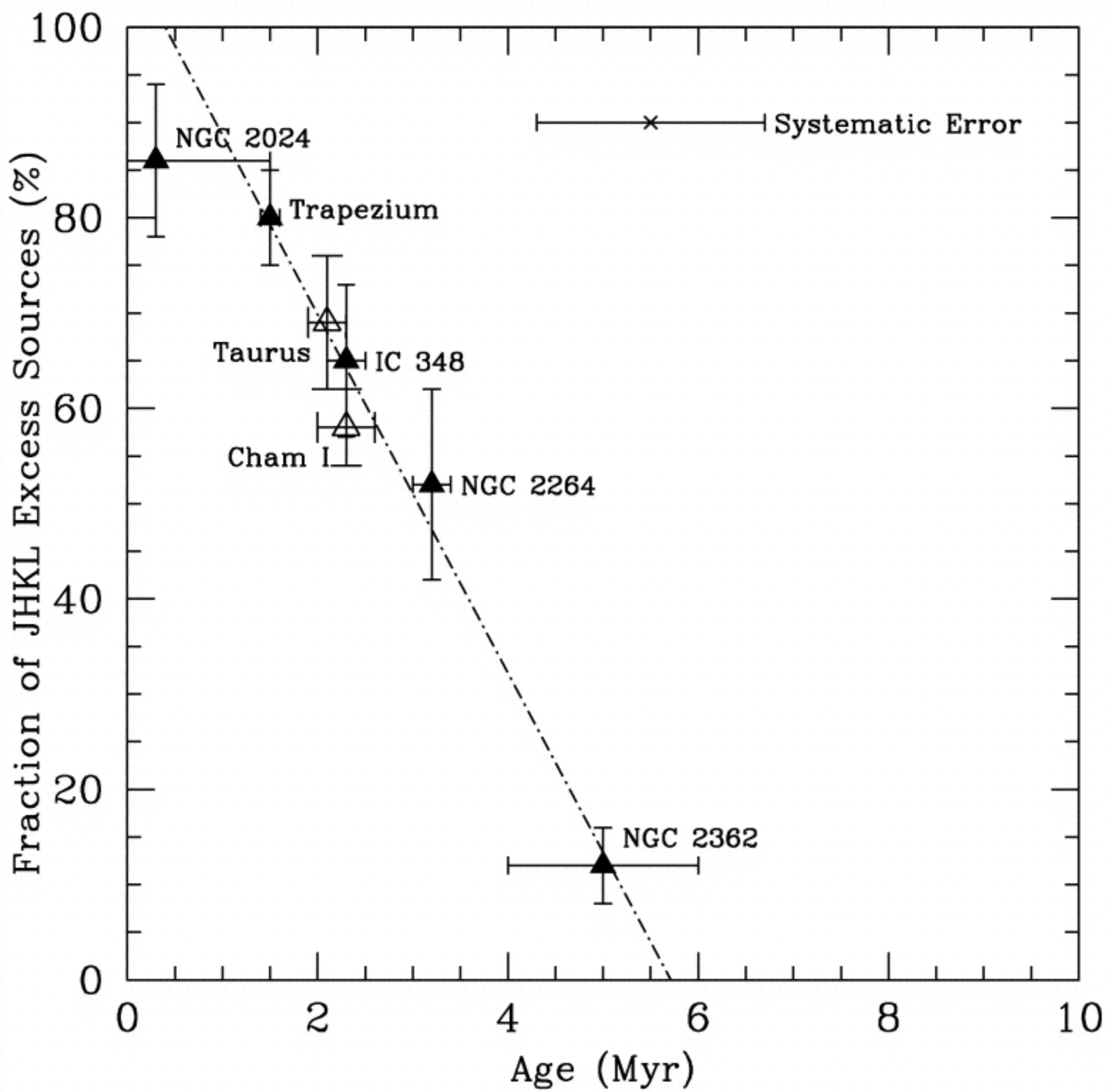

[Haisch et al. 2001]

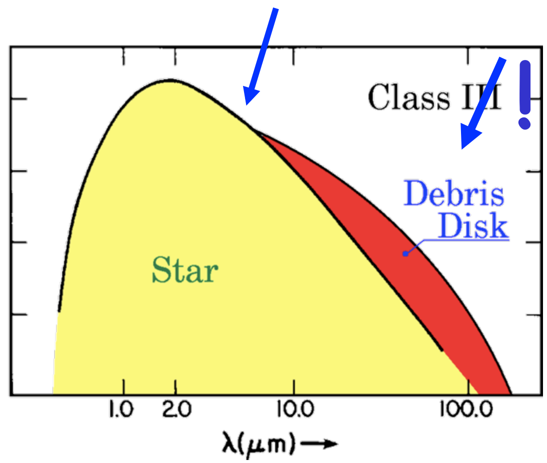

Inner disk region which
can be traced in
the near-infrared,
disappears after
a few million years

Inner disk region: Dust depletion

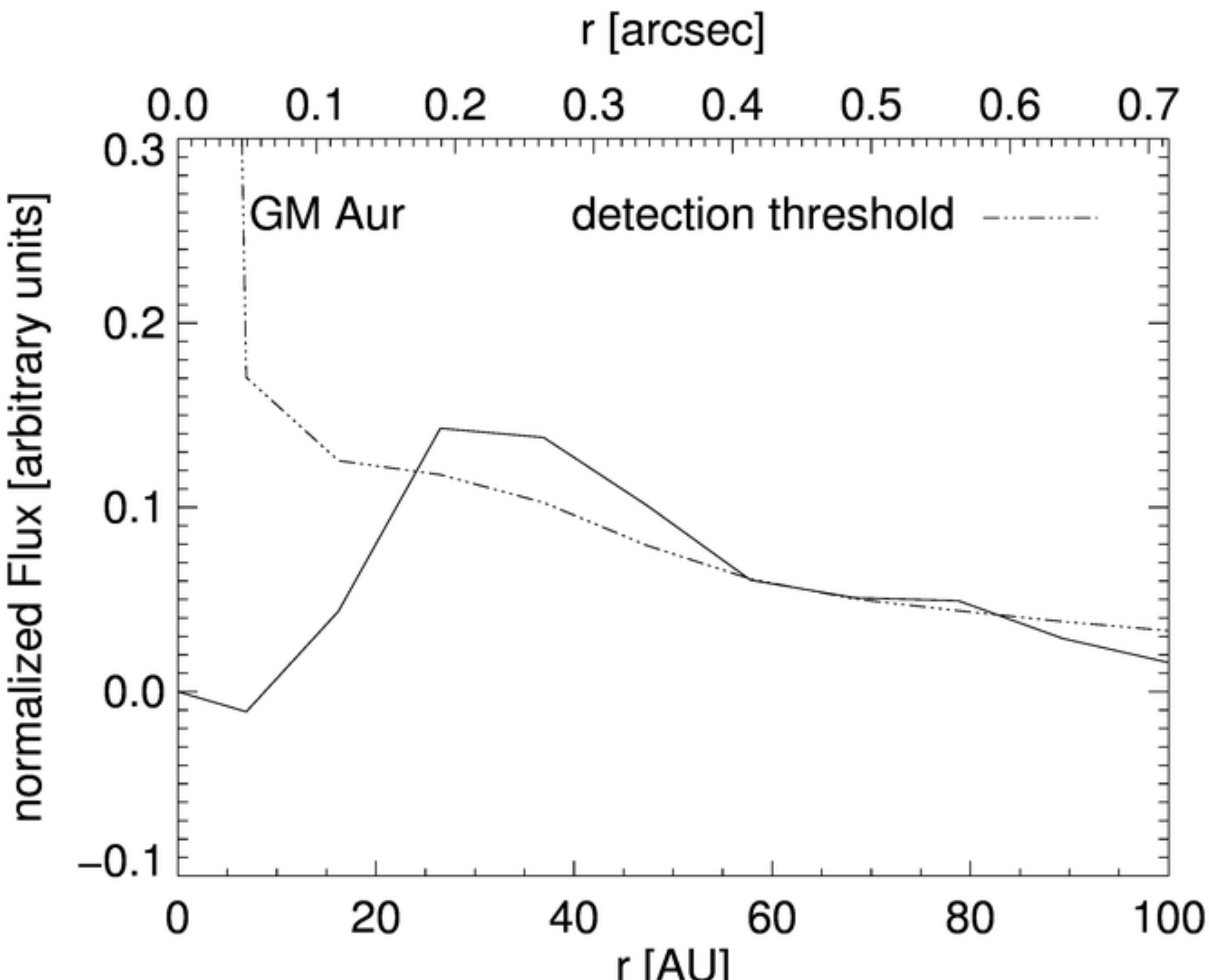

Observed flux residuals of GM Aur (VISIR/VLT, ESO)

[Gräfe, et al., 2011]

Inner disk region: Dust depletion

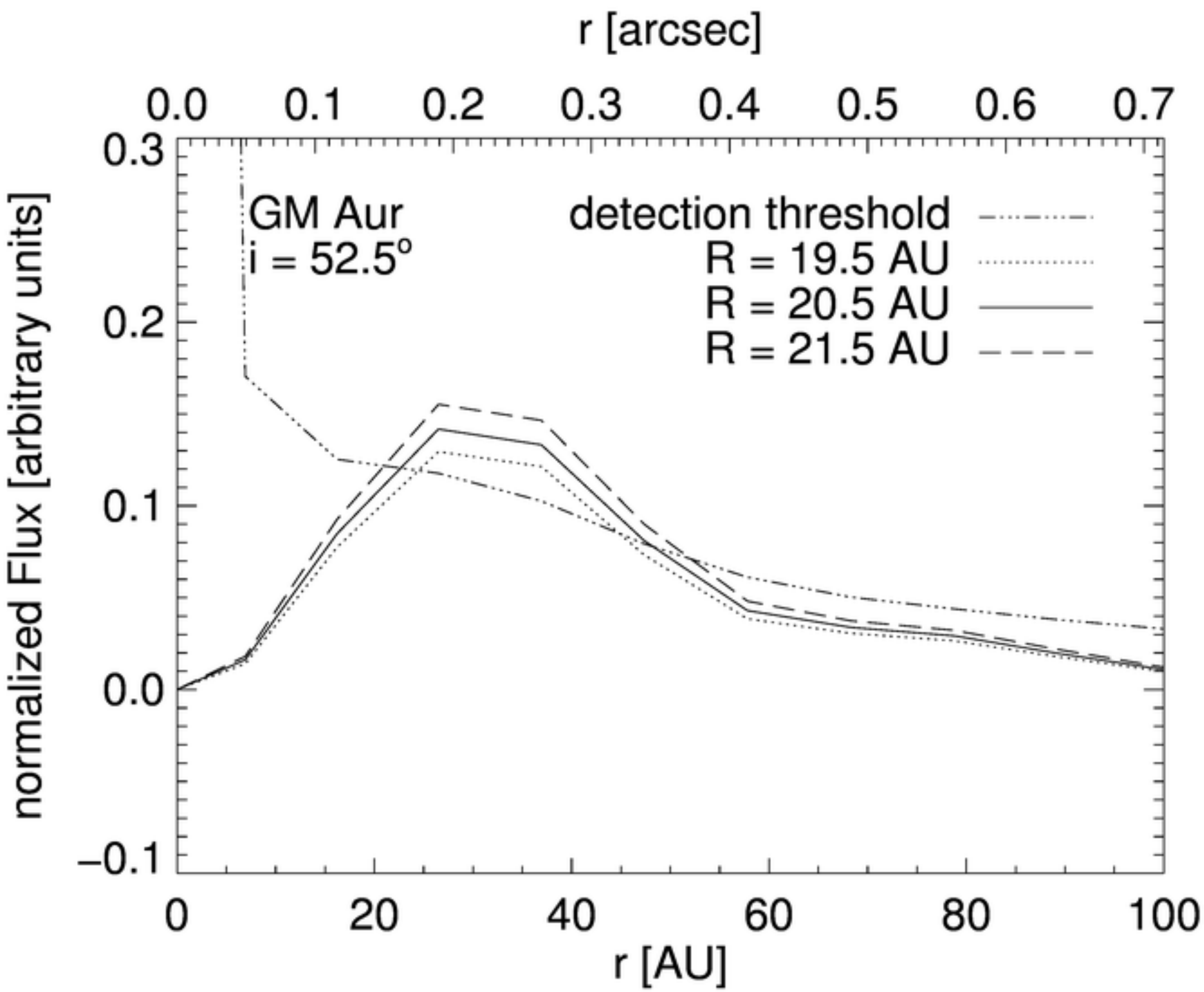

Modeled flux residuals of GM Aur

[Gräfe, et al., 2011]

For comparison

Dutrey et al. 2008:
Inner disk radius:
19 +/- 4 AU

Inner disk region: Dust depletion

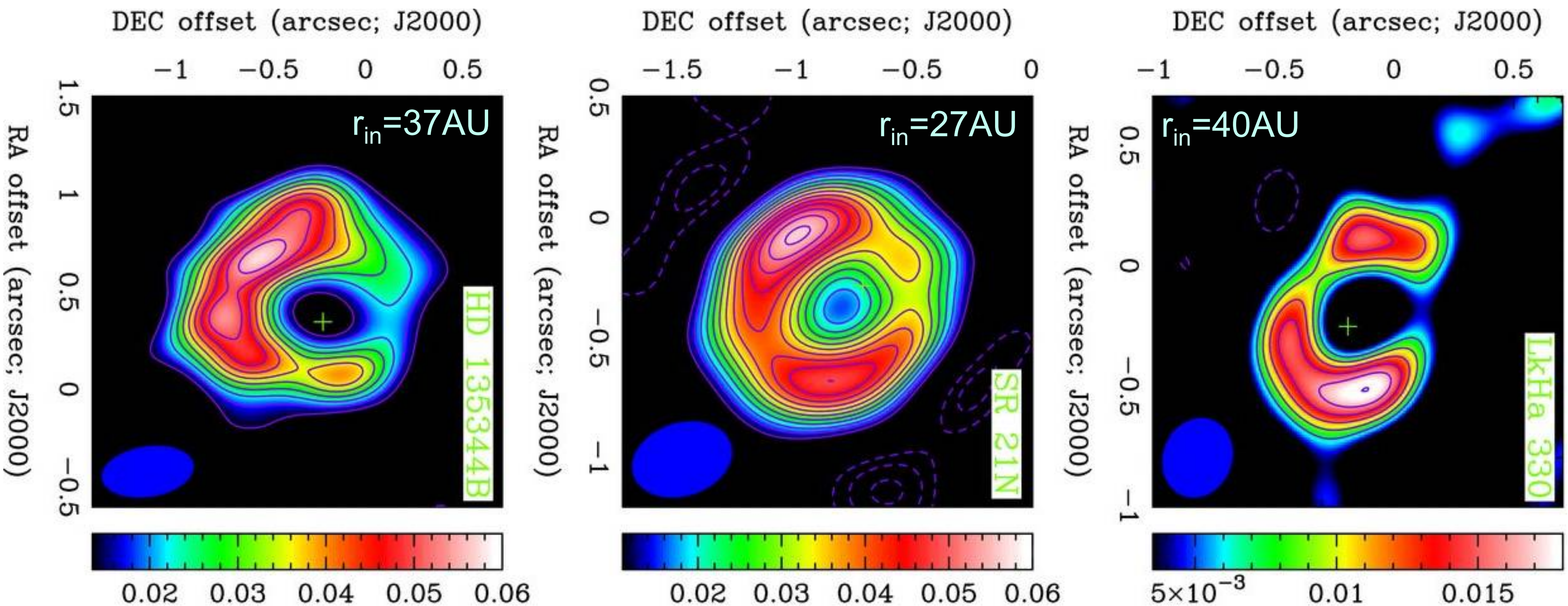

340 GHz dust continuum images of LkHα 330 (top), SR 21N (middle), and HD 135344B (bottom). The crosses mark the literature coordinates of the central star.

[Brown et al. 2009]

Photoevaporation

- Heating of the disk surface by the central star or a nearby O star (T_{Gas} ~10^4K)
- Removal of hot gas from the disk surface
- Criterion:

Sound speed > Escape velocity

$$c_S^2 = \frac{kT}{\bar{\mu} m_H} > \frac{GM}{r} = v_{\mathrm{Escape}}^2$$

$$\Rightarrow r > \frac{GM\bar{\mu} m_H}{kT}$$

In reality: Critical radius r_{cr} ~$0{,}15r$ (considering the surface structure of the disk)

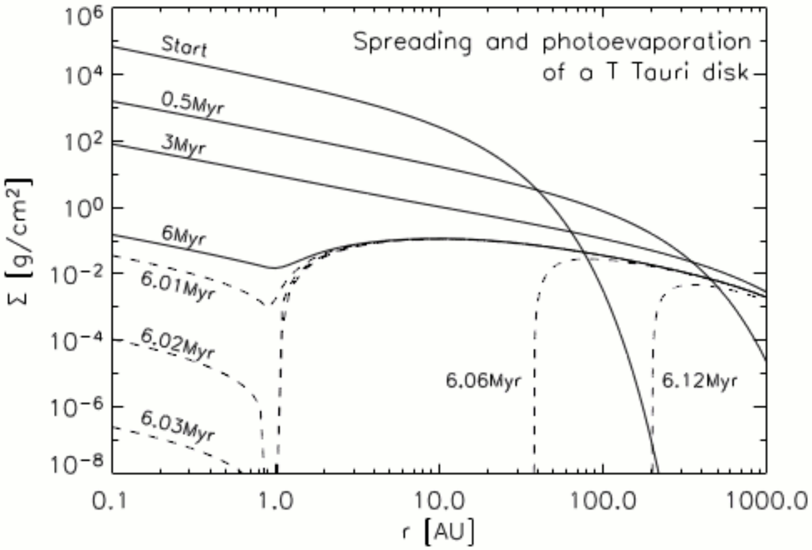

Fig. 11.— Evolution of the surface density of a EUV-photoevaporating disk (Figure adapted from *Alexander et al.*, 2006b). This simulation starts from a given disk structure of about 0.05 $M_\odot$ (marked with 'Start' in the figure). Initially the disk accretes and viscously spreads (solid lines). At $t = 6 \times 10^6$ yr the photoevaporation starts affecting the disk. Once the EUV-photoevaporation has drilled a gap in the disk at $\sim$ 1 AU, the destruction of the disk goes very rapidly (dashed lines).The inner disk quickly accretes onto the star, followed by a rapid erosion of the outer disk from inside out. In this model the disk viscosity spreads to $>$ 1000 AU; however, FUV-photoevaporation (not included) will likely truncate the outer disk.

[from „Protostars and Planets V“]

Evaporation: Orion

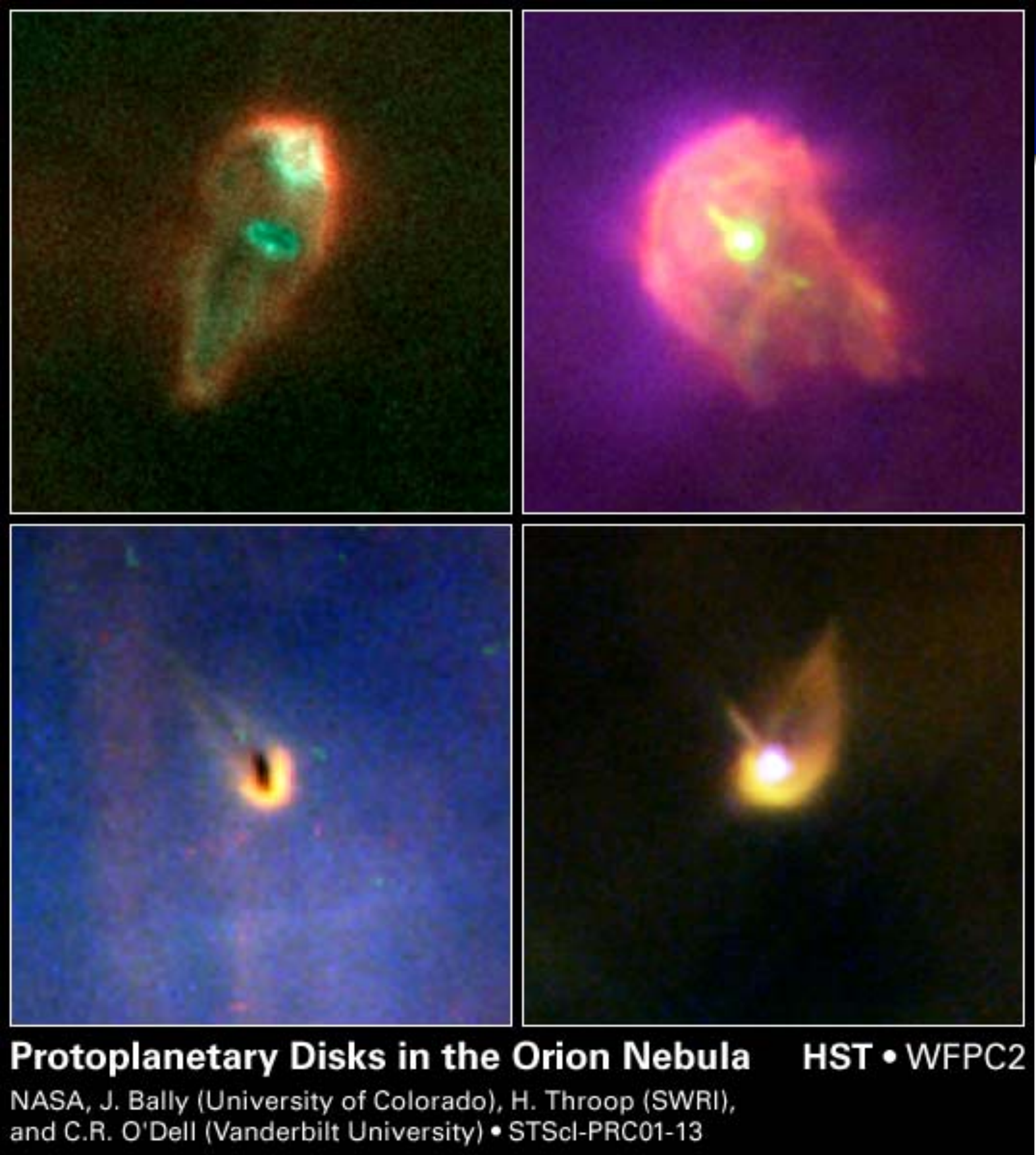

Disk dispersal within ~10^5yr

1) „Evaporation " of the disk surface

2) Removal by winds of nearby O stars

Evaporation: NGC 3603

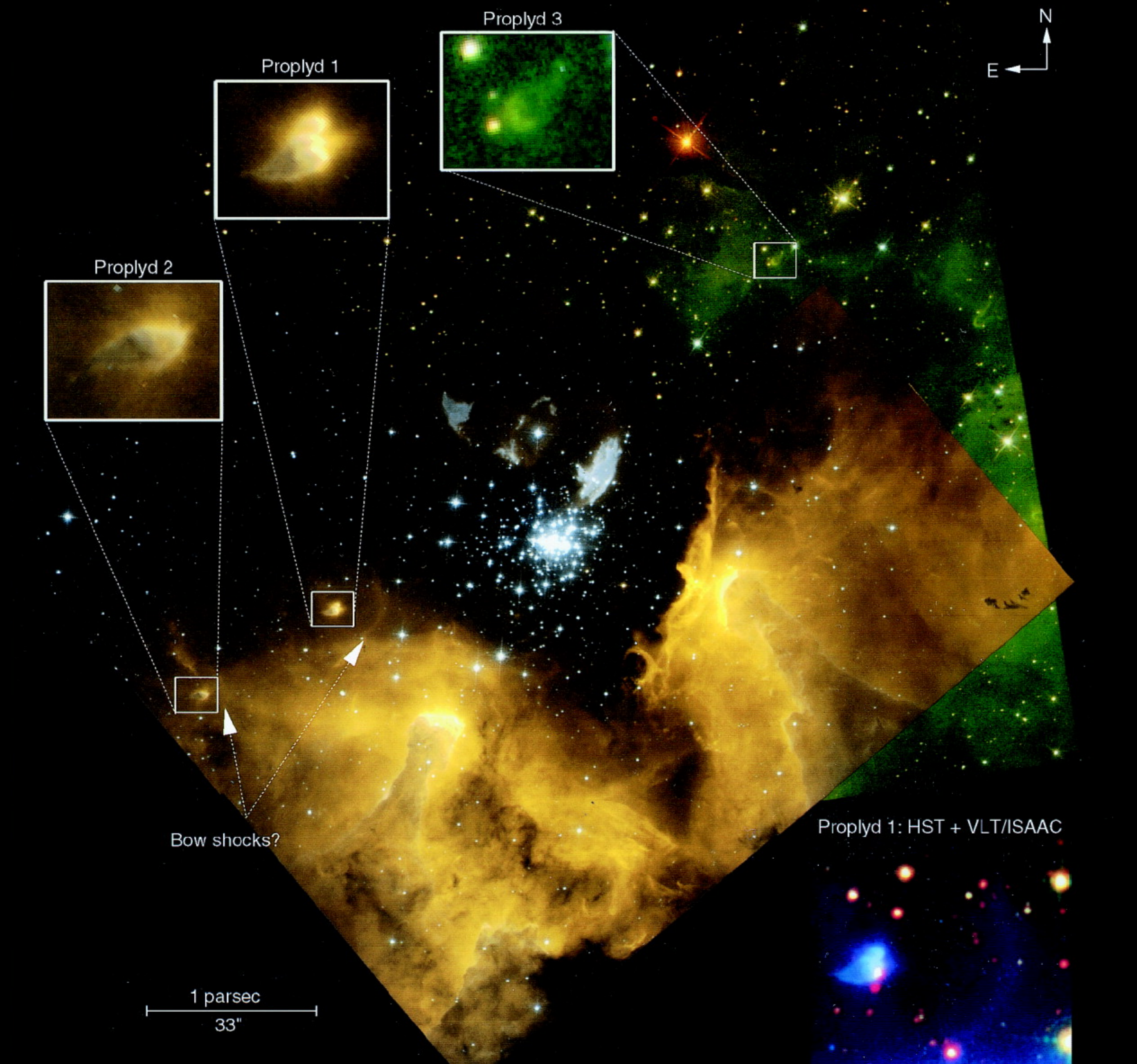

Brandner et al. 2000

Dispersal of 95% of all disks after ~140,000 yr

WFPC2 observations of NGC 3603. North is up and east is to the left. The upper part of the image consists of the archive data with the following color coding: F547M (*blue*), F675W (*green*), F814W (*red*). Overlaid are our new WFPC2 data with the F656N data in the red channel, the average of F656N and F658N in the green channel, and F658N in the blue channel. The location of the three proplyd-like emission nebulae is indicated. The insert at the lower right is a combination of WFPC2 F656N (*blue*) and F658N (*green*) and VLT/ISAAC K_s (*red*) observations.

- **Accretion onto the central star**

viscous timescale: $t_\nu \propto r^2/\nu, \quad \nu \propto r \;\Rightarrow\; t_\nu \propto r$

$$t_\nu \cong 10^5\,\text{yr}\left(\frac{\alpha}{0{,}01}\right)^{-1}\left(\frac{r}{10\,AU}\right)$$

Viscous timescale
(„Timescale of radial drift “):
Timescale on which a disk ring moves by a distance *r* in radial direction (ν: viscosity)

- **Close stellar encounter**

$$t_{\mathrm{SE}} \cong 2\cdot 10^7\,\text{yr}\left(\frac{n_*}{10^4\,\text{pc}^{-3}}\right)^{-1}\left(\frac{\text{v}}{1\text{km/s}}\right)\left(\frac{r_{\mathrm{d}}}{100\text{AU}}\right)$$

n_* – Stellar number density,
r_{d} – Outer disk radius after encounter,
v – Velocity dispersion of the stars

- **Stellar winds**

$$t_{\mathrm{WS}} = f(v_{\mathrm{w}}, \text{disk flaring})$$

- **Photoevaporation**

for $r>r_{\mathrm{g}}$:

$$t_{\mathrm{PE}} \cong 10^7\,\text{yr}\left(\frac{\Phi_i}{10^{41}\,\text{s}^{-1}}\right)^{-1/2}\left(\frac{\Sigma_0}{\Sigma_0(\text{min})}\right)$$

Φ_i – (EUV) Extreme Ultraviolet luminosity of the star
Σ_0 – Surface density at a reference radius
Σ_0(min) – Corresponding value for the „minimum mass solar nebula“

Further reading: „Protostars and Planets IV“, p. 401+

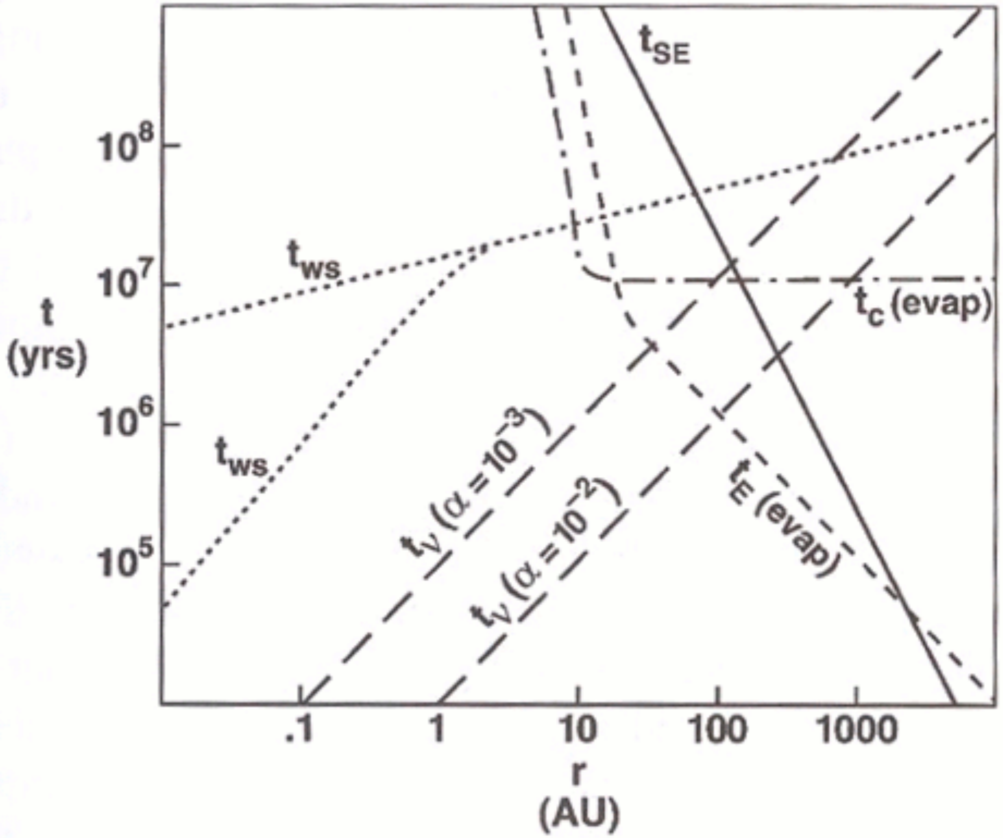

Figure 1. Timescales for disk dispersal: t_ν is the viscous timescale for $\alpha = 10^{-2}$ and 10^{-3}; t_{SE} is the stellar encounter (tidal stripping) timescale for Trapezium cluster conditions (see sections II.B and III); t_{ws} and t'_{ws} are stellar wind stripping timescales for wind and disk parameters summarized in section III; t_c(evap) is the photoevaporation timescale by the central star (strong wind case), and t_E(evap) is the photoevaporation timescale for an external star (Trapezium conditions) for the conditions summarized in sections II.D and III.

[from „Protostars and Planets IV"]

Are there no more disks
after a few Million years?

Debris Disks
Beta Pic

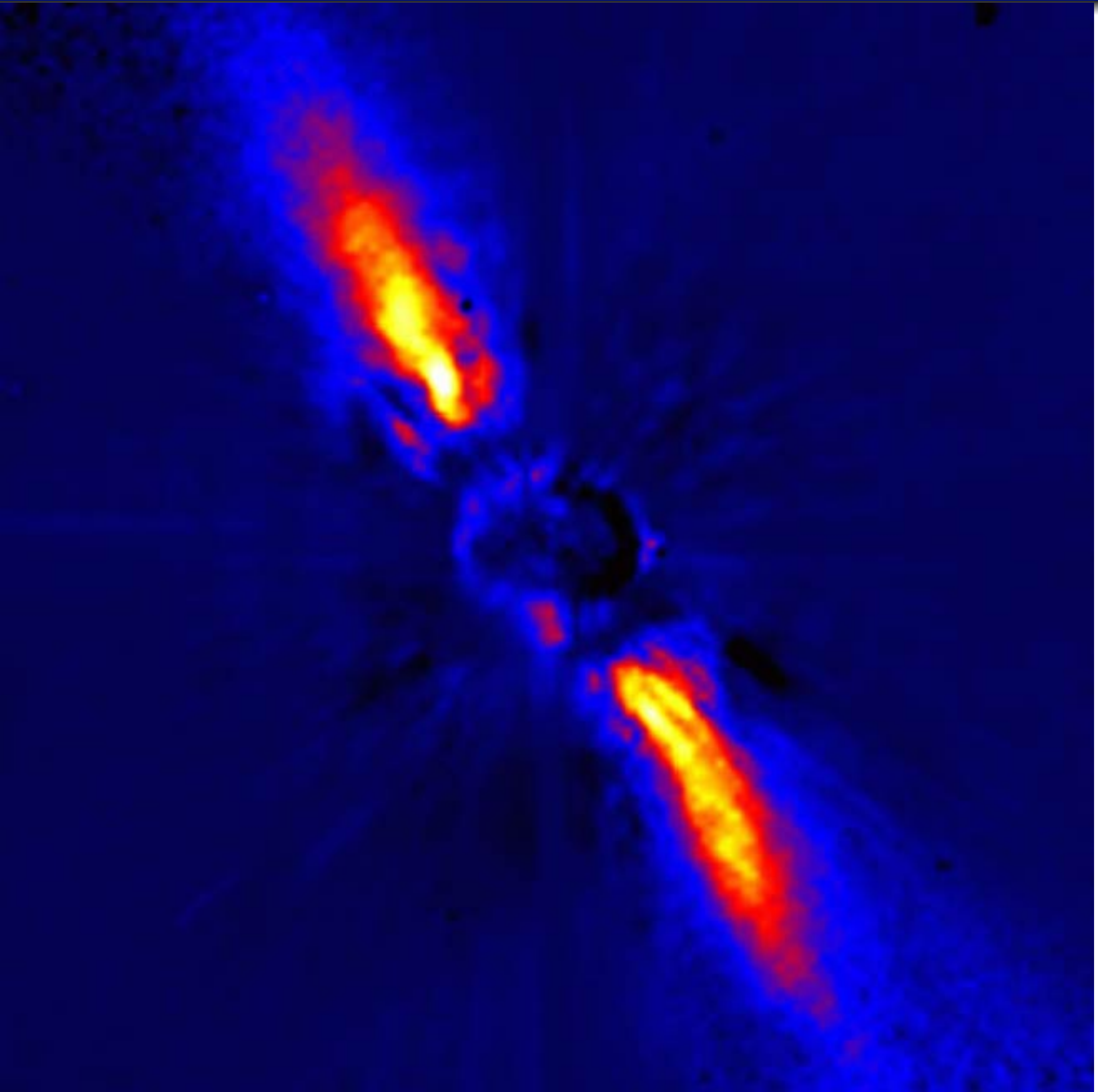

Spectral typ: A5 V

T_{eff}= 8250K

Distance:
19,3pc

Age:
8-20 Myr

Disk radius
~500 AU

First main-sequence star for which an image of its disk was obtained in the visible wavelength range (Smith & Terrile 1984)

[ESO/Beuzit et al. 1997; near-infrared]

Debris Disks
AU Mic

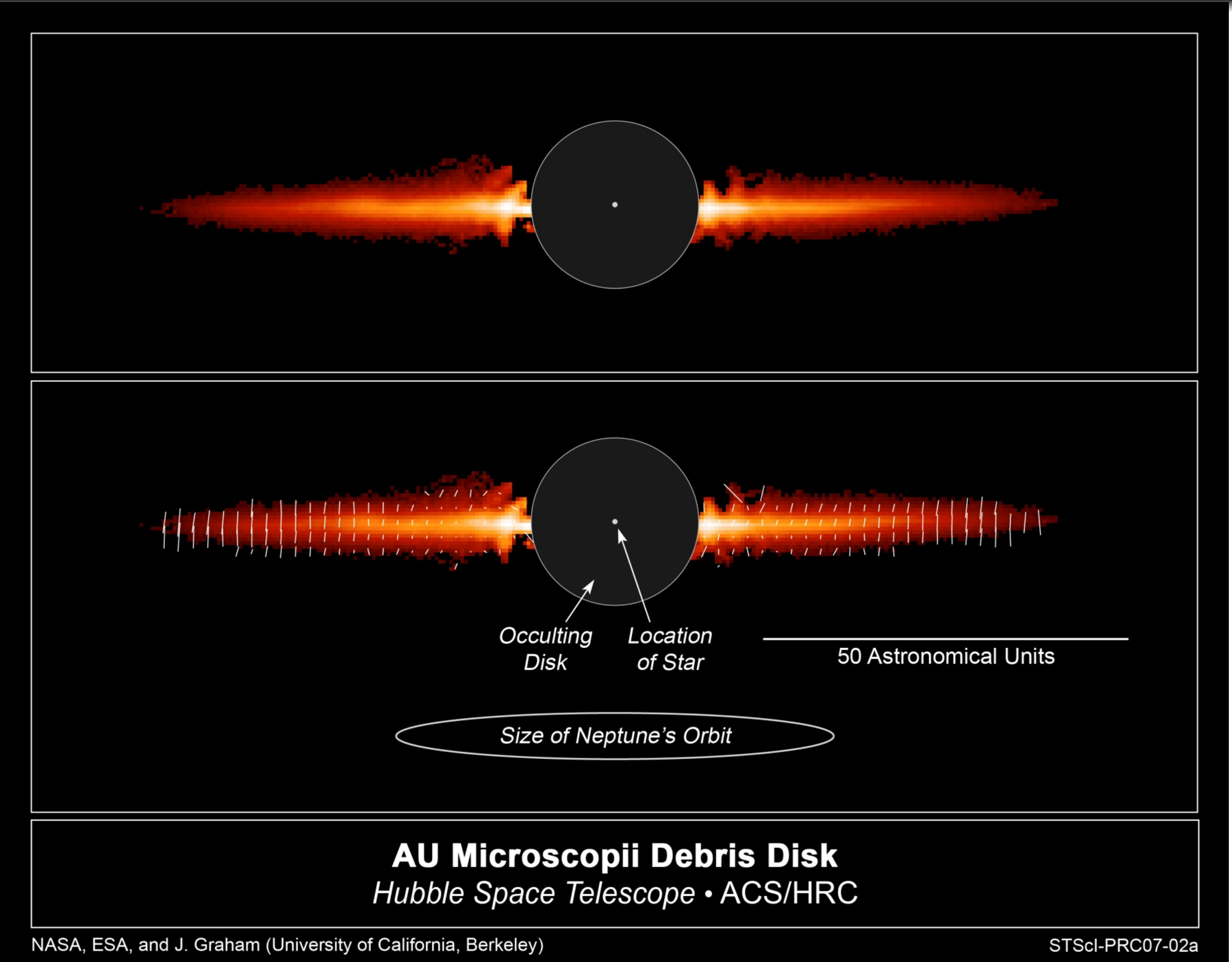

Spectral typ: M

T_{eff}= 3730K

Distance: 10pc

Age: **12 Myr**

Disk radius ~210 AU

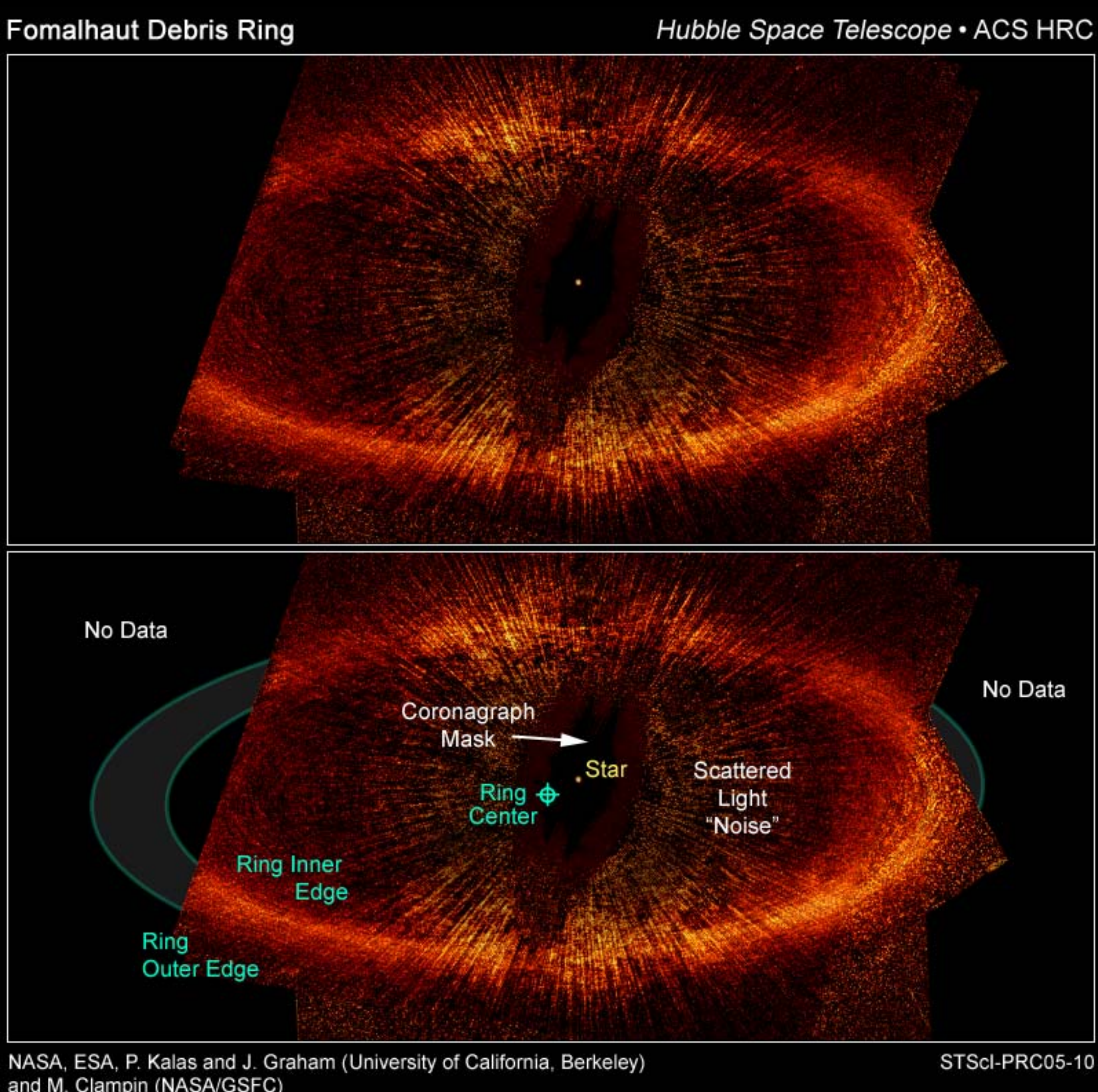

Debris Disks
Fomalhaut

Spectral type:
A3 V

T_{eff}= 8500K

Distance:
7,66pc

Age:
200-300 Myr

Disk radius
~158 AU

Zodiacal light

Age of the star:
4,6 x 10^9 yr

ESO/Y.Beletsky

Evolution of debris disks

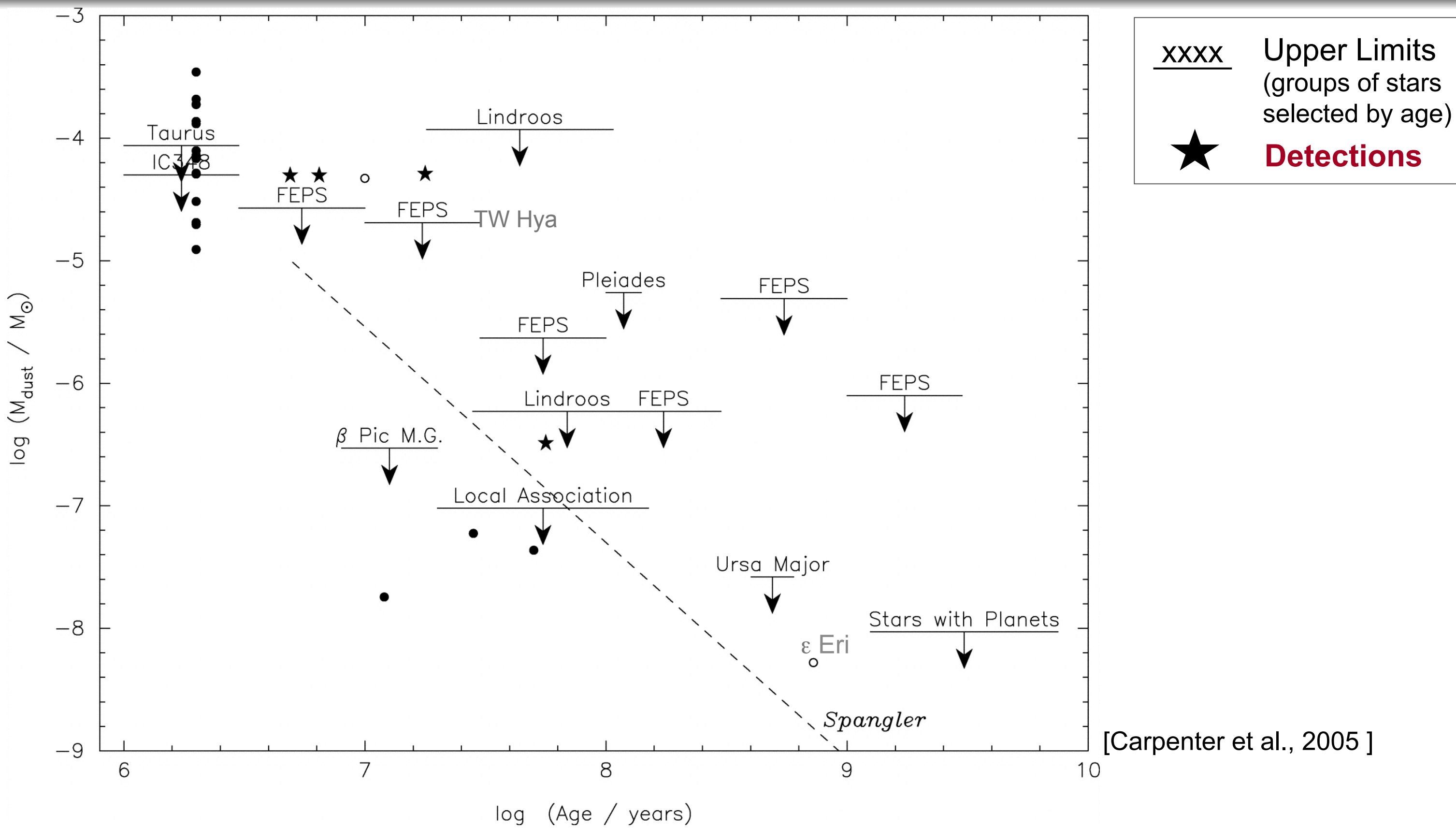

[Carpenter et al., 2005]

<u>Spitzer Space Observatory: Results:</u>

- Mass ~ typically several lunar masses
- Gas content: negligible
- Abundance
    - A stars: >33% (Su et al. 2006)
    - FGK stars: 10%-15% (Bryden et al. 2006, Beichman et al. 2006, Trilling et al. 2008)

Rem.: Abundance = f(detection limit of the survey)

Origin of „second generation“ dust

Age of those stars around which debris disks have been found: 10 Myr ... 10 Gyr
but: Lifetime of dust particles in an optically thin disk: < 1Myr

Important time scale: Poynting Robertson timescale *[explanation follows]*

$$t_{\mathrm{PR}} \cong 710\mathrm{yr}\left(\frac{r_{\mathrm{Dust}}}{\mu m}\right)\left(\frac{\rho}{1g/cm^{-3}}\right)\left(\frac{R}{1AE}\right)^{2}\left(\frac{L_{\mathrm{Star}}}{1\mathrm{L}_{\mathrm{Sun}}}\right)^{-1}(1+A)^{-1}$$

r_{Dust} – Dust grain radius, ρ – Dust grain density, R – Distance: Dust grain - Star,
L_{Star} – Stellar luminosity, A – Albedo *(Burns et al. 1979)*

⇒ No primordial dust
⇒ Dust must be replenished continuously

Mechanism: Collision of planetesimals

=> Debris disks provide information about

- Planetesimals, which produce the dust via collisions
- Planets, which modify the spatial distribution of the dust

Dynamics: Dust distribution

Forces in debris disks

Remember:	Disks around	YSOs	:	gas-rich, optically thick
	- " -	MS stars	:	gas-poor, optically thin

[r_{Dust} – Particle radius]

Gravity ~ $(r_{Dust})^3$ => dominates for large particles

- Gravity of the central star
- Gravitational forces of planets

(Radiation) Pressure forces ~ $(r_{Dust})^2$ => become important with decreasing particle size

- Radiation pressure
- Poynting-Robertson effect
- Stellar wind (corpuscular radiation)

Electromagnetic Lorentz force ~ r_{Dust} => important only for very small particles

Other forces

- Collisions
- Yarkovski Effect

Radiation pressure

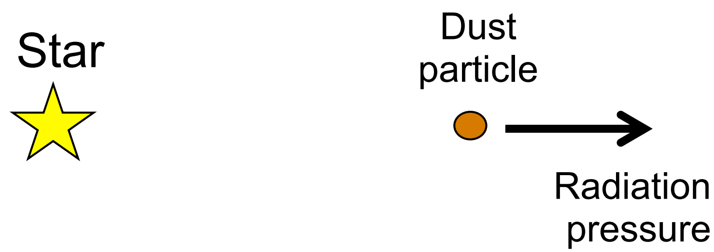

$$\vec{F}_{RP} = -\frac{S(r)AQ_{RP}}{c}\frac{\vec{r}}{r}$$

with S(r) – Flux density: $L_*/4\pi r^2$,
A – Geometrical cross section
Q_{PR} – Efficiency of momentum transfer

Stellar radiation => Dust particle => Momentum transfer

$$\Rightarrow \vec{F}_{RP} = -\frac{L_*(r)AQ_{RP}}{4\pi c r^2}\frac{\vec{r}}{r} \qquad \Rightarrow \vec{F}_{RP} \propto \frac{1}{r^2}\frac{\vec{r}}{r}$$

Note:
- *Same functional dependence F(r) as in the case of the gravitational force*
- *Motion of particle neglected*

$$\beta \equiv \frac{|\vec{F}_{RP}|}{|\vec{F}_G|} = -\frac{L_*(r)AQ_{RP}}{4\pi c}\frac{1}{GM_* m_{\mathrm{Dust}}} = f(\text{Dust properties})\, f(\text{Stellar parameters})$$

$$\Rightarrow \vec{F}_{RP} = -\beta \vec{F}_G$$

=> Reduction of Gravitational force by factor (1-β)

Remarks:

- Resonances „sorted“, according to value of β=f(grain size. Chemical composition)
- $Q_{RP} = Q_{abs} + (1-g)Q_{sca}$, g – Scattering asymmetriy factor (Henyey &Greenstein, 1941)

Gravity vs. Radiation pressure

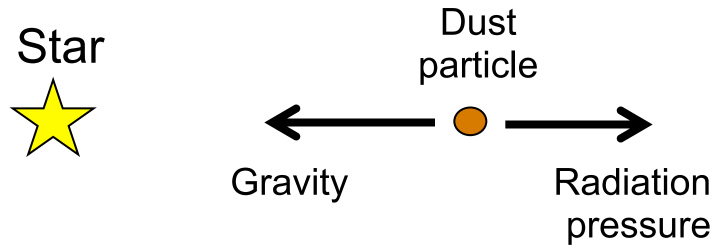

Resulting force: $\vec{F} = -\frac{GM_*(1-\beta)m}{r^2}\frac{\vec{r}}{r}$

Ideal absorber:

$$\beta = 0.574 \left(\frac{L_\star}{L_\odot}\right)\left(\frac{M_\odot}{M_\star}\right)\left(\frac{1\,\mathrm{g\,cm^{-3}}}{\rho}\right)\left(\frac{1\ \mu\mathrm{m}}{s}\right)$$

(s – particle size, ρ – bulk density; Burns, 1979)

Resulting particle orbits and corresponding structure of a debris disk

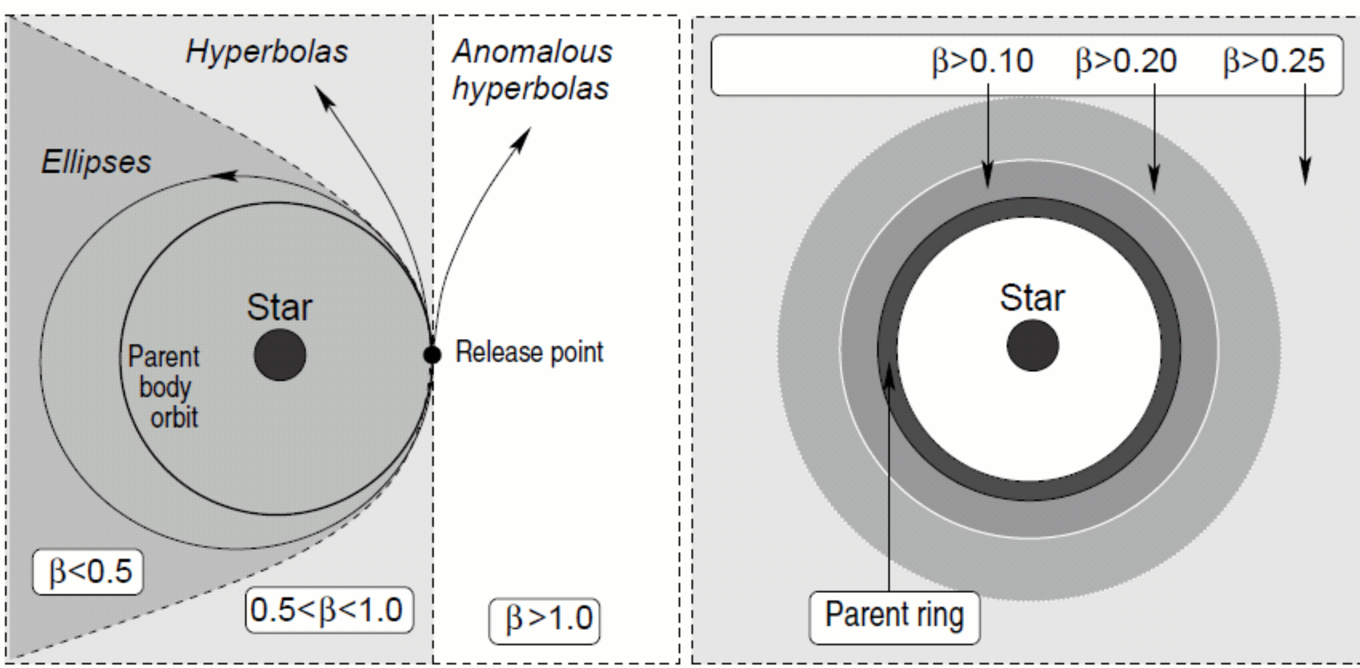

[from Krivov, 2010]

Poynting-Robertson Effect

Schematic illustration of the Poynting-Robertson effect

(a) … in the rest frame of the dust particle

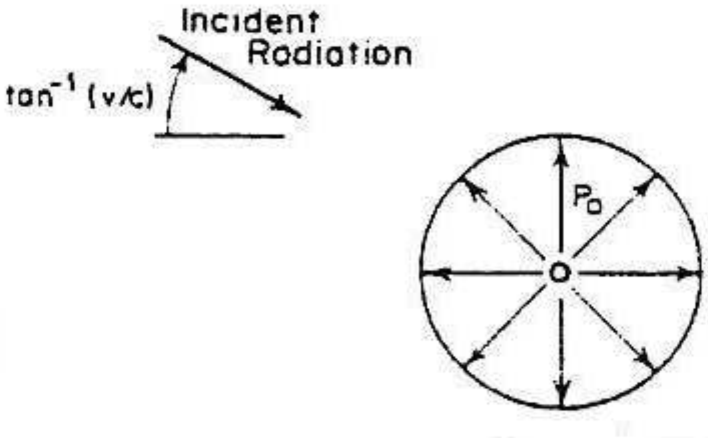

(b) … in the rest frame of the star

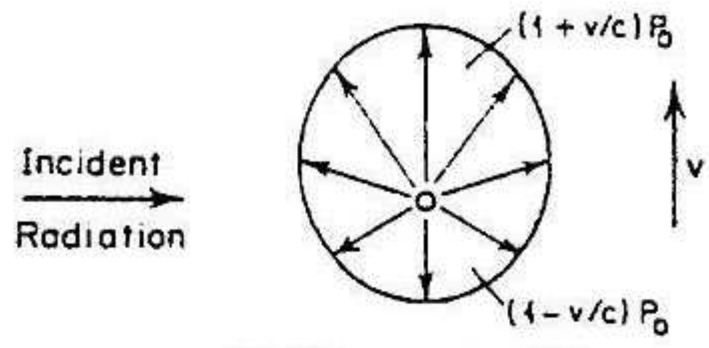

[from Burns et al. (1979); The length of the arrows depicts the power of the re-radiated energy]

$$\vec{F}_{PR} = -\frac{S'(r)AQ_{RP}}{c^2}\vec{v}$$

with

$$S' = S\left[1-\frac{v}{c}\right]$$

„Modified radiation pressure“

=> Particle loses angular momentum and spirals towards the star

Stellar wind

Corpuscular radiation (Origin: Corona of the central star)

- Protons, electrons, α particles, small fraction of heavy ions
- Momentum transfer => Dust grains

1. **Pressure force**

   Example: Sun

   - *Typical velocity: ~400 km/s*
   - *Low density and velocity*
     - $\Rightarrow$ *Momentum flux density ~400x smaller than that of the radiation field*
     - $\Rightarrow$ *Influence on the dynamics of the dust negligible*

2. **Drag force („Stellar Wind Drag")**

   – „Counterpart " to Poynting-Robertson effect

   – Significant, since wind velocity only ~1-2 orders of magnitude larger than the orbital velocity of the dust grains => Abberation angle much larger than in the case of photons

   - $\zeta = F_{SW} / F_{PR} = c/v_{SW}$ * ratio of momentum flux densities

     Example: Solar system

     - *ζ = 0,3 for dust grains > 0,1μm (Gustafson 1994, Holmes et al. 2003)*
     - *For smaller dust grains: ζ > 1 => long-time evolution of particle trajectories*

Lorentz force, Collisions

Lorentz force

- Photoemission of electrons => Dust usually carries a positive charge
- Interplanetary magnetic field => Lorentz force
  => Deflection of dust particles primarily in **vertical** direction
- Azimuthal component of the (primarily toroidal) magnetic field ~ 1 / r
- Charge of the dust grain q ~ Particle size (r_{Dust})

$$\Rightarrow \quad \frac{F_L}{F_G} \propto \frac{qB}{m_{\text{Dust}}/r^2} \propto \frac{r_{\text{Dust}}/r}{r_{\text{Dust}}^3/r^2} = \frac{r}{r_{\text{Dust}}^2}$$

$\Rightarrow$ **Lorentz force only of importance for**
a) small dust grains
in
b) a large distance from the central star

Collisions

- Important for dust grains with a long Poynting-Robertson timescale
  (in that case many collisions might occur)
- Important for large grains
  Example: Solar system
  Important for grains > 10µm - 80µm
  (Dohnanyi 1978, Leinert et al. 1983, Grün et al.1985)

Yarkovsky Effect

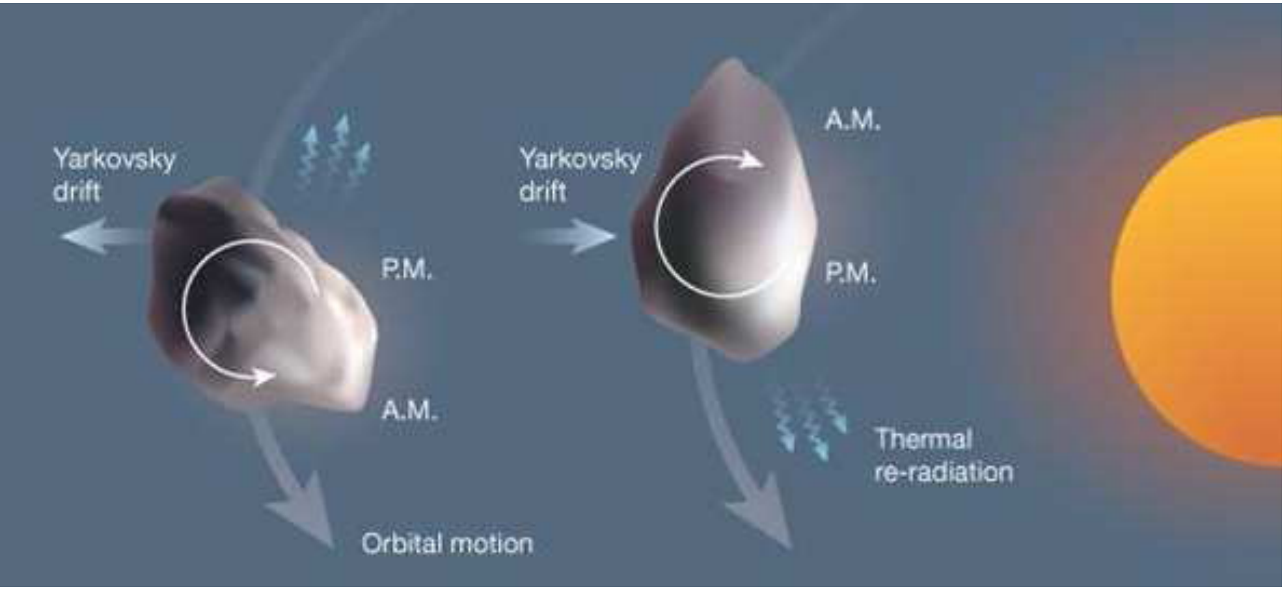

Illustration of the Yarkovski effect
[Figure from Binzel 2003]

Daily heating an cooling of a rotating body
=> anisotropic thermal reemission

Limited ability of a body to redistribute the absorbed stellar radiation
=> "Afternoon hemisphere" warmer than "Morning hemisphere" (Burns et al. 1979)

Higher thermal reemission from warm side
=> Resulting force may accelerate or decelerate meter-sized bodies
(Öpik 1951; Grün et al. 2001)

Example

The debris disk around q1 Eri

q1 Eri

Stellar parameters

- Spectral type: F8
- Distance : 17.4 pc
- Age : ~ 2 Gyr

Planet (Mayor et al. 2003, Butler et al. 2006)

- M sin i: 0.93 $M_{Jupiter}$
- Semi-major axis: 2.03 AU
- Eccentricity : 0.1

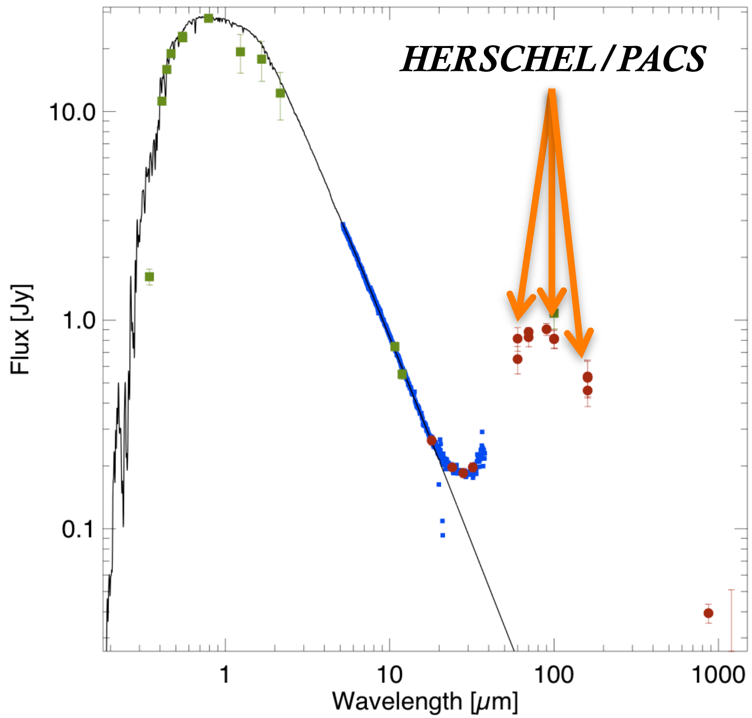

[Liseau et al. 2010]

Dust ring

- IRAS, ISO and Spitzer: cold dust, with a luminosity ~1000 times that of the Kuiper Belt
- Sub-mm APEX/LABOCA images:
  Disk extent up to several tens of arcsec (Liseau et al. 2008)
- HST images suggest a peak at 83 AU (4.8”, Stapelfeldt et al., in prep.)

q1 Eri

Herschel Space Observatory (Key project: DUNES):

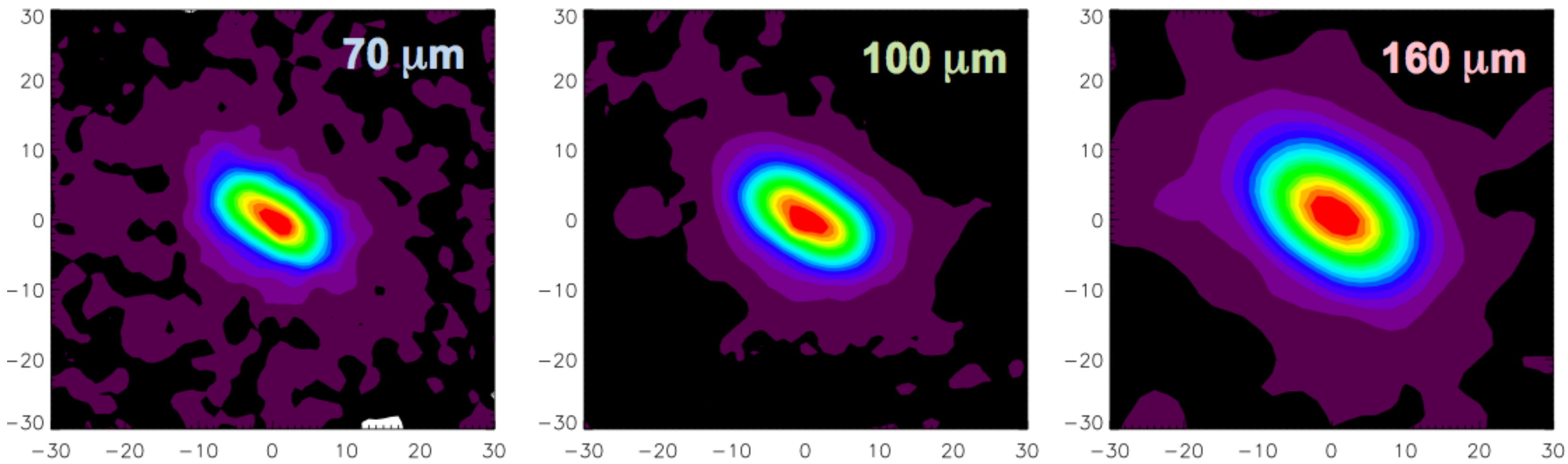

[Liseau et al. 2010]

- Disk spatially resolved at all PACS wavelengths
- Disk marginally resolved along the minor axis: inclination > 55°

Detailed <u>simultaneous</u> modeling of the SED and PACS images required to unveil the disk structure, dust properties and dynamical history

Further material will be added as soon as corresponding article is published

[Augereau et al., in prep.]

Planets in debris disks

Searching for planets/low-mass companions in debris disks: Success!

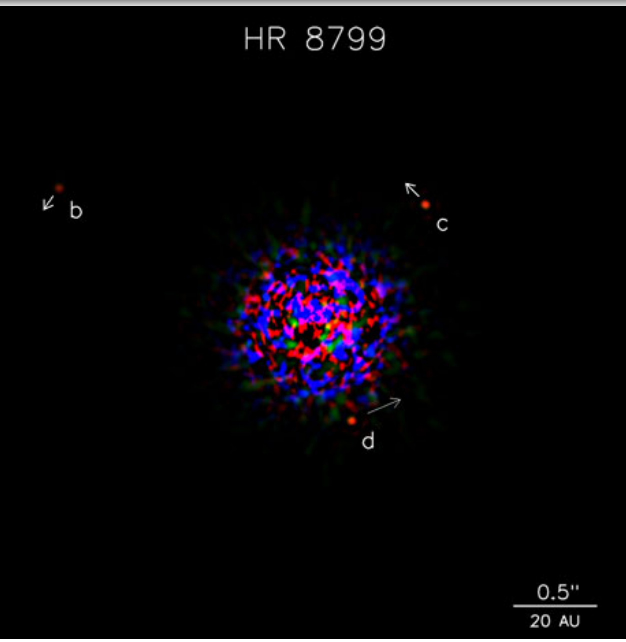

HR 8799 *[Marois et al. 2008]*
(Pegase, d~140ly, 60-100Mio yr, disk diameter: 2000AU?)

<u>Companions</u>
Orbital axis: 67AU, 37AU, 24AU
Masses: 7,10,10$M_{Jupiter}$
(based on age of the system)
Arrows: Movement within 4 years

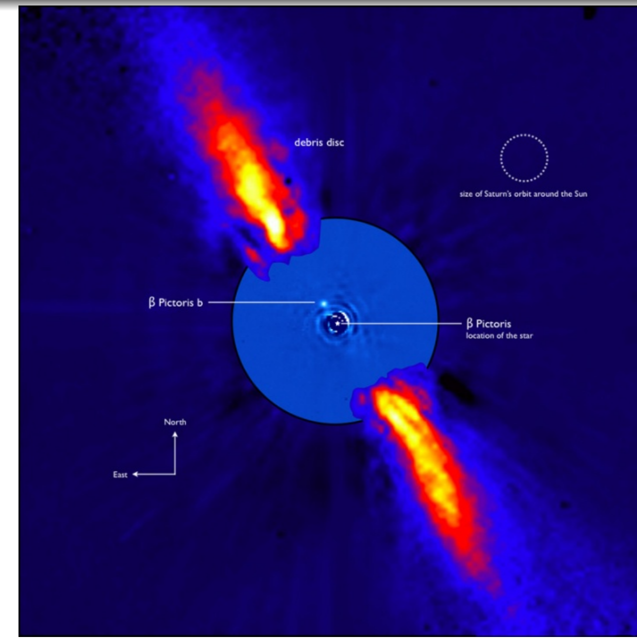

β **Pictoris** *[Lagrange et al. 2008]*
(Pictor, d~63ly, 800Mio yr, disk diameter: ~800AU)
Companion: 8$M_{Jupiter}$?

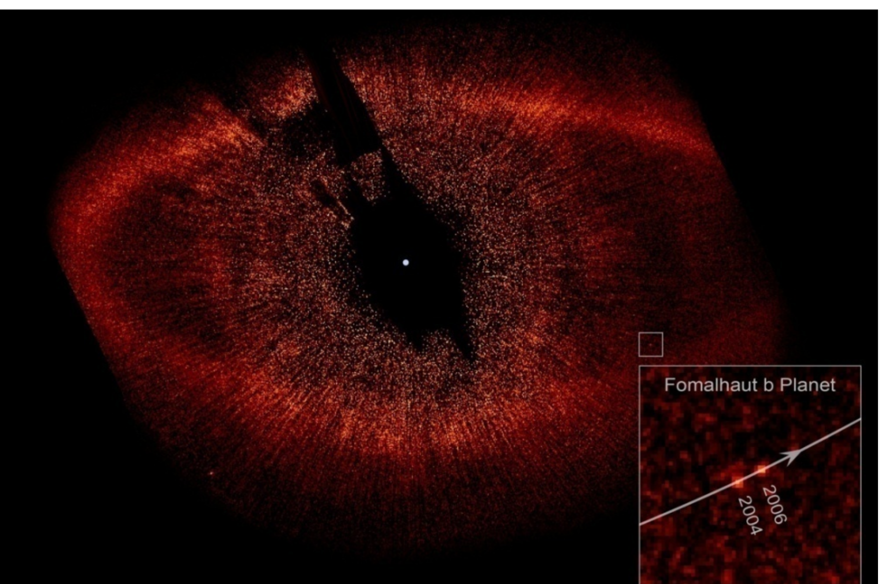

Fomalhaut *[Kalas et al. 2008]*
(Piscis Austrinus, d~25ly, 200-300Mio yr, disk diameter ~200AU)

<u>Fomalhaut B</u>
Orbital radius: 113 AU, orbital period: 872yr,
Large-scale ring system?

Giant Planets in Debris Disks

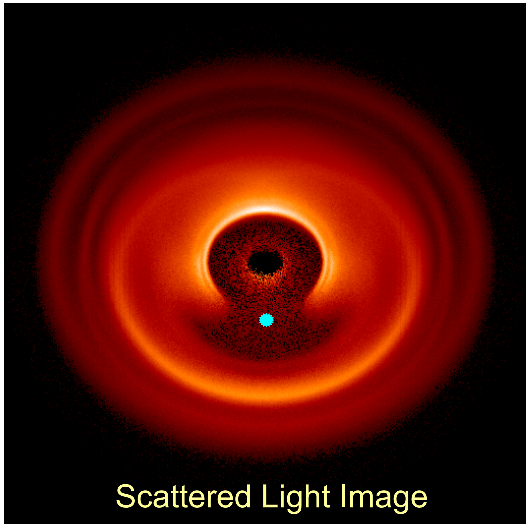

[Rodmann & Wolf]

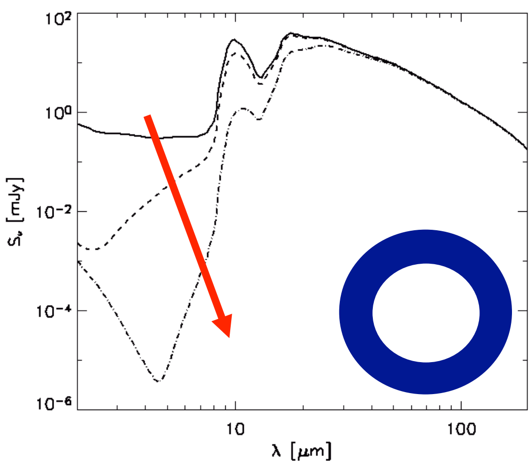

[Wolf & Hillenbrand 2003, 2005]

Planet → **Resonances** and **Gravitational scattering** →

Asymmetric resonant dust belt with one or more clumps, intermittent with one or a few off-center cavities

+

Central cavity void of dust.

- Resonance Structures: **Indicators of Planets**

  [1] Location

  → [2] Major orbital parameters

  [3] Mass of the planet

Note: Relative brightness distribution of individual clumps in optical to near-infrared scattered light images may sensitively depend on the disk inclination (asymmetry of the scattering function)

- Decreased mid-infrared SED

Example:
Highly structured disk aound εEridani

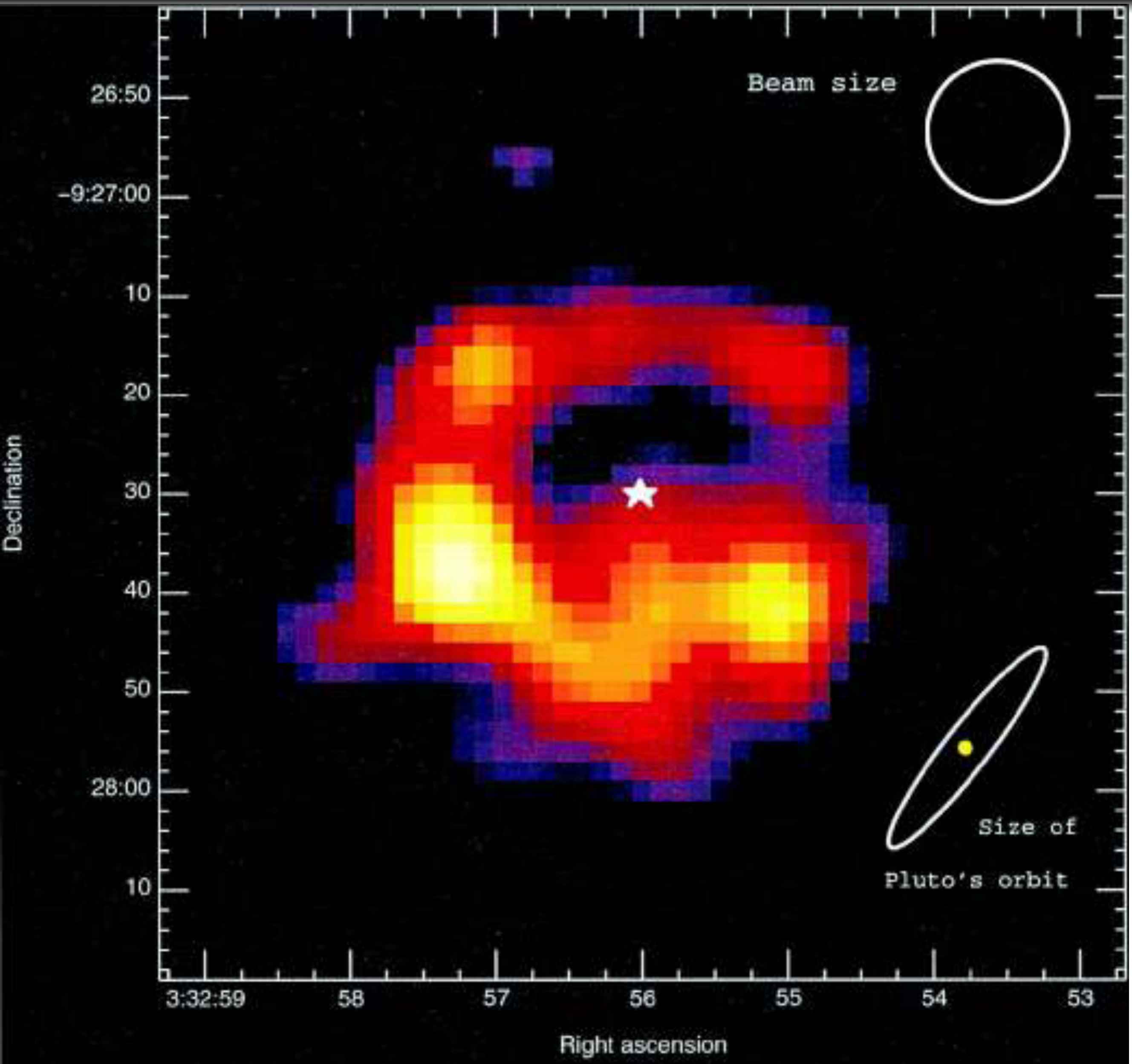

850μm, continuum

[Greaves et al. 1998]

Structures in Debris Disks

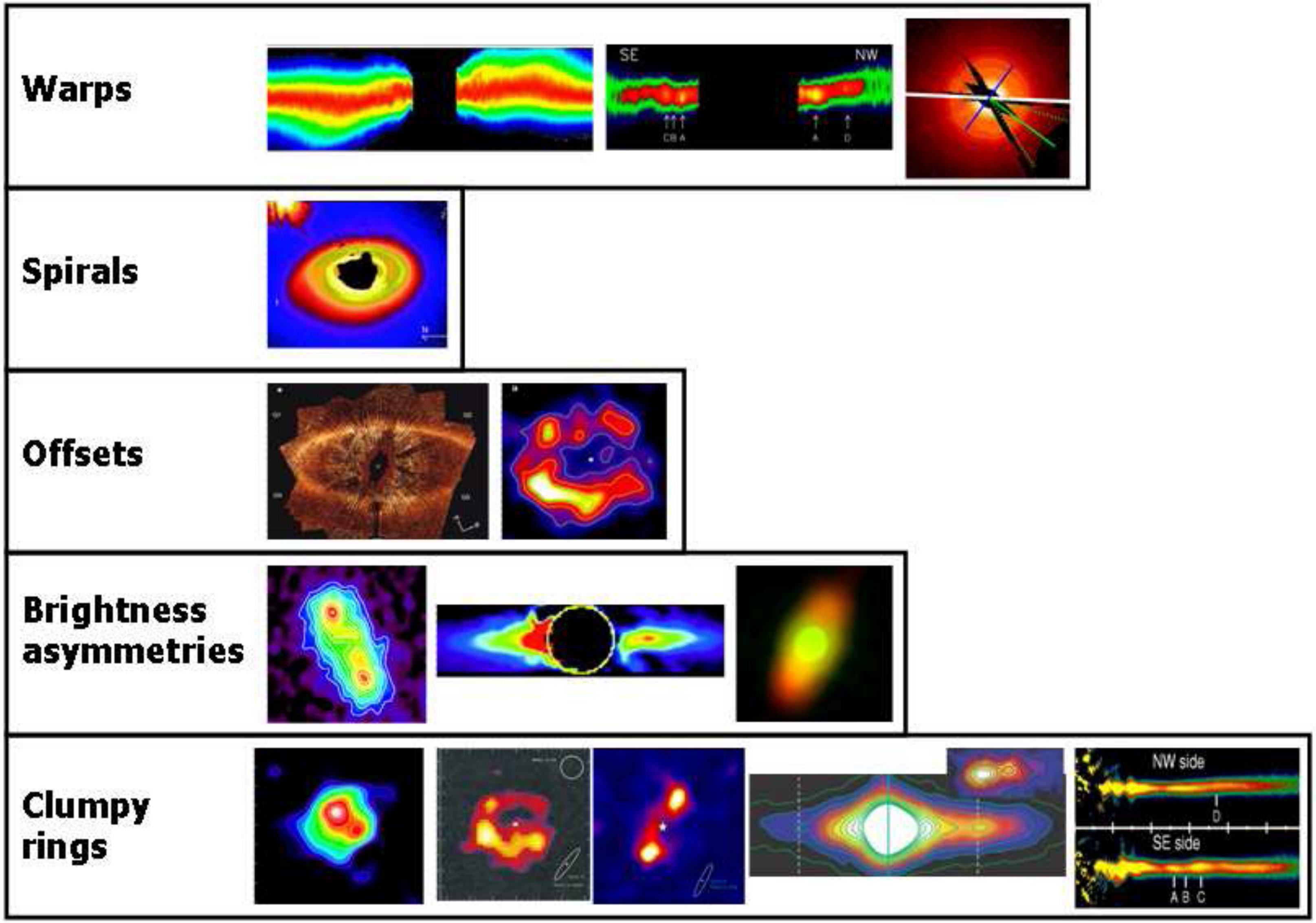

[Moro-Martin et al.]

Structures in Debris Disks

Figure caption:

Spatially resolved images of nearby debris disks showing a wide diversity of debris disk structure. From left to right the images correspond to:

(1st row)	**β-Pic**	(0.2–1 μm; Heap et al., 2000),
	AU-Mic	(1.63 μm; Liu, 2004),
	TW Hydra	(0.2–1 μm; Roberge, Weinberger & Malumuth, 2005);
(2nd row)	**HD 141569**	(0.46–0.72 μm; Clampin et al., 2003);
(3rd row)	**Fomalhaut**	(0.69–0.97 μm; Kalas et al., 2005) and
	eps-Eri	(850 μm; Greaves et al., 2005);
(4th row)	**HR4796**	(18.2 μm; Wyatt et al., 1999),
	HD 32297	(1.1 μm; Schneider, Silverstone, & Hines, 2005),
	Fomalhaut	(24 and 70 μm; Stapelfeldt et al., 2004);
(5th row)	**Vega**	(850 μm; Holland et al., 1998),
	eps-Eri	(850 μm; Greaves et al., 1998),
	Fomalhaut	(450 μm; Holland et al., 2003),
	β-Pic	(12.3 μm; Telesco et al., 2005),
	AUMic	(0.46–0.72 μm; Krist et al., 2005).

[Moro-Martin 2008]

Constraining the existence of planets through analysis of disk structures:

Imaging required!

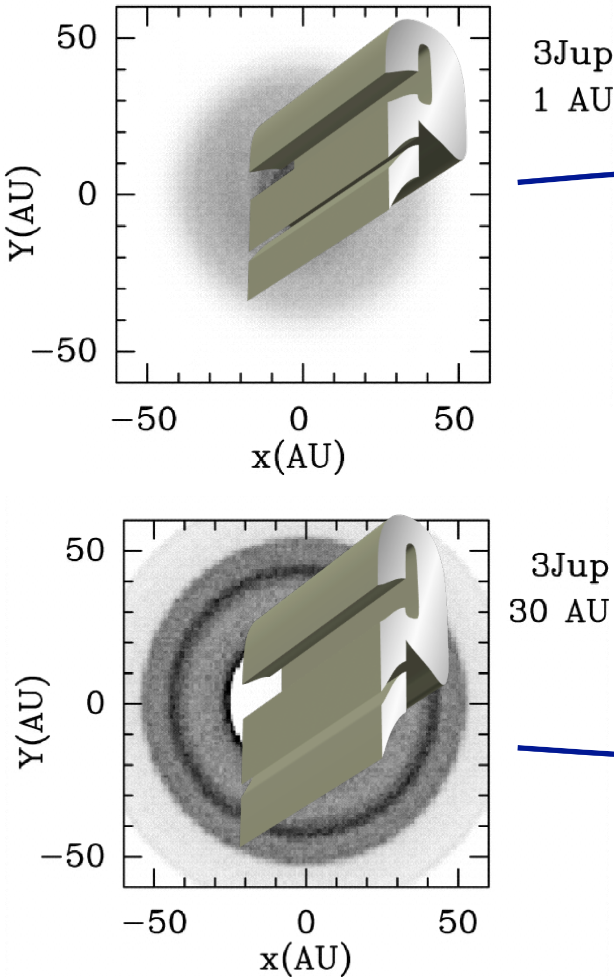

First guess

Planets of **different mass** at **similar orbit**

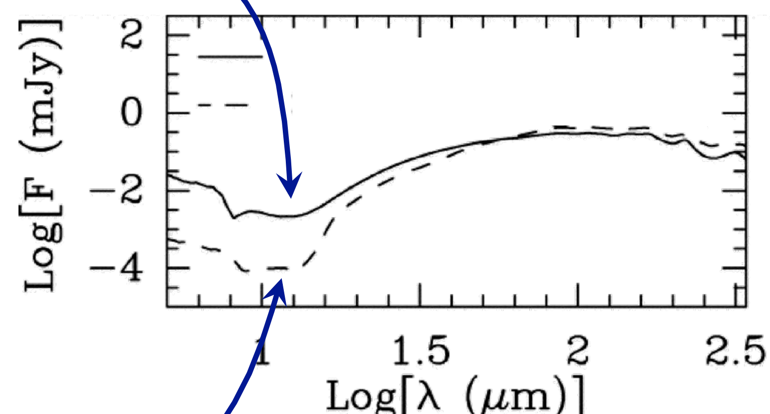

Solution

Planets of **same mass** at **different orbits**

Important: Influence of dust composition

[Moro-Martin, Wolf, & Malhotra 2005]

Again: SED analysis limited

SEDs can be well reproduced, but not unambiguously

(1) Optically thin => SED = f (T(R), $Q_{abs, sca}$)

⇒ Azimuthal/Vertical structure (e.g., patterns indicating embedded planets) can *not* be derived

(2) Many of the debris disks which were observed with the Spitzer Space Observatory show no or only very weak emission in the range < 20…30μm

⇒ Often only weak constraints for the chemical composition of dust can be derived

(3) Unambiguous dust/geometrical parameters difficult to derive
(e.g., Wolf & Hillenbrand 2003)

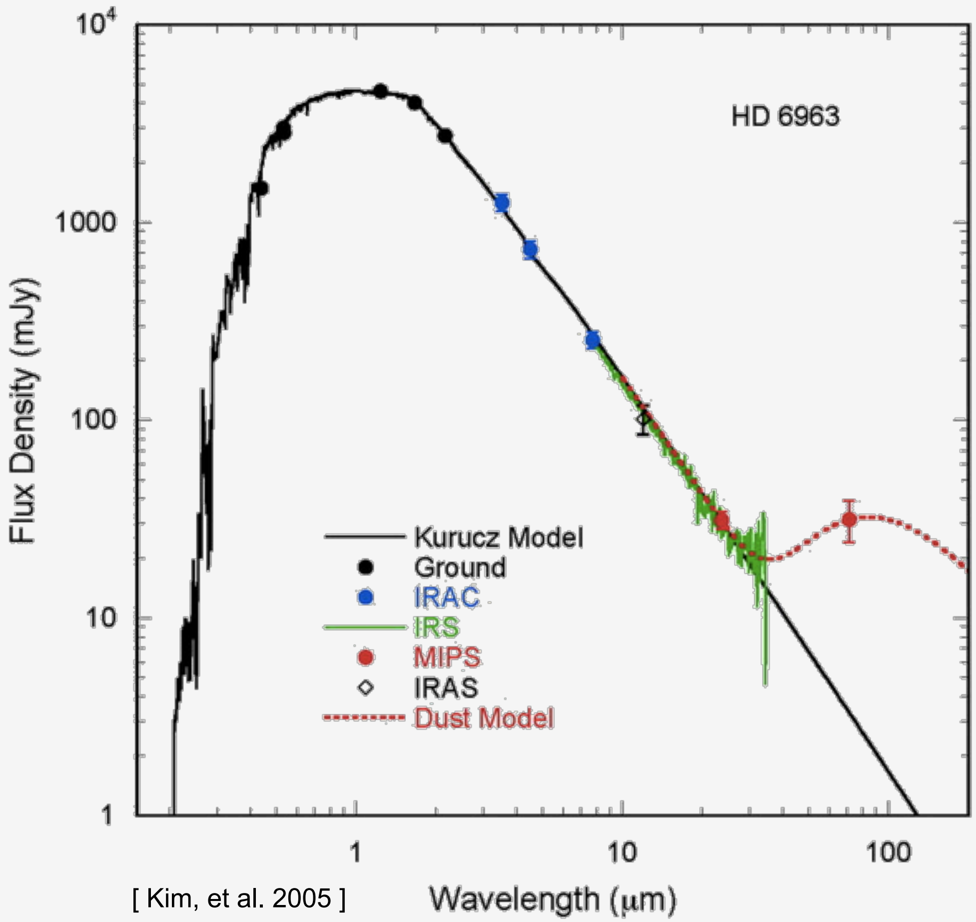

[Kim, et al. 2005]

Imaging? Debris disks: Low surface brightness => Difficult to observe

ALMA sensitivity sufficient for large surveys?

What comes next?

Multi-wavelength / Multi-scale intensity measurements

- Inner (<10AU) disk structure: Test of disk / planet formation evolution models
- Distribution of gas species: – Self-consistent modeling of dust and gas distribution
  – Chemical processes in circumstellar disks

Polarimetry

- High-contrast observing techniques
- Break degeneracies, Magnetic field measurement

Near-future goal: Planet-disk interaction

- Usually much larger in size than the planet
- Specific structure depends on the evolutionary stage of the disk
- High-resolution imaging performed with observational facilities which are already available or will become available in the near future will allow to trace these signatures.

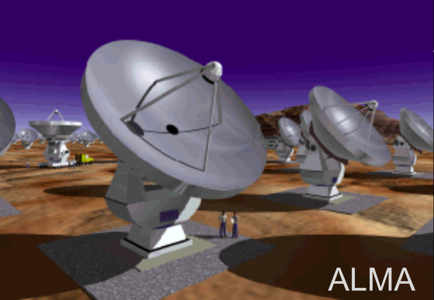

[Wolf & D‘Angelo 2005]

Thank you.

References of the figures

Papers

Andre, P. & Montmerle, T. 1994: From T Tauri stars to protostars: Circumstellar material and young stellar objects in the rho Ophiuchi cloud, ApJ, 420, 837

Apai, D., Pascucci, I., Brandner, W., Henning, Th., Lenzen, R., Potter, D. E., Lagrange, A.-M., Rousset, G. 2004: Grain growth and dust settling in a brown dwarf disk. Gemini/T-ReCS observations of CFHT-BD-Tau 4, A&A, 415, 671

Bacciotti, F., Ray, T. P., Mundt, R., Eislöffel, J., Solf, J. 2002: Hubble Space Telescope/STIS Spectroscopy of the Optical Outflow from DG Tauri: Indications for Rotation in the Initial Jet Channel, ApJ, 576, 222

Bate, M. R., Lubow, S. H., Ogilvie, G. I., Miller, K. A. 2003: Three-dimensional calculations of high- and low-mass planets embedded in protoplanetary discs, MNRAS, 341, 213

Beckwith, Steven V. W., Sargent, Anneila I., Chini, Rolf S., Guesten, Rolf. 1990: A survey for circumstellar disks around young stellar objects, AJ, 99, 924

Beckwith, Steven V. W. 1999: Circumstellar Disks, osps.conf, 579

Binzel, R. P. 2003: Planetary science: Spin control for asteroids, Nature, 425, 131

Brandner, W., Grebel, E. K., Chu, You-Hua, Dottori, H., Brandl, B., Richling, S., Yorke, H. W., Points, S. D., Zinnecker, H. 2000: HST/WFPC2 and VLT/ISAAC Observations of Proplyds in the Giant H II Region NGC 3603, AJ, 119, 292

Brown, J. M., Blake, G. A., Qi, C., Dullemond, C. P., Wilner, D. J., Williams, J. P. 2009: Evidence for Dust Clearing Through Resolved Submillimeter Imaging, ApJ, 704, 496

References of the figures

Papers

Burns, J. A., Lamy, P. L., Soter, S. 1979: Radiation forces on small particles in the solar system, Icarus, 40, 1

Carpenter, J. M., Wolf, S., Schreyer, K., Launhardt, R., Henning, T. 2005: Evolution of Cold Circumstellar Dust around Solar-type Stars, AJ, 129, 1049

Cotera, A. S., Whitney, B. A., Young, E., Wolff, M. J., Wood, K., Povich, M., Schneider, G., Rieke, M., Thompson, R. 2001: High-Resolution Near-Infrared Images and Models of the Circumstellar Disk in HH 30, ApJ, 556, 958

D'Angelo, G., Henning, T., Kley, W. 2002: Nested-grid calculations of disk-planet interaction, A&A, 385, 647

Ertel, S., Wolf, S., Metchev, S., Schneider, G., Carpenter, J. M., Meyer, M. R., Hillenbrand, L. A., Silverstone, M. D. 2011: Multi-wavelength modeling of the spatially resolved debris disk of HD 107146, A&A, 533, A132

Fujiwara, H., Honda, M., Kataza, H., Yamashita, T., Onaka, T., Fukagawa, M., Okamoto, Y. K., Miyata, T., Sako, S., Fujiyoshi, T., Sakon, I. 2006: The Asymmetric Thermal Emission of the Protoplanetary Disk Surrounding HD 142527 Seen by Subaru/COMICS, ApJ, 644, L133

References of the figures

Papers

Fukagawa, M., Hayashi, M., Tamura, M., Itoh, Y., Hayashi, Saeko S., Oasa, Y., Takeuchi, T., Morino, J., Murakawa, K., Oya, S., Yamashita, T., Suto, H., Mayama, S., Naoi, T., Ishii, M., Pyo, Tae-Soo, Nishikawa, T., Takato, N., Usuda, T., Ando, H., Iye, M., Miyama, Shoken M., Kaifu, N. 2004: Spiral Structure in the Circumstellar Disk around AB Aurigae, ApJ, 605, L53

Gledhill, T. M. & Scarrott, S. M. 1989: Evidence for circumstellar disks around nebulous stars in the Taurus dark clouds, MNRAS, 236, 139

Gräfe, C., Wolf, S., Roccatagliata, V., Sauter, J., Ertel, S. 2011: Mid-infrared observations of the transitional disks around DH Tauri, DM Tauri, and GM Aurigae, A&A, 533, A89

Greaves, J. S., Holland, W. S., Moriarty-Schieven, G., Jenness, T., Dent, W. R. F., Zuckerman, B., McCarthy, C., Webb, R. A., Butner, H. M., Gear, W. K., Walker, H. J. 1998: A Dust Ring around epsilon Eridani: Analog to the Young Solar System, ApJ, 506, L133

Guilloteau, S., Dutrey, A., Pety, J., Gueth, F. 2008: Resolving the circumbinary dust disk surrounding HH 30, A&A, 478, L31

Haisch, K. E., Jr., Lada, E. A., Lada, C. J. 2001: Disk Frequencies and Lifetimes in Young Clusters, ApJ, 553, L153

Hatchell, J., Fuller, G. A., Ladd, E. F. 1999: Hot molecular bullets in HH 111 and CEP E, A&A, 346, 278

References of the figures

Papers

Kalas, P., Graham, J. R., Chiang, E., Fitzgerald, M. P., Clampin, M., Kite, E. S., Stapelfeldt, K., Marois, C., Krist, J. 2008: Optical Images of an Exosolar Planet 25 Light-Years from Earth, Science, 322, 1345

Kenyon, S. J. & Hartmann, L. 1995: Pre-Main-Sequence Evolution in the Taurus-Auriga Molecular Cloud, ApJS, 101, 117

Kessler-Silacci, Jacqueline E., Hillenbrand, Lynne A., Blake, Geoffrey A., Meyer, Michael R. 2005: 8-13 μm Spectroscopy of Young Stellar Objects: Evolution of the Silicate Feature, ApJ, 622, 404

Kim, J. S., Hines, Dean C., Backman, D. E., Hillenbrand, L. A., Meyer, M. R., Rodmann, J., Moro-Martín, A., Carpenter, J. M., Silverstone, M. D., Bouwman, J., Mamajek, E. E., Wolf, S., Malhotra, R., Pascucci, I., Najita, J., Padgett, D. L., Henning, T., Brooke, T. Y., Cohen, M., Strom, S. E., Stobie, Elizabeth B., Engelbracht, C. W., Gordon, K. D., Misselt, K., Morrison, J. E., Muzerolle, J., Su, Kate Y. L. 2005: Formation and Evolution of Planetary Systems: Cold Outer Disks Associated with Sun-like Stars, ApJ, 632, 659

Krivov, A. V. 2010: Debris disks: seeing dust, thinking of planetesimals and planets, RAA, 10, 383

Lada,Charles J. 1987: Star formation - From OB associations to protostars, IAUS, 115, 1

Lagage, P., Doucet, C., Pantin, E., Habart, E., Duchêne, G., Ménard, F., Pinte, C., Charnoz, S., Pel, J. 2006: Anatomy of a Flaring Proto-Planetary Disk Around a Young Intermediate-Mass Star , Science, 314, 621

References of the figures

Papers

Leinert, Ch., van Boekel, R., Waters, L. B. F. M., Chesneau, O., Malbet, F., Köhler, R., Jaffe, W., Ratzka, Th., Dutrey, A., Preibisch, Th., Graser, U., Bakker, E., Chagnon, G., Cotton, W. D., Dominik, C., Dullemond, C. P., Glazenborg-Kluttig, A. W., Glindemann, A., Henning, Th., Hofmann, K.-H., de Jong, J., Lenzen, R., Ligori, S., Lopez, B., Meisner, J., Morel, S., Paresce, F., Pel, J.-W., Percheron, I., Perrin, G., Przygodda, F., Richichi, A., Schöller, M., Schuller, P., Stecklum, B., van den Ancker, M. E., von der Lühe, O., Weigelt, G. 2004: Mid-infrared sizes of circumstellar disks around Herbig Ae/Be stars measured with MIDI on the VLTI, A&A, 423, 537

Lin, Shin-Yi, Ohashi, N., Lim, J., Ho, Paul T. P.; Fukagawa, M. Tamura, M. 2006: Possible Molecular Spiral Arms in the Protoplanetary Disk of AB Aurigae, ApJ, 645, 1297

Liseau, R., Eiroa, C., Fedele, D., Augereau, J.-C., Olofsson, G., González, B., Maldonado, J., Montesinos, B., Mora, A., Absil, O., Ardila, D., Barrado, D., Bayo, A., Beichman, C. A., Bryden, G., Danchi, W. C., Del Burgo, C., Ertel, S., Fridlund, C. W. M., Heras, A. M., Krivov, A. V., Launhardt, R., Lebreton, J., Löhne, T., Marshall, J. P., Meeus, G., Müller, S., Pilbratt, G. L., Roberge, A., Rodmann, J., Solano, E., Stapelfeldt, K. R., Thébault, Ph., White, G. J., Wolf, S. 2010: Resolving the cold debris disc around a planet-hosting star . PACS photometric imaging observations of q1 Eridani (HD 10647, HR 506), A&A, 518, L132

References of the figures

Papers

Lucas, P. W. & Roche, P. F. 1997: Butterfly star in Taurus: structures of young stellar objects, MNRAS, 286, 895

Marois, C., Macintosh, B., Barman, T., Zuckerman, B., Song, I., Patience, J., Lafrenière, D., Doyon, René. 2008: Direct Imaging of Multiple Planets Orbiting the Star HR 8799, Science, 322, 1348

Moro-Martín, A. 2008: On the solar system -- debris disk connection, IAUS, 249, 347

Moro-Martín, A., Wolf, S., Malhotra, R. 2005: Signatures of Planets in Spatially Unresolved Debris Disks, ApJ, 621, 1079

Oppenheimer, B. R., Brenner, D., Hinkley, S., Zimmerman, N., Sivaramakrishnan, A., Soummer, R., Kuhn, J., Graham, J. R., Perrin, M., Lloyd, J. P., Roberts, L. C., Jr., Harrington, David M. 2008: The Solar-System-Scale Disk around AB Aurigae, ApJ, 679, 1574

Paardekooper, S.-J. & Mellema, G. 2004: Planets opening dust gaps in gas disks, A&A, 425, L9

Padgett, D. L., Brandner, W., Stapelfeldt, K. R., Strom, S. E., Terebey, S., Koerner, D. 1999: HUBBLE SPACE TELESCOPE/NICMOS Imaging of Disks and Envelopes around Very Young Stars, AJ, 117, 1490

References of the figures

Papers

Przygodda, F., van Boekel, R., Abraham, P., Melnikov, S. Y., Waters, L. B. F. M., Leinert, Ch. 2003: Evidence for grain growth in T Tauri disks, A&A, 412, L43

Quanz, S. P., Schmid, H. M., Geissler, K., Meyer, M. R., Henning, T., Brandner, W., Wolf, S. 2011: Very Large Telescope/NACO Polarimetric Differential Imaging of HD100546—Disk Structure and Dust Grain Properties between 10 and 140 AU, ApJ, 738, 23

Sauter, J., Wolf, S., Launhardt, R., Padgett, D. L., Stapelfeldt, K. R., Pinte, C., Duchêne, G., Ménard, F., McCabe, C.-E., Pontoppidan, K., Dunham, M., Bourke, T. L., Chen, J.-H. 2009: The circumstellar disc in the Bok globule CB 26. Multi-wavelength observations and modelling of the dust disc and envelope, A&A, 505, 1167

Schegerer, A., Wolf, S., Voshchinnikov, N. V., Przygodda, F., Kessler-Silacci, J. E. 2006: Analysis of the dust evolution in the circumstellar disks of T Tauri stars, A&A, 456, 535

Stanke, T., McCaughrean, M. J., Zinnecker, H. 2002: An unbiased H2 survey for protostellar jets in Orion A. II¥@. The infrared survey data, A&A, 392, 239

Testi, L., Bacciotti, F., Sargent, A. I., Ray, T. P., Eislöffel, J. 2002: The kinematic relationship between disk and jet in the DG Tauri system, A&A, 394, L31

van Boekel, R., Min, M., Leinert, Ch., Waters, L. B. F. M., Richichi, A., Chesneau, O., Dominik, C., Jaffe, W., Dutrey, A., Graser, U., Henning, Th., de Jong, J., Kohler, R., de Koter, A., Lopez, B., Malbet, F., Morel, S., Paresce, F., Perrin, G., Preibisch, Th., Przygodda, F., Scholler, M., Wittkowski, M. 2004: The building blocks of planets within the `terrestrial' region of protoplanetary disks, Nature, 432, 479

References of the figures

Papers

Winters, W. F., Balbus, Steven A., Hawley, J. F. 2003: Gap Formation by Planets in Turbulent Protostellar Disks, ApJ, 589, 543

Wolf, S. & D'Angelo, G. 2005: On the Observability of Giant Protoplanets in Circumstellar Disks, ApJ, 619, 1114

Wolf, S., Gueth, F., Henning, T., Kley, W. 2002: Detecting Planets in Protoplanetary Disks: A Prospective Study, ApJ, 566, L97

Wolf, S. & Hillenbrand, L. A. 2003: Model Spectral Energy Distributions of Circumstellar Debris Disks. I. Analytic Disk Density Distributions, ApJ, 596, 603

Wolf, S., Padgett, D. L., Stapelfeldt, K. R. 2003: The Circumstellar Disk of the Butterfly Star in Taurus, ApJ, 588, 373

Wolf, S., Schegerer, A., Beuther, H., Padgett, D. L., Stapelfeldt, K. R. 2008: Submillimeter Structure of the Disk of the Butterfly Star, ApJ, 674, L101

References of the figures

Books

Beckwith, S. V. W., Henning, T., Nakagawa, Y. 2000: Protostars and Planets IV, University of Arizona Press, p. 533

Reipurth, B., Jewitt, D., Keil, K. 2007: Protostars and Planets V, University of Arizona Press

Najita, J. R., Carr, J. S., Glassgold, A. E., Valenti, J. A. 2007: Protostars and Planets V, University of Arizona Press

Stahler, S. W. & Palla, F. 2004: The formation of stars, Wiley-VCH, p.3

Waelkens, C. 2002: The Century of Space Science, Volume I. Kluwer Academic Publishers, p.857

Appendix

Accretion in circumstellar disks

(Introduction)

Accretion disk – Angular momentum transport

- *accretio* (lat.) - accretion, growth
- Flow of gas from the disk (supporte by centrifugal forces) onto a compact central object is one of the most important concepts in astrophysics

Examples:

- *Protoplanetary accretion disk around young stellar objectse*
- *Close binary stars*
- *Active Galactic Nuclei, Quasars*

1. Isolated, self-gravitating system (Mass M, Angular momentum L): Energetically "most favourable" configuration: Entire mass in the center, entire angular momentum at very large radii

   Solar system: Sun: 99.9% of total mass

   2% of total angular momentum (Jupiter!)

2. Dissipation of Energy: Results in transport of matter (mass) to smaller radii and transport of angular momentum to larger radii
3. Mechanism of energy dissipation:

   "Internal friction" in differentially rotating disks

   Viscose Accretion disks

What causes viscosity?

Energy release

Accretion of mass *m* onto the surface of a body with mass M_* and radius R_*

$$\Delta E_{\mathrm{acc}} = \frac{G \cdot M \cdot m}{R_*}$$

⇒ Ratio M_* / R_* ("compactness" of the object) determines E_{acc}

⇒ In Solar nebula: Energy release negligible, but important in the case of massive star formation
(e.g. Omukai & Palla 2003 "Formation of the first stars by accretion", ApJ 589, 677)

⇒ Important in following cases:

1) Neutron star

$$\left.\begin{array}{l} R_* = 10\ \mathrm{km} \\ M_* = 1\ \mathrm{M_{Sonne}} \\ m = 1\mathrm{g} \end{array}\right\} \Delta E_{\mathrm{acc}} \approx 1.3 \times 10^{13}\ \mathrm{Ws}$$

H fusion: $\Delta E_{\mathrm{Fusion}} \approx 0.007 mc^2 \approx 6.3 \times 10^{11}\ \mathrm{Ws} \approx 5\% \Delta E_{\mathrm{acc}}$

2) Black holes
3) White dwarfs

Assumptions / Simplifications

1. **Disk mass** is **small** in comparison to the mass which determines the gravitational potential (in which the disk evolves)
   - Self-gravitation of the disk insignificant
   - Keplerian orbits

2. **Geometrical extent** (vertical direction) is **small** compared to the disk radius: <u>Thin disk approximation</u>

3. **Radial pressure and temperature gradients** are not important for the dynamics of the system

   (i.e., if steady-state solution exist, the disk must be supported by centrifugal force)

   => Orbital velocity always almost Keplerian, superposed with a much smaller radial velocity component

Accretion: Simple model

- Model:
  Disk: Single rings, coupled by friction

- Differential Rotation: $r \Uparrow \;\; \Rightarrow \;\; \Omega \Downarrow$
  Example: Keplerian disk
  $$\Omega = [\, G\, M / r^3 \,]^{1/2} \sim \mathbf{r}^{-3/2}$$

- Friction between inner (faster) and outer (slower rotating) ring:

  => $\Omega_{inner} \Downarrow$, $\Omega_{outer} \Uparrow$

  => Angular momentum transfer: inner ring => outer ring
  => Inner material ("decelerated") moves inward,
  Outer material ("accelerated") moves outward

- Friction => Angular momenum transfer
  => Mass flux: inward,
  Release of potential energy

Gas disk: Kinematic viscosity

- Gas disk: Situation slightly more difficult…
  1) Matter diffuses in both directions at all radii
  2) Instead of friction: **Viscosity**
  (caused e.g. by magnetic fields: coupling in plasma phase)

- In general: turbulent flow => radial mixing =>
  - Matter exchange at different radii
  - Viscous tension
  - Angular momentum transfer between different radial regions

- Description: kinematic Viscosity ($\nu \sim w\,\lambda$)
  - Turbulence of gas described by
    - w - "typical" random velocity of gas elements
    - λ - mean free path (before mixing with other material)

Transport of angular momentum

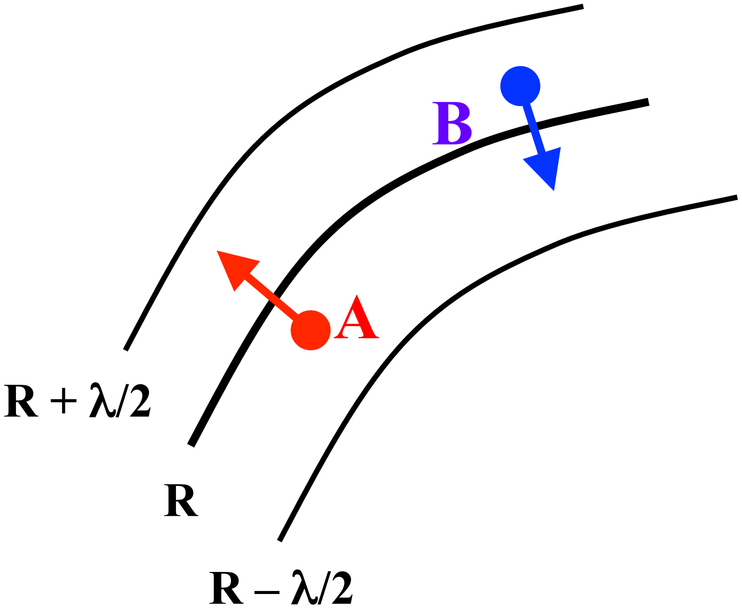

Transport of angular momentum at radius R
(caused by different angular momenta of the inward and outward drifting matter):

A) $R-\lambda/2 \rightarrow R \rightarrow R+\lambda/2$ (outward)

B) $R+\lambda/2 \rightarrow R \rightarrow R-\lambda/2$ (inward)

$\mathrm{d}\Omega/\mathrm{d}R \neq 0 \Rightarrow$ Shear forces

Observer at radius *R* (rotating with the disk)

A) Angular momentum of the matter coming from $R-\lambda/2$ (approx.):

$$\Delta J_{\mathrm{in}} \propto \left(R-\lambda/2\right)^2\left[\Omega\left(R-\lambda/2\right)-\Omega(R)\right] \approx \left(R-\lambda/2\right)^2\left[-\lambda/2\,\frac{\mathrm{d}\Omega}{\mathrm{d}R}\right]$$

B) Analog

Transport of angular momentum

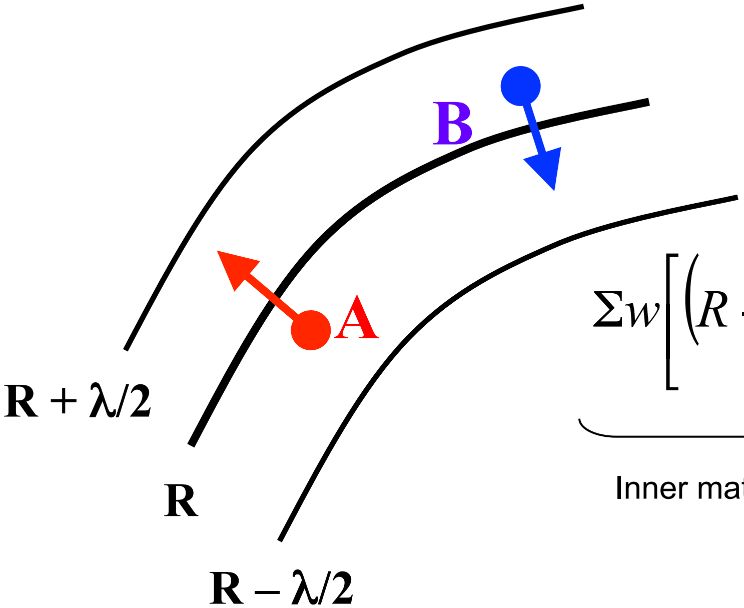

Resulting transport of angular momentum in outward direction (at radius R) per unit length for a disk with mass density per unit area Σ (surface density) :

$$\underbrace{\Sigma w\left[\left(R-\frac{\lambda}{2}\right)^2\left(-\frac{\lambda}{2}\frac{\mathrm{d}\Omega}{\mathrm{d}R}\right)-\left(R+\frac{\lambda}{2}\right)^2\left(\frac{\lambda}{2}\frac{\mathrm{d}\Omega}{\mathrm{d}R}\right)\right]}_{\text{Inner material diffuses with volecity } w \text{ outwards, outer material with the same velocity inwards}} \approx -\Sigma w\lambda R^2\frac{\mathrm{d}\Omega}{\mathrm{d}R}$$

$\lambda << R,$
$\lambda <<$ Distances, over which Ω is varying significantly

=> Torque (on outer ring caused by inner ring) :

$$G = -2\pi R\cdot\Sigma\nu R^2\frac{\mathrm{d}\Omega}{\mathrm{d}R}, \quad \text{where} \quad \nu = \lambda w$$

Discussion: 1) $\frac{\mathrm{d}\Omega}{\mathrm{d}R} < 0$ (e.g. Keplerian disk): outward flow of angular momentum

2) $\frac{\mathrm{d}\Omega}{\mathrm{d}R} = 0$ Stiff body => no shear forces => no angular momentum transport

Thin disk approximation

- In many cases the material which is to be accreted has a sufficiently high angular momentum to form an accretion disk
- Usual approximation: Gas flow constrained to a thin layer

  => approximation: 2D gas flow

  => "Thin disk approximation"

see Frank, King & Draine: "Accretion Power in Astrophysics"

For description of

a) Radial disk structure

b) Temporal evolution

c) Stationary thin disk

d) Local structure of thin disks

Mass transport in a thin disk

Application of the model for the case of a geometrically thin disk (example)

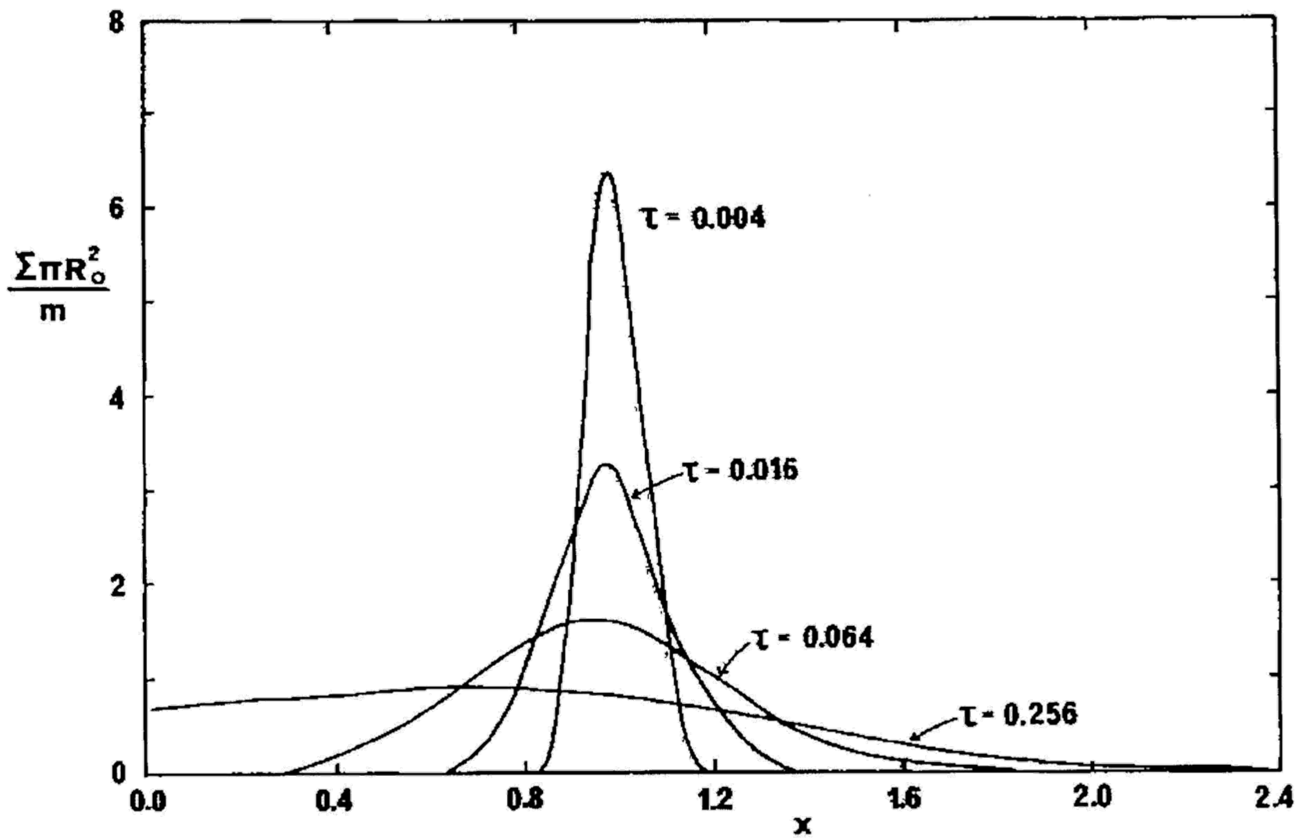

Figure 1 The viscous evolution of a ring of matter of mass m. The surface density Σ is shown as a function of dimensionless radius $x = R/R_0$, where R_0 is the initial radius of the ring, and of dimensionless time $\tau = 12\nu t/R_0^2$ where ν is the viscosity.

[from Lynden-Bell & Pringle, 1974]

Instabilities causing viscosity

Motivation

Why do particles / gas parcels not move on stable (e.g. Keplerian) orbits, but give away part of their angular momentum to neighboring particles?

Remember: Concept of kinematic viscosity ($\nu \sim w \, \lambda$)

Rem.: 1) If viscosity is caused by random gas diffusion ("molecular viscosity): kinematic viscosity good approach

2) Problem:

Molecular viscosity much too small to be of importance in astrophysical disks!

Ansatz: Other processes must creat "effective turbulent viscosity", which can then be described by proper values of the following parameters:

$$\nu_{turb} \sim w_{turb} \, \lambda_{turb}$$

Concept: α parametrization

- Problem
  Missing theory of turbulence, allowing to derive w_{turb} and λ_{turb}

- Ansatz

  1. $\lambda_{\text{turb}} \le H$ Typical size of a gas element < vertical extent of the disk
  2. $w_{\text{turb}} \le c_{\text{Sound}}$ For $w_{\text{turb}} > c_{\text{Sound}}$: Thermalization of turbulent motions by shocks

$$\Rightarrow \quad \underline{\underline{\nu = w_{\text{turb}} \cdot \lambda_{\text{turb}} = \alpha \cdot H \cdot c_{\text{Sound}}}}$$

This approach is only a useful parametrization

a) Lack of knowledge (w_{turb} , λ_{turb}) => Lack of knowledge (α), except for $\alpha \le 1$;
but: $\alpha>1$ possible in small disk regions with supersonic turbulence

b) α not necessarily constant throughout the disk

=> α to be constrained through disk observations:
Measurement: Line width (Hα) => Accretion rate, Assumption $\Sigma(r)$ => α

Currently discussed sources of viscosity: a) Magneto-rotational instability

b) Gravitational instability

Further Reading

Books

"Accretion Processes in Star Formation"
L. Hartmann; Cambridge University Press 1998

“**Accretion power in Astrophysics**”
J. Frank, A. King, & D. Raine; Cambridge University Press 1992

Papers

“**Theory of Accretion Disks I / II**”
Papaloizou, J.C.B., Lin, D., 1995, Ann.Rev.Astron.Astrophys., 33, 505
Lin, D.N.C. & Papaloizou, J.C.B., 1996, Ann.Rev.Astron.Astrophys., 34, 703

“**Accretion Discs in Astrophysics**”
Pringle, J.E., 1981, Ann. Rev. Astron. & Astrophys., 24, 337

“**Evolution of Viscous Discs**”
Lynden-Bell, D. & Pringle, J.E., 1974, Mon. Not. R. Astr. Soc., 168, 603

“**Black Holes in Binary Systems. Observational Appearance**”
Shakura, N.I. & Sunyaev, R.A., 1973, Astron. & Astrophys., 24, 337